University
of Southampton

UNIVERSITY OF SOUTHAMPTON

EFFECTS OF MALATHION ON THE VASCULAR FUNCTION IN HUMAN SKIN

Submitted by Paraskevi Boutsiouki

for the degree of Doctor of Philosophy

FACULTY OF MEDICINE, HEALTH AND BIOLOGICAL SCIENCES
DIVISION OF INFECTION, INFLAMMATION AND REPAIR

FEBRUARY 2002

UNIVERSITY OF SOUTHAMPTON

ABSTRACT

FACULTY OF MEDICINE, HEALTH AND BIOLOGICAL SCIENCES

DIVISION OF INFECTION, INFLAMMATION AND REPAIR

Doctor of Philosophy

EFFECTS OF MALATHION ON VASCULAR FUNCTION IN HUMAN SKIN

by Paraskevi Boutsiouki

While the effects of acute exposure to high levels of organophosphorus insecticides like malathion on human health are well documented, the mechanisms underlying the responses of the cutaneous vasculature to short and/or long term exposure to low-doses of organophosphates (OP's) are less well understood. The skin is considered as the major route of absorption of OP's and other xenobiotics. However, the toxic nature of OP's and the lack of appropriate techniques for their study have meant that the mechanisms of transdermal absorption of topically applied malathion and the role of cutaneous blood flow in its distribution within the tissue have yet to be resolved. Once absorbed malathion has its main toxic effects through the inhibition of acetylcholinesterase (AChE) found in both neuronal and non-neuronal cells. Inhibition of AChE results in the accumulation of acetylcholine (ACh) and overstimulation of the cholinergic receptors in the tissue. One consequence of this is an increase in blood flow due to the action of ACh on the vascular endothelium and the vascular smooth muscle.

This work examines the effects of a single low-dose of malathion on the cutaneous vasculature in healthy human skin in vivo. The percutaneous delivery of malathion to the tissue space was established using dermal microdialysis. Scanning laser Doppler imaging was used to assess changes in skin blood flow following exposure to a single low-dose of malathion. The effects of changes in local blood flow on the distribution of malathion within the tissue space were also investigated. In addition the mechanisms by which malathion exerts its effects on the vasculature were investigated both directly by the assay of ACh and nitric oxide in dermal dialysates and indirectly using the response to exogenous ACh as a measure of AChE activity. The role of cutaneous muscarinic receptors in the malathion-induced changes in vascular perfusion was also addressed in this study using dermal iontophoresis to deliver agonists and/or antagonists in the skin and laser Doppler fluximetry to monitor the responses of the vasculature to these agents.

The results from the present study demonstrate that malathion is absorbed through the skin and can have direct vasodilator effects which are mediated in part by the increase in tissue levels of ACh and subsequent stimulation of cutaneous muscarinic receptors. This study also showed that tissue levels of malathion are dependent upon local skin blood flow and thus malathion through its effects on the vasculature can influence its own systemic distribution. In addition the results in this study confirm that the responses to ACh are only in part modulated by nitric oxide and demonstrate that at high concentrations ACh has neurogenic effects manifest as flare and itch.

Together these findings result in a better understanding of the factors that contribute to the systemic distribution of malathion following its topical application to the skin, as well as of the mechanisms by which OP's modulate the physiological responses of the cutaneous vasculature. The latter provides valuable information about the potential toxic effects following acute exposure to low-doses of OP's.

LIST OF CONTENTS

LIST OF FIGURES

Chapter 1

Chapter 2

Chapter 3

Chapter 4

Chapter 5

Chapter 6

Chapter 7

LIST OF TABLES

Chapter 1

Chapter 5

Chapter 6

Chapter 7

AKNOWLEDGEMENTS

I would like to thank my supervisor, Dr Geraldine Clough, for her everlasting guidance, help and encouragement throughout this project and Professor Martin Church for his support and enthusiasm.

A particular thanks to Katerina Klagkou who helped me to develop a method for the assay of acetylcholine in my samples. I am also grateful to all the individuals who were brave enough to volunteer for my experiments and enabled this work to be performed.

Last but not least my gratitude to my mum, Faidra and dad, Nikolaos as well as to my closest friends for their love and understanding throughout the challenging years of this project.

I also would like to aknowledge the generous financial support provided by the Sir Jules Thorn Charitable Trust.

DECLARATION AND PUBLICATIONS

Apart from the mass spectrometry studies on the levels of acetylcholine in dermal dialysate, which were performed by Ms Katerina Klagkou, all the studies presented in this thesis were performed solely by the author.

A substantial amount of the work presented in this thesis has been published:

Boutsiouki P, Thompson JP, Clough GF (2000) Effects of malathion on the microcirculation of healthy human skin *in vivo* J Physiol **523** 142P

Boutsiouki P, Thompson JP, Clough GF (2000) Effects of local blood flow on the percutaneous absorption of malathion in human skin *in vivo* J Vasc Res **37** (Suppl 1) 40

Boutsiouki P, Thompson JP, Clough GF (2001) Effects of local blood flow on the percutaneous absorption of the organophosphorous compound malathion: a microdialysis study in man Arch Toxicol **75** 321-328.

Boutsiouki P, Clough GF (2001) Role of nitric oxide in the vascular response to acetylcholine in human skin *in vivo* J Physiol **531** 20P

Boutsiouki P, Thompson JP, Clough GF (2001) Long-term effects of low dose of malathion on the microcircualtion of healthy human skin *in vivo* J Vasc Res **38** 398

Clough GF, Boutsiouki P, Church MK, Michel CC (2001) Recovery of small diffusible molecules by microdialysis in human skin *in vivo* effects of blood flow J Vasc Res **38** 404

Boutsiouki P, Thompson JP, Clough GF (2001) .Microvascular responses to acute low-dose exposure to malathion in human skin *in vivo* FASEB J **15** A52

Boutsiouki P, Clough GF (2001) Long-term modulation of the microvascular response to acetylcholine by acute low-dose exposure to malathion in humans *in vivo* J Physiol **536** 164P

The only thing greater than the power of mind
is the courage of the heart

'Beautiful Mind'-2002

Abbreviations

ACh	Acetylcholine
AChE	Acetylcholinesterase
AU	Arbitrary Units
CaM	Calmodulin
cAMP	Cyclic Adenosine Monophosphate
cGMP	Cyclic Guanosine Monophosphate
CGRP	Calcitonin gene related peptide
CNS	Central Nervous System
DOH	Department of Health
EDHF	Endothelium - derived Hyperpolarizing Factor
FBF	Forearm Blood Flow
FU	Fluoresence Units
GC	Gas Chromatography
G_i	Inhibitory G protein
GTN	Glyceryltrinitrate
ICAM	Inter - Cellular Adhesion Molecule
IPPSF	Isolated Perfused Porkine Skin Flap
LD_{50}	Lethal $Dose_{50}$
LDF	Laser Doppler Fluximetry
L - NAME	N^G - nitro - L - arginine methyl ester
L - NMMA	N^G - mono - methyl - L - arginine
MW	Molecular Weight
N	Avogadro's Constant
NA	Noradrenaline
NaI	Sodium Iodide
NK_1	Neurokinin 1
$NaNO_2$	Sodium nitrate
NO	Nitric Oxide
NO_2^-	Nitrite
$NO_2^\bullet$	Nitrogen Dioxide
NOA	Nitric oxide analyzer
NOS	Nitric oxide synthase

NPY	Neuropeptide Y
NTE	Neuropathy target esterase
OP	Organophosphate
OPIDN	Organophosphorus induced delayed neuropathy
PACAP	Pituitary adenylate cyclase activating peptide
PGI_2	Prostaglandin I_2
PI	Phosphoinositide
PNS	Peripheral nervous system
ppm	Parts per million
PU	Perfusion units
QNB	Quinuclidinyl benzilate
RR	Relative recovery
sem	Standard error of the mean
SLDI	Scanning laser Doppler Imaging
SNP	Sodium nitroprusside
SP	Substance P
UVB	Ultraviolet light B
VAS	Visual analoque scale
VIP	Vasoactive intestinal peptide

CHAPTER 1: GENERAL INTRODUCTION

1.1 Organophosphates

Organophosphates (OP's) are widely used as pesticides in agriculture, public health, veterinary, domestic and medicinal application. Other organophosphorus esters are used as lubricants and plasticisers. Human exposure to OP's is therefore extensive. OP's have their main action by the irreversible inhibition of esterases, most notable acetylcholinesterase (AChE). The inhibition of AChE by OP's will lead to the rapid accumulation of acetylcholine (ACh) and the subsequent cholinergic symptoms (Department of Health, 1999). In humans these symptoms include disturbances of the peripheral and the central nervous systems, myopathy, cardiotoxicity and suppression of the immune system. In the past few years, reports on the adverse health effects resulting from exposure to OP's have significantly increased. Although the adverse effects of acute high-dose exposure to OP's on the central and peripheral nervous system are well documented and related to the inhibition of AChE, the mechanisms underlying the effects of low-dose exposure to OP's on the periphery are yet to be investigated. This study explores the effects of a single low-dose of the organophosphorous compound malathion on the peripheral vasculature and its inhibitory action on the AChE activity, in human skin *in vivo*.

Malathion has a relatively low toxicity towards mammals and is therefore licensed for house–hold use and as a human medicine for the treatment of head lice and scabies. As a result malathion comes in direct contact with human skin. There have been many attempts to model the kinetics of transdermal absorption of malathion. However, mainly due to the lack of sensitive experimental techniques these studies have been restricted to isolated tissue experiments and animal models. Hence despite the widespread interest in the skin as a major route of absorption for both therapeutic and environmental agents, the mechanisms of transdermal absorption and the factors (e.g. local blood flow and metabolism) that influence the disposition of topically applied OP's within the skin remain poorly understood. Several studies have demonstrated that clearance of small diffusible molecules from the dermis is highly dependent upon local blood flow (Riviere & Williams, 1992; Singh & Roberts, 1994). Thus it may be speculated that agents that affect cutaneous blood flow will also influence their own distribution. The present study investigates the rate of the percutaneous absorption of malathion and the relationship between tissue levels of malathion and changes in local skin blood flow.

1.1.1: General characteristics of malathion and its use in agriculture and as a human medicine

Malathion is the common name for the organophosphate O,O–dimethyl–S–(1,2–dicarbethoxyethyl)phosphorodithioate. Malathion is a deep brown to yellow liquid at room temperature, with a characteristic odour. It is only slightly soluble in water (145 ppm) but is miscible in many organic solvents. The octanol–water partition coefficient ($LogK_{ow}$) for malathion lies between 2.36 and 2.89 (World Health Organization IPCS Database, 1993; Hazardous substances databank, 1997). Malathion, has a relatively low mammalian toxicity compared with several other OP's (LD_{50} for malathion is 60–1300 mg kg^{-1}, compared with chlorfenvinphos LD_{50} 1-30 mg kg^{-1}) (Minton & Murray, 1988). However, the oxygen analogue of malathion, malaoxon **(Figure 1.1)** is a potent inhibitor of AChE and is formed as a metabolite of malathion (Johnson & Wallace, 1987; Ward *et al.*, 1993; Rodriguez *et al.*, 1997). The resistance of mammals to malathion and other OP's is due to mammal's higher capacity for metabolic inactivation of OP's rather than any inherent resistance of the mammalian target proteins.

Malathion is formulated for agricultural use as wettable powders, emulsifiable concentrates, dusts and ultra–low volume concentrates. Coformulants are added in order to increase the stability of the OP during storage, or to increase contact between the OP and the target organism, or to reduce inactivation in the target species. It has been suggested that the coformulants can have profound effects on the rates of dermal absorption of OP's and may themselves have toxic effects (Department of Health, 1999). Malathion preparations for human use for the treatment of head lice and other lice manifestations may be found in aqueous or alcohol based formulations containing 0.5–1 % malathion **(Table 1.1)**. In the present study Derbac M (0.5 % malathion) in the form of head lice shampoo and an aqueous based malathion formulation (1 % malathion) were used to explore the rate of the percutaneous absorption of malathion and the mechanisms underlying its effects on the microcirculation in human skin *in vivo*.

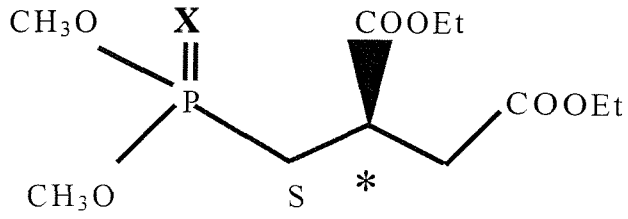

Figure 1.1 Chemical structure of organophosphates: When **X** = S malathion, when **X** = O malaoxon. Stereoisomers of both malathion and malaoxon occur due to an asymmetric carbon centre (*). Rodriguez and colleagues showed that the stereoisomers of malaoxon are significantly different in their ability to inhibit cholinesterase enzymes (Rodriguez *et al.*, 1997).

NAME	MALATHION CONCENTRATION	RECOMMENDED CONTACT TIME	FORMULANTS
Derbac M shampoo	0.5% w/w	12–24 h 1 treatment	Aqueous base
Quellada M shampoo	0.5%		Aqueous base
Suleo M shampoo	0.5% w/v	10–12 h 1 treatment	Isopropyl alcohol
Prioderm lotion	0.5% w/v	12 h for scabies 2–12 h for lice	Isopropyl alcohol
Prioderm a) cream b) shampoo	1% w/w	~5–10 min 3 treatments over 9 days	Alcohol base

Table 1.1 Summarises the different commercial formulations of malathion available for use as human medicines: Formulations of malathion can be found as shampoos and lotions in the form of aqueous and alcohol based preparations. The concentration of malathion in these formulations ranges from 0.5 to 1 % and the time of application vary from 5-10 min up to 24 h with single or repeat treatments. Derbac M as well as an aqueous based malathion (1 %) formulation prepared in the laboratory was used in the present study to explore the percutaneous absorption of malathion in human skin *in vivo*.

1.1.2: Clinical symptoms after exposure to malathion and other OP's in humans.

All OP's used in pesticide products or veterinary medicines are capable of producing cholinergic symptoms in man **(Table 1.2)** due to the inhibition of AChE and the accumulation of ACh at receptors in the brain and spinal cord, at neuromuscular junctions, at ganglia of the autonomic nervous system and at parasympathetic nerve endings. The severity of these effects depends upon the reactivity of the OP, the route of exposure and the relative bio-activation and inactivation of the OP in the tissue.

1.1.2a Acute high-level OP exposure: Acute effects (i.e. short–term effects usually related to high-doses) after exposure to OP's are well documented in a number of epidemiological studies. Signs and symptoms of exposure are usually seen after exposure when the level of red blood cell AChE activity falls by more than 30–50 %. The duration of these effects depends on the OP. High-dose intoxication with some short–lived agents (such as sarin) is relatively transient whereas with other pesticides particularly after dermal exposure, the intoxication can be longer lasting (Camara *et al.*, 1997). Exposure to high-doses of OP's can cause prolonged effects in muscle and brain. For example, muscle necrosis has been observed in man after malathion and diazinon intoxication. This is also known as the intermediate syndrome the symptoms of which cannot be reversed by treatment with atropine or oximes. The best-known lasting effect of acute exposure to high–dose of OP is organophosphorus-induced delayed neuropathy (OPIDN). Symptoms begin 1–3 weeks after exposure and are related to inhibition of the neuropathy target esterase (NTE). The condition does not respond to treatment with anticholinergic drugs or oximes and recovery is slow and often incomplete (Department of Health, 1999).

1.1.2b Chronic low–level OP exposure: Because of the known potential of these agents to cause acute toxicity there is much concern about the long–term effects that may result after low-level OP exposure. Furthermore contact with OP's arises more often during occupational exposure e.g. sheep dipping and crop spraying and is associated with chronic exposure to low–level of the OP. However, the clarification of the long–term effects that may result after low–level OP exposure is more complicated by the lack of a major clinical episode (for example respiratory failure, or convulsions) and a notable underlying biological mechanism (Department of Health, 1999; Camara *et al.*, 1997).

RECEPTOR	SITE	SYMPTOMS AND SIGNS
Muscarinic and Nicotinic	Central nervous System	Anxiety, headache, confusion, respiratory depression, failure to concentrate, giddiness
Muscarinic	Glands (parasympathetic nervous system) Smooth muscle (gastro-intestinal tract, heart and pupil)	Excessive secretion e.g. saliva tears and sweat Diarrhoea, bradycardia, miosis and failure to focus
Nicotinic (N1) Nicotinic (N2)	Autonomic (increased sympathetic drive) Neuromuscular junction	Hypertension and tachycardia Fasciculation of muscle followed by weakness and paralysis

Table 1.2 The cholinergic symptoms observed after exposure to OP's: The table summarises the possible cholinergic symptoms that may occur after exposure to OP's. The severity of the symptoms depends on the OP agent, the duration and route of exposure. OP intoxication is usually reversed by administration of atropine and oxime treatment to reactivate AChE (redrawn and modified from Department of Health (1999)).

1.1.3: Other toxic effects of OP's.

1.1.3a Effects of malathion on the immune system: Immune cells (macrophages, mast cells and lymphocytes) appear to be regulated by ACh. The effects of malathion and malathion metabolites on human and rat basophilic cells and mast cells have been previously investigated by Xiong who suggested that malathion and its metabolites can cause the release of histamine from both basophilic cells and mast–cells (Xiong & Rodgers, 1997). They also examined the effects of acute and long–term (90 days) malathion exposure on serum histamine levels after administration of malathion via oral and dermal routes to mice and rats. Acute exposure to malathion resulted in an increase in serum histamine levels in rats that was maximal at 4 h, whereas repeated administration of malathion increased macrophage function and led to mast cell degranulation at doses as low as 0.1mg/kg/day for 90 days (Rodgers & Xiong, 1997; Rodgers & Xiong, 1997a). Cases of non-specific skin rash, urticaria as well as angioedema after repeated spraying of a mixture of malathion corn syrup bait have been reported in Southern California (Schanker *et al.*, 1992) although the mechanisms underlying these responses have yet to be determined. Irritant responses after patch test with malathion and other OP's in farmers with contact dermatitis but not in healthy farmers have also been reported (Sharma & Kaur, 1990) and may be related to the interaction of malathion with the immune system.

1.1.3b Inhibition of nitric oxide synthase: Malathion has been shown to interfere with nitric oxide synthase (NOS). Studies in rat brain *in vitro* demonstrate the inhibition of NOS activity by malathion, carbaryl and kepon to be concentration-dependent. This results from the interaction of these OP's with calcium/calmodulin (Ca^{2+}/CaM) complex on which the NOS activity is well known to be dependent (Rao *et al.*, 1999).

1.1.3c Genotoxic effects: Studies in cell culture reveal that malathion exposure is associated with specific mutations in human T-lymphocytes although the mechanism is still unknown (Pluth *et al.*, 1996). The ability of malathion to induce alterations in the morphology of spermatogenic cells and elicit damage of the germinal epithelium was studied *in vivo* in mice. Results demonstrate that malathion has a teratogenic effect on mice spermatid differentiation perhaps due to an alkylating effect on the DNA that disturbs the normal assembling of tail structural protein components (Contreras & Bustos-Obregón, 1999).

1.2 Mechanisms underlying the toxicity of malathion and other OP's

Organophosphates mimic biological esters such as acetylcholine (ACh) and can inhibit acetylcholinesterase (AChE) that leads to the accumulation of ACh **(Figure 1.2A)** at peripheral and central cholinergic synapses and subsequent signs of cholinergic over stimulation. Most OP's produce acute intoxication as a result of inhibition of AChE and if severe this can have longer-lasting secondary consequences such as permanent disability. All these effects are reasonably well understood and show a dose threshold. However, the mechanisms underlying the effects associated with low-level exposure to OP's in non-poisoned subjects are yet to be investigated. It has been suggested that if OP's play a causal role this will not necessarily be via AChE inhibition **(Figure 1.2)**. Several studies have shown that in addition to AChE, OP's bind to other proteins and inhibit a number of other enzymes, such as plasma pseudocholinesterase, neuropathy target esterase (NTE), A–esterases, carboxyesterases, as well as other esterases and proteases (Ray *et al.*, 2001) **(Figure 1.2 B)**. In general many enzyme systems have the potential for interaction with OP's, some of which are more sensitive than AChE. The possible biological consequences of exposure to OP's and the subsequent inhibition of these enzymes is highly dependent on the functional role of these enzymes in the tissue and are not yet fully understood.

Evidence for possible direct interaction of the OP's with the cholinergic receptors has also been provided, mainly from *in vitro* studies (Katz *et al.*, 1997) **(Figure 1.2 C)**. However, the mode of action of the OP's on the receptors and the significance of these direct effects compared with the inhibition of AChE are not clear. Furthermore, recent studies have demonstrated a widespread expression of ACh and AChE activity in non-neuronal cells such as endothelial cells, keratinocytes and mast cells (Wessler *et al.*, 1998). Non-neuronal ACh mediates its cellular actions via cholinergic receptors that are expressed on these cells and appears to be involved in the regulation of basic cell and immune functions (Wessler, 1999). Interaction of OP's with the non-neuronal cholinergic system is possible and may play role in the pathogenesis of inflammatory disease. Deficiency in skin cholinesterase for example and subsequent increase in the amount of ACh released normally in the skin was suggested as a possible mechanism underlying cholinergic urticaria (Magnus & Thompson, 1954). The effects of a single low-dose exposure to malathion on the endothelium of the peripheral vasculature and the possible mechanisms underlying these effects are explored in the present study *in vivo* in humans.

1.2.1: Inhibition of AChE and other esterases by malathion.

Acetylcholinesterase is present in large amounts in the membranes surrounding the synapse or the neuro–effector junction and also in erythrocytes and blood plasma and is responsible for the rapid hydrolysis of ACh in the tissue. Enzyme activity to inactivate ACh is also abundantly expressed in non-neuronal cells such as fibroblasts and the non–innervated part of skeletal muscle fibres (Wessler *et al.*, 1998). Non–specific cholinesterase (pseudo–cholinesterase) is also expressed in different tissues such as rabbit and human lung and is involved in the hydrolysis of free ACh. Magnus and colleagues have shown that in human skin pseudocholinesterase exists in considerably greater amounts than AChE (Magnus & Thompson, 1954). In the same study the activities for both AChE and pseudocholinesterase were measured in normal skin, obtained either by biopsies or at surgical operation from different anatomical sites. Their results indicate that healthy human skin has cholinesterase content such that 0.015 M ACh is hydrolysed at the rate of 442 ± 30 µl CO_2/g/h in male volunteers and 592 ± 45 µl CO_2/g/h in females. There were no significant differences in the activities of cholinesterase between anatomical sites, although pseudo–cholinesterase activity was found to be greater in the dermis compared with that in the epidermis (Magnus & Thompson, 1954).

Inhibition of AChE by malathion is mainly characterised by the progressive covalent reaction of malathion with the serine site of the target protein **(Figure 1.3 Step 2)** and the irreversible ageing reaction **(Figure 1.3 Step 4)**. Any serine hydrolase, due to its serine site (E-OH) that is the essential feature for the enzyme-OP covalent reaction, may be a potential target protein for the action of malathion **(Figure 1.3 Step 2)**. Due to the two distinct features (covalent reaction and ageing process) of the inhibition of esterases by malathion the extent of the biological effects after exposure to malathion will depend on both the concentration of malathion and the duration of exposure. Hence the effects after high-dose short-term exposure and low-dose long-term exposure to malathion can be equivalent *in vitro*. The factors that affect the rate of clearance of malathion from the tissue *in vivo* such as the cutaneous circulation are of great significance since these factors will limit both the duration and the severity of the adverse effects of malathion. These factors will be discussed further in **section 1.3** of the present chapter.

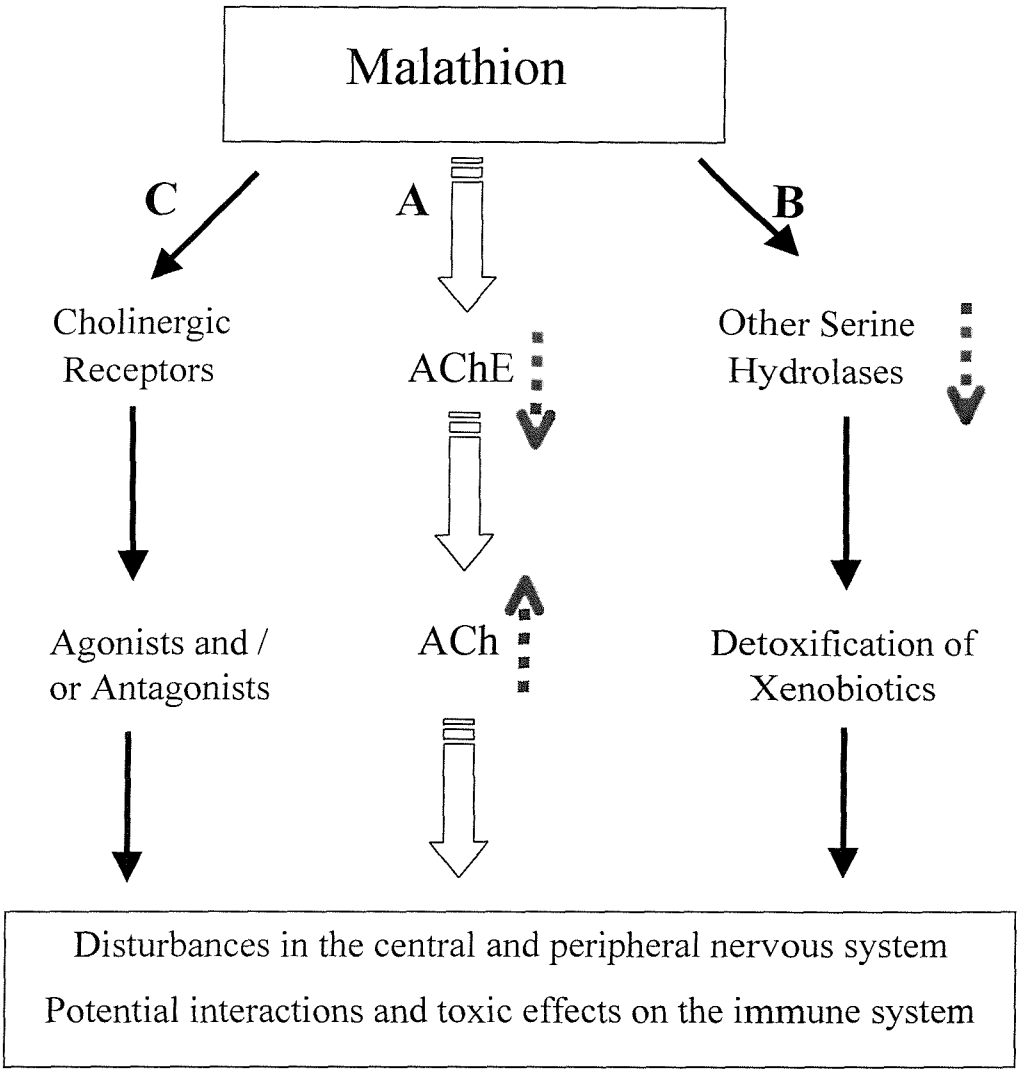

Figure 1.2 Potential mechanisms underlying the toxic effects following exposure to OP's: The scheme summarises the possible pathways that may be altered after exposure to malathion and could lead to mild or severe toxic effects. The main mechanism of action (**A**) is the inhibition (⇣) of acetylcholinesterase (AChE), which leads to an increase (⇡) in the levels of acetylcholine (ACh) in the tissue. Over stimulation of cholinergic receptors by excess ACh could lead to disturbances of central and peripheral nervous system (CNS and PNS) or cell death in non-neuronal systems. Inhibition (⇣) of other serine hydrolases (**B**) for example carboxylesterases by OP's has been demonstrated *in vitro*. Carboxylesterases are mainly xenobiotic metabolising enzymes. However, at least one type of esterase has been shown to be important in metabolising cholesterol esters and in testosterone biosynthesis (Ray *et al.*, 2001). In addition to their potent anti-cholinesterase action malathion and other OP's can have their effects directly through their interaction with muscarinic and nicotinic receptors (**C**). Their mode of action (agonist or antagonist) has yet to be resolved as it depends on the OP agent and the location of the receptors.

1.2.1a Stages involved in the inhibition of AChE by malathion: The hydrolysis of ACh by AChE involves transfer of the acetyl group from ACh to the esteratic site of the enzyme, followed by rapid hydrolysis to give acetate and the active enzyme. The process by which AChE can be inhibited by malathion and other OP's involves several steps that are outlined in **Figure 1.3**. Malathion initially inhibits cholinesterase by reversible binding (phosphorylation) and the formation of the Michaelis–Menten complex **(Figure 1.3 Step 1)**. A covalent reaction is followed with the leaving group (X) being eliminated **(Figure 1.3 Step 2)**. At this stage the phosphorylated enzyme is fairly stable resulting in relatively slow recovery **(Figure 1.3 Step 3)** from intoxication. This delay leads to prolonged inhibition. A second covalent reaction may occur before reactivation of the enzyme. This is known as "ageing" of the phosphorylated form of the enzyme **(Figure 1.3 Step 4)**. Step 4 involves a covalent cleavage of a bond within the enzyme–malathion adduct and the formation of a negative charge which stabilises it. Once this ageing reaction has occurred, reactivation of the enzyme is not possible and the enzyme is irreversibly inactivated.

1.2.1b Factors that affect inhibition and reactivation of AChE: The rates for the reactivation as well as the ageing process are highly dependent on the animal species, the chemical group attached to the enzyme and the length of exposure. Results from *in vitro* studies performed with different cholinesterases (ChE) from different species indicate that the stereoisomers of malaoxon **(Figure 1.1)** differ significantly in their ability to inhibit ChE enzymes. The rate constant (k_i) for human AChE after treatment with R–malaoxon was 1.27×10^5 compared with 1.09×10^4 for S–malaoxon (Rodriguez *et al.*, 1997). Kinetic studies indicate that dimethoxy OP's (e.g. malathion) have faster rate constants for all steps compared to diethoxy compounds (e.g. parathion) and are therefore less potent inhibitors and have lower toxicity (Camara *et al.*, 1997). Hence for dimethoxy phosphorylated AChE the half life for hydrolysis **(Figure 1.3, Step 3)** is 4.6 h, whereas for the ageing reaction **(Figure 1.3, Step 4)** is 4.3 h (Ray, 1998). This means that the ageing reaction can be faster than the spontaneous reactivation reaction, leading to irreversible inhibition of the enzyme. Therefore the factors that affect the clearance of OP's from the tissue such as the cutaneous circulation and metabolism will determine the duration and the mode (reversible or irreversible) of the AChE inhibition and consequently determine the severity of the toxic effects of the OP agent.

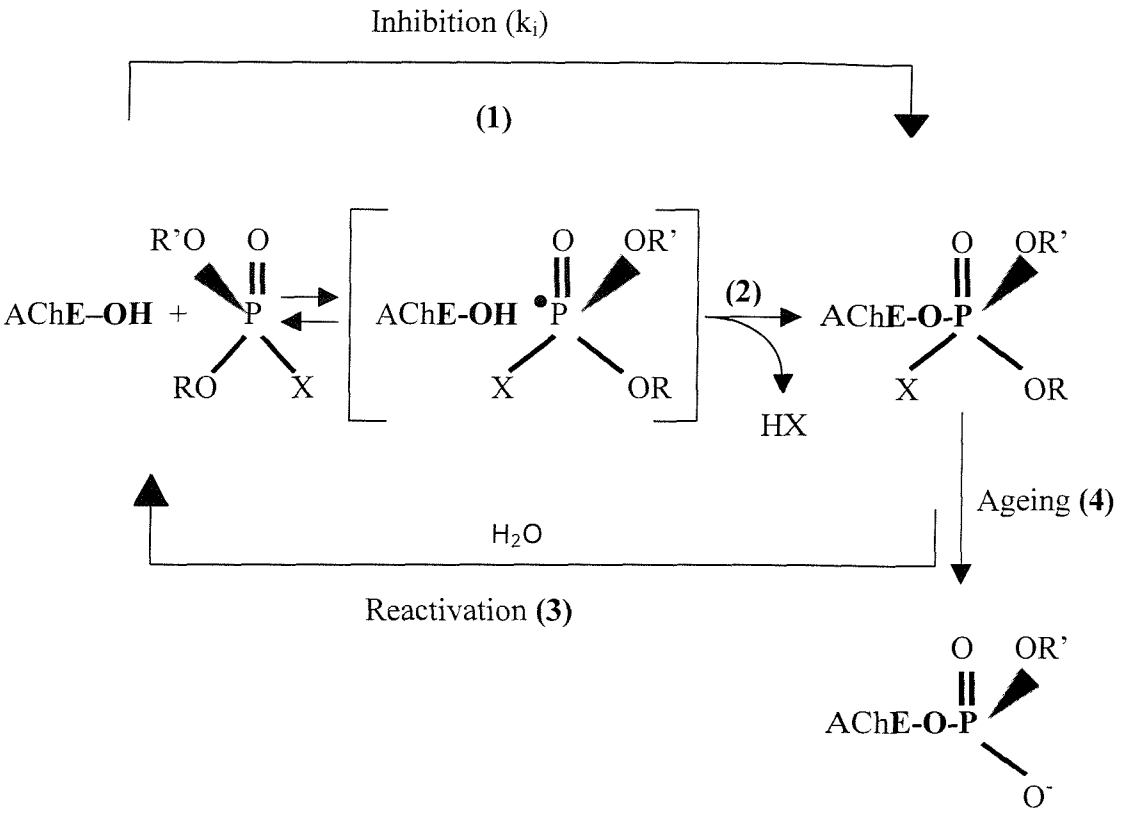

Figure 1.3 The stages involved in the inhibition of AChE by OP's: AChE is the main target protein for OP's to exert their inhibitory action. However, any serine hydrolase is a potential target for inhibition by OP's due to their serine site (**E-OH**), which is essential for the formation of the enzyme-OP complex **(step 1)**. The two main features of the inhibitory action of OP's on these proteins are the reversible formation of the enzyme–OP complex **(step 2)** and the subsequent irreversible ageing reaction **(step 4)** which is highly dependent on the nature of the OP agent (modified and redrawn from Jianmongkol *et al.*, 1999).

(1) : Reversible formation of enzyme–substrate (OP) complex

(2) : Phosphorylation of the enzyme with the loss of the leaving group X (Covalent reaction).

(3) : Reactivation of the enzyme spontaneously or following the addition of an oxime

(4) : Inactivation or aging of the enzyme on cleavage of an alkyl group (Ageing process).

1.2.2: Interactions of malathion and other OP's with cholinergic receptors.

In addition to their ability to inhibit AChE and other serine hydrolases, malathion and other OP's can directly interact with cholinergic receptors (**Figure 1.2**) (Bakry *et al.*, 1988; Eldefrawi *et al.*, 1992; Ward *et al.*, 1993). There is much confusion as to whether this interaction of OP' s with the receptor may contribute to their toxic effects. Despite the good evidence that OP's can act directly on cholinergic receptors it has proved very difficult to identify the mechanism of action of the OP (either an agonist or antagonist) at these receptors. A number of studies have investigated the regulation of the pathways involved with the cholinergic receptors in the presence and absence of an OP as a possible way of elucidating the mechanism of action of different OP's on these receptors (Eldefrawi *et al.*, 1992; Ward & Mundy, 1996; Katz *et al.*, 1997).

Cholinergic receptors can be divided into two types, muscarinic and nicotinic based on the pharmacological action of various agonists and antagonists. Acetylcholine can bind to both muscarinic and nicotinic receptors, yet the responses elicited by activating each receptor differ in several ways. Muscarinic responses are slow, may produce excitation or inhibition and involve second messenger systems, whereas nicotinic responses are of fast onset and short duration, excitatory in nature and involve the direct opening of an ion channel. The possible consequences of the overstimulation and/or inhibition of these receptors by OP's will depend on the mode of action of the OP on the receptor as well as on the nature of the receptor at its location in the tissue.

1.2.2a Muscarinic Receptors: Muscarinic receptors are widely distributed within the parasympathetic nervous system and regulate different functions at different tissues. Five different subtypes of muscarinic receptors have been identified (M_1-M_5) distinct for their association with different second messenger systems and their distribution within the tissues. M_3 receptors for example are found in the smooth muscle and in the heart regulate cardiac contractions, but can also result in cutaneous relaxation. Generally, M_1, M_3 and M_5 receptors are coupled to phospholipase C by one or two G proteins. Stimulation of the receptor activates phosphoinositide (PI) hydrolysis that leads to the release of calcium and is therefore thought to be involved in cardiac muscle contraction (Eglen *et al.*, 1996). By contrast in the smooth muscle of the blood vessel wall PI hydrolysis results in the production of nitric oxide in the endothelium and activation of guanylate cyclase, which

catalyses the formation of cyclic guanosine monophosphate (cGMP) and results in vascular relaxation. Stimulation of M_1 and M_3 on endothelial cells also leads to potassium and chloride channel activation as well as the release of arachidonic acid and subsequent production of prostaglandins that elicit relaxation in the adjacent smooth muscle via increase of cyclic adenosine monophosphate (cAMP).

M_2 and M_4 subtypes are coupled to adenylate cyclase by an inhibitory G protein (G_i) and activation of these subtypes results in the inhibition of cAMP formation. The muscarinic receptors expressed on non-neuronal cells are of the classic subtypes M_1-M_5 that couple to G–proteins to stimulate arachidonic acid release and cAMP production and open K^+ and Ca^{2+} dependent channels (M_1 and M_3) or inhibit adenylate cyclase and open K^+ channels (M_2 and M_4), or (M_5). Thus interaction of OP's with these receptors may result in a variety of clinical and biological symptoms ranging from prolonged contraction of the heart muscle to cell death.

1.2.2b Nicotinic Receptors: Nicotinic receptors are ion channel-coupled receptors and mediate the influx of Na^+ and Ca^{2+} ions and efflux of K^+ from the cell. They are found in the autonomic nervous system, the neuromuscular junction and the brain as well as in various non-neuronal cells such as keratinocytes (Grando, 1997). Generally an agonist will bind to the α-subunit of the nicotinic receptor making the membrane more permeable to cations causing a local depolarization, which results in muscle contraction when summed with the action of other receptors. Interruption of nicotinic pathways in non-neuronal systems by nicotinic receptor blockers results in cell death (Grando, 1997). The evidence for the direct actions of different OP's on the nicotinic receptors comes from *in vitro* studies in cultures of neuronal cells. In a recent study (Katz *et al.*, 1997) the ability of chlorpyrifos, parathion and their oxons to bind to nicotinic receptors was studied in relation to their anticholinesterase activity. The findings from this study demonstrate that these OP's bind to and affect the nicotinic receptors independently from their action on AChE. In the same study it was also suggested that chlorpyrifos, parathion and in a lesser extend their oxons, bind to an allosteric site on the nicotinic receptor that is distinct from the agonist site that bind ACh and α–bugarotoxin. Binding of OP's to this site would cause desensitization of the receptor and increased binding of the non-competitive antagonist TCP and consequently the inhibition of the nicotinic receptor function leading to cell death (Katz *et al.*, 1997).

1.2.3 Summary of the potential mechanisms underlying the toxic effects of malathion and other OP's on humans.

In summary the adverse effects observed after exposure to malathion are mainly the result of the inhibition of AChE by the OP and the subsequent increase in the levels of ACh in the tissue which in turn leads to over stimulation of cholinergic receptors. Because of the two distinct steps involved in the inhibition of AChE by OP's the toxic effects observed after exposure to OP's depend both on time of exposure and the concentration of the OP. Thus both the duration and severity of the effects of the OP will be highly dependent on the rate of clearance of the OP from the tissue space.

While AChE inhibition by OP's is the major reason for OP's acute toxicity, modulation of cholinergic receptors by OP's may add to the toxic effects after exposure to OP's. However there is much confusion on how significant are the effects of this interaction of the OP with the receptors compared with the effects that result from inhibition of AChE by OP's. This is mainly due to the fact that the reactions of the OP's with the receptors are reversible and in general occur at relatively high concentrations compared with the irreversible inhibition of AChE by OP's.

A variety of serine hydrolases other than AChE represent potential targets for OP inhibition due to their serine site that is the essential feature for the interaction of the OP with the protein. Serine hydrolases are thought to be involved in the immunotoxic effects of OP's due to the role that these enzymes play in the complement and thrombin systems. The possible mechanisms underlying the effects of malathion on the peripheral vasculature via its inhibition of AChE and the potential participation of the muscarinic receptors are explored in the present study in human skin *in vivo*. This study also investigates the release of different vasoactive mediators such as nitric oxide and histamine in response to a single low-dose of malathion and increased levels of ACh in the tissue.

1.3 Factors that affect the toxicity of OP's

The severity of the toxic effects of OP's will depend on 1) the route and length of exposure and 2) the rate of clearance of the OP from the tissue.

1.3.1 Route and extend of exposure

Exposure to malathion and other OP's can result from ingestion of contaminated food and water, inhalation of aerosols such as sprays and dusts and dermal exposure during handling or medical treatments. Oral exposure is usually associated with high dose intake e.g. in suicidal attempts and frequently results in acute cholinergic symptoms and death. Less serious oral exposure has also been reported in agricultural workers through smoking or eating without having first washed their hands.

The skin is the major route for the absorption of the majority of OP's. Dermal exposure can occur during treatment of head lice, handling of the concentrate and application of the diluted OP during crop spraying or sheep dipping. In addition, handling of treated sheep may result in exposure due to residues in the fleece. Although dermal exposure to OP's results in low dose intake **(see section 1.4.1)**, the duration of the exposure may be extended and can therefore lead to severe intoxication. For example a previous study showed that when increasing concentrations of malathion powder were applied to healthy volunteers and their clothing, up to 5 times a week for 8 or more weeks approximately 2% of the malathion applied was excreted as malathion and metabolites in the urine. This was calculated to represent a repeated dermal absorbed dose of 3.2 mg/kg/day (Bulletin of World Health Organization, 1960).

1.3.2 Bio-activation and detoxification in the tissue

The severity of the toxic effects observed after exposure to OP's is highly dependent on the rate of bio-activation and detoxification of the OP and their removal of the OP from the tissue. Mammals can bio-activate and detoxify OP's through various pathways that involve a range of enzyme systems. The consequences of metabolism depend upon the biological activities of the tissue and the physicochemical characteristics of the parent compound and its metabolite(s). If detoxification of OP's does not occur then the OP's can undergo metabolic oxidation resulting in desulphuration (e.g. conversion of malathion to malaoxon) and other chemical substitutions of their side chains or groups.

These oxidations are catalysed by cytochrome P–450 enzymes (mainly CYP3A) predominantly esterases. These enzymes are involved in both the activation and detoxification of thion OP's like malathion and parathion. Changes in their activity have therefore complex effects and the overall change in toxicity depends upon the balance between the two processes. Carboxylesterases although irreversibly inhibited by OP's also play an important role in detoxification of OP's as inhibition of these enzymes leads to non–toxic metabolites. For example OP's like malathion that contain esterified carboxylic acid side chains are hydrolysed by carboxylesterases to produce more water–soluble and less toxic metabolites (Maxwell, 1992).

The enzymes involved in the hydrolysis and oxidation of OP's have been detected in human skin but are also present in other tissues with high activities in liver, intestine and plasma. Heymann *et al.* demonstrated that human skin contains at least four different carboxylesterases, two of which are sensitive and two insensitive to inhibition by OP's (Heymann *et al.*, 1993). Significant activity of A–esterases which are also involved in the hydrolysis of OP's was found in the skin, as demonstrated *in vitro* in rat liver, lung, skin and blood (McCracken *et al.*, 1993). Significant metabolism of parathion to paraoxon and p–nitrophenol, as well as hydrolysis of carbaryl to naphthol was also observed using an *in vitro* model of porcine skin after topical application of the OP's (Chang *et al.*, 1994). Immunolocalisation and histochemical localisation studies have indicated that xenobiotic metabolising enzymes in the skin are located in the basement membrane of the epidermis in the hair follicle sheath and in the sebaceous glands, so that diffusing material must pass through these cells for metabolism (Heymann *et al.*, 1993). The presence of these enzymes in the skin is of great importance for the present study that investigates the percutaneous absorption of malathion and explores the possibility of its metabolic activation to malaoxon in human skin *in vivo*.

1.4 The skin as a route of absorption of malathion and other OP's

The skin is a major route for the absorption of both therapeutic and environmental agents. The skin receives up to one third of the cardiac output and along with the various enzymatic systems found within its components, the skin plays an important role in the degradation and elimination of xenobiotics. The skin is an important route for the absorption of malathion especially when malathion is used clinically as human miticide and comes in direct contact with the skin. The various xenobiotic metabolising enzymes that are located within the different compartments of the skin play an important role in the rate of bio-activation and detoxification of malathion and can therefore determine the severity of its toxic effects.

1.4.1 Structure and function of the skin

The most obvious function of the skin is to provide a protective barrier between the body and the environment. The skin prevents the penetration of micro-organisms and harmful destructive chemicals, absorbs radiation from the sun and prevents loss of fluids. The immunological functions of the skin depend both on cells in the epidermis and on the dermal cellular constituents. The skin contains several types of sensory receptor, which detect incoming stimuli of touch, pain, vibration, pressure, warmth, cold and itch. Because of its extensive vasculature the skin is also important for the regulation of body temperature and is involved in elimination and excretion of xenobiotics.

The human skin consists of three anatomical layers **(Figure 1.4)**:

The epidermis is a multilayer structure consisting of two main parts: the stratum corneum and the viable epidermis. The most superficial layer of the epidermis is the stratum corneum, which consists of eight to sixteen layers of flattened, stratified and fully keratinised dead cells. The stratum corneum contains about 15 % water, 70 % protein and 15 % lipid, when it becomes hydrated it can contain up to 75 % water. The epidermal barrier is localised to the stratum corneum. The barrier depends on both the cornified material of the keratinocytes and the intercellular material, particularly lipids (Elias, 1983). Regional differences in permeability and drug absorption are related to the lipid content and not to the thickness of the stratum corneum (Rook, Wilkinson & Ebling, 1998). The three principal layers of the viable epidermis are the stratum basale, stratum

spinosum and the stratum granulosom. The basal cells of the stratum basale form the epidermal border of the dermo-epidermal junction and adhere to the dermis by cytoplasmic intercellular bridges. The increased interface surface caused by the papillae structure of the junction interface facilitates the diffusion of nutrients from the dermis into the epidermis. The junction does not provide any significant barrier function even for large macromolecules. The stratum basale additionally contains melanocytes, responsible for pigmentation, Langerhans cells involved in immune response and Merkel cells associated with sensory reception (Stenn *et al.*, 1986; Rook, Wilkinson & Ebling, 1998).

The dermis ranges from 2–3 mm thick and in man constitutes between 15-20 % of total body weight. The dermis consists of a matrix of loose connective tissue composed of fibrous protein, filamentous and amorphous connective tissue. The principal cell constituents of the dermis are fibroblasts, however macrophages and mast cells are also present. Nerves, blood vessels and skin appendages are also located in the dermis.

The hypodermis is composed of loose fibrous connective tissue, which contains fat and elastic fibres. The base of the hair follicles is present in this layer, together with the secretory portion of the sweat glands, cutaneous nerves and blood and lymph networks. It has been suggested that if the drug reaches this layer it has entered the systemic circulation, however the fat deposits may serve as a deep compartment for the drug (Washington & Washington, 1989).

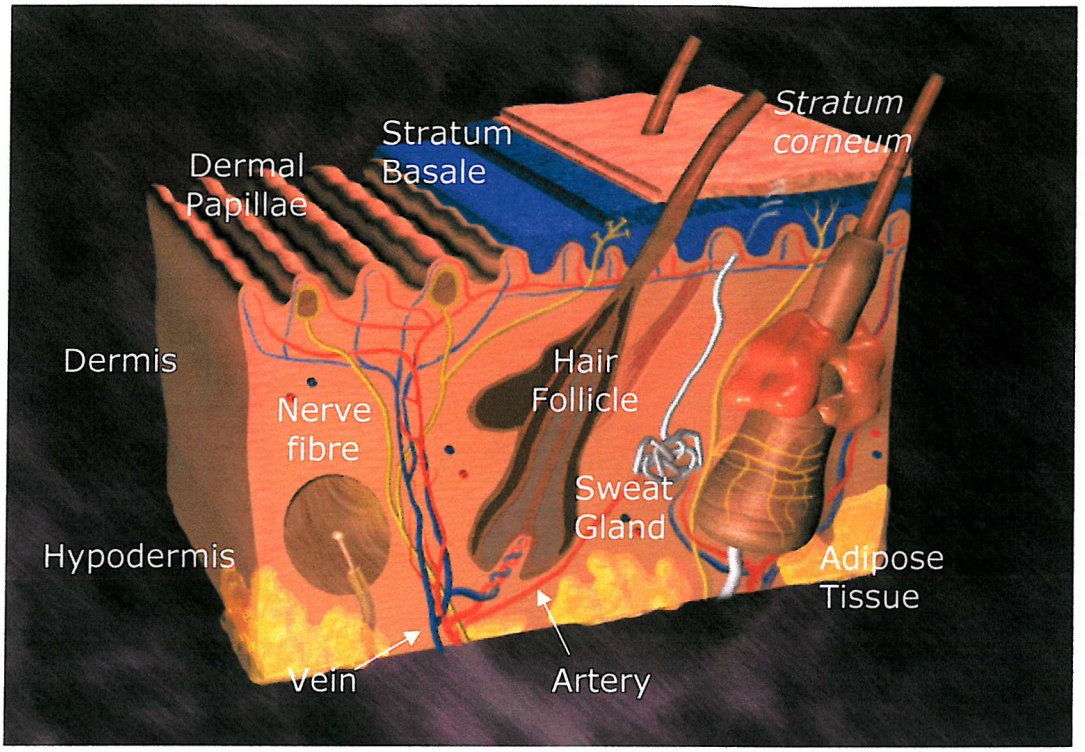

Figure 1.4 Anatomy of the skin (BodyWorks 6.0, CD Rom, Medical Library). The above figure illustrates the different layers that compose the human skin along with the main functional constituents that are located within the different layers.

The functional constituents of the skin:

The skin appendages penetrate the epidermis and the stratum corneum. These, epidermis–derived, structures consist of the hair follicles, sebaceous glands and sweat glands. The extent of hair growth plays an important role in the penetration and absorption of xenobiotics through the skin. The sebaceous glands vary in size from between 0.2–2 mm in diameter and are found in the upper hair follicle. The absence of stratum corneum from the structure of the glands potentially introduces a cutaneous entrance for drugs with low stratum corneum permeability. The lipids maintain a pH of about 5 on the skin surface and can cause problems for the adhesives in transdermal delivery systems.

Nerve fibres in the skin conduct the sensations of touch, pain, warmth, cold and itch. Nerve endings either exist freely in the skin or are encapsulated as specialised sensory receptors, such as Meissner's or Pacinian corpuscles. The neural supply of free nerve endings in the skin is mainly located in the dermis but a small amount of nerve endings penetrate the basal membrane and enter the epidermis (Reilly *et al.*, 1997). The sensory nerves are myelinated (Aδ–fibres) or non–myelinated (C–fibres), but as they run peripherally an increasing number lack myelin sheaths (Reilly *et al.*, 1997; Rook, Wilkinson & Ebling, 1998). Nerve fibres are found in close association with blood vessels in the skin, hair follicles, sweat glands and other dermal components, particularly mast cells. It is also possible that there are functional interactions between the nerve fibres and epidermal cell types such as Langerhans cells and melanocytes (Misery, 1997; Asahina *et al.*, 1995). Orthodromic stimulation of afferent C–fibres leads to local neurogenic inflammatory response via the release of neuropeptides and the subsequent interaction with mast cells and the vasculature (Foreman, 1988; Eady, 1993; Ansel *et al.*, 1997).

The cutaneous microvasculature plays an important role in thermoregulation and nutrition of the skin as well as in the clearance of small diffusible molecules from the dermis (Riviere and Williams, 1992; Singh and Roberts, 1994). Thus it may be speculated that agents that affect cutaneous blood flow will also influence their own distribution within the tissue space. A deep plexus of arteries and veins is found in the subcutaneous tissue and this sends out branches to the hair follicles and various glands. A second vascular plexus is located on the sub–papillary region of the dermis. From this plexus, small branches are sent towards the surface layers of the skin (Braverman, 1997). The

capillaries do not enter the epidermis, but they come within 150 and 200 μm from the outer surface of the skin. The capillary wall consists essentially of a single layer of endothelial cells that possess an inherent tone that contributes to the control of blood flow. The muscle of the smallest arterioles has a tone of its own that is responsible for the periodic opening and closing of pre-capillary sphincter. Both the activity of the muscle and the endothelial tone are influenced by nervous stimuli and to a large part by local chemical changes–autoregulation. Hence xenobiotics that are able to induce a neurogenic response and/or local chemical changes (e.g. elevation of nitric oxide (NO)) will alter the cutaneous perfusion.

1.4.2 Percutaneous absorption of malathion

The skin is an important route for the absorption of malathion. There have been many attempts to model the kinetics of transdermal absorption and to measure the rates of penetration of a wide range of OP's both *in vitro* in isolated skin preparations and *in vivo* in animal models and in man.

***In vitro* studies:** *In vitro* experiments using whole skin epidermis and dermis have been valuable for studying the mechanisms of percutaneous absorption of malathion and other OP's. The *in vitro* percutaneous absorption of malathion from aqueous ethanol solution was estimated at 8.77 % of applied dose (Wester *et al.*, 1996). *In vitro* studies using different OP's revealed a 1.35 % absorption of applied dose of methyl-parathion dissolved in an acetone vehicle versus a 5.20 % absorption of applied dose of methyl-parathion in the form of commercial formulation (Sartorelli *et al.*, 1997). However, a principal assumption made in these studies is that living processes such as an intact microcirculation and tissue metabolism have little or no effect on the mechanisms and/or kinetics of the percutaneous absorption of OP's.

An alternative *in vitro* technique developed for examining the percutaneous absorption processes in intact living skin is the isolated perfused porcine skin flap (IPPSF). The presence of a functional microcirculation and viable epidermis and dermis in the IPPSF allows more realistic studies of percutaneous absorption. Topical administration of ^{14}C-labelled malathion and parathion resulted in radiolabel recovery of 94.6 % and 93.4 % of applied dose respectively (Carver *et al.*, 1989). More recent studies revealed that malathion tends to be retained in the skin and subcutaneous fat (34.19 % of applied dose)

compared to 0.23 % of applied dose found in the vascular space (Chang *et al.*, 1994).

***In vivo* studies in animals:** The percutaneous absorption of malathion and other OP's has been studied in various *in vivo* models, however only limited data exist regarding the capacity of these models to predict skin penetration in man. Studies with the weanling pig revealed that 5 % of the radiolabelled malathion dose remained in the skin and 1 % in the subcutaneous fat. In the same studies the total radioactivity recovery for malathion in the hairless dog was estimated as 94 % of the applied dose whereas in the human skin grafted to athymic nude mouse was 95 % of the applied dose (Reifenrath *et al.*, 1984).

***In vivo* studies in man:** Percutaneous absorption of topically applied malathion in man, as measured by total excretion in the urine after 120 h application on the ventral forearm, was found to be 8.2 % of the applied dose whereas for other OP's such as parathion, ethion, and guthion was 9.7 %, 3.3 %, and 15.9 % of topical application respectively (Feldmann & Maibach, 1974). The percutaneous absorption of a single dose malathion application in a more recent study was 4.5 % of the applied dose. Repeated application of malathion did not change the percutaneous absorption of the initial day, and an average of 3.5 % of the applied dose was absorbed (Wester *et al.*, 1983).

Thus data concerning the rate at which malathion is absorbed into the dermis are inconclusive originating as they do from indirect measurements of OP's in urine and blood samples. Furthermore, the physiological factors that influence the disposition of topically applied malathion within the dermis and its subsequent systemic distribution, such as tissue composition, tissue metabolism and cutaneous perfusion, which can only be determined *in vivo* in preparations where a viable dermis and dermal microcirculation are present, have been explored only in part due to the lack of temporal and spatial experimental techniques.

Several studies have demonstrated that clearance of small diffusible molecules from the dermis is highly dependent upon local blood flow (Riviere & Williams, 1992; Singh & Roberts, 1994). Thus it is hypothesised that agents that affect cutaneous blood flow will influence their own systemic distribution. The aim of the present study was to measure the rate of percutaneous absorption of malathion in human skin *in vivo* and to explore the relationship between tissue levels of malathion and changes in local skin blood flow.

1.5 Factors that affect the percutaneous absorption and tissue distribution of topically applied malathion and other OP's.

The percutaneous absorption of malathion and other OP's is determined by various factors including the site of application, the nature of the OP and the properties of the barrier. Thus factors that may disrupt the skin barrier will enhance the penetration of OP's through the skin and may also affect its distribution in the tissue. Once the topically applied OP enters the dermis its distribution within the tissue space depends on the ability of the OP to diffuse into underlying tissues bypassing the dermal blood supply as well as on the dermal microcirculation. Therefore, factors that may affect cutaneous perfusion will also affect their distribution within the tissue space and subsequently their systemic uptake.

1.5.1 The formulant, barrier properties and site of application

The factors that have been shown to influence the absorption of malathion following topical application include the treatment regimen, the formulant, occlusion and the skin site of application. Repeat treatments and hot baths before treatments, which reduce the barrier and cause increase in local skin blood flow, are also factors that will favour the systemic absorption of malathion after topical application. Enhanced absorption and toxicity have been reported for some OP formulations in organic solvents, compared with the pure compound or an aqueous preparation (Baynes & Riviere, 1998; Committee on Toxicity of Chemicals in Food, 1999). This is because organic formulations facilitate the diffusion of the OP through the lipid layer of the skin and may therefore augment its systemic distribution. Qiao & Riviere demonstrated *in vivo* in swine that occlusion, which prevents evaporation of the OP from the site of application, enhanced the penetration and metabolism of [ring–U–^{14}C] parathion resulting in increased percutaneous absorption and urinary excretion of total ^{14}C. However in this study, it wasn't possible to distinguish differences in ^{14}C percutaneous absorption between sites of application, because of the differences in transport from the epidermis into blood, in local tissue distribution and in the cutaneous metabolism. Systemic bioavailability though for parathion was higher from the back than from the abdomen (Qiao & Riviere, 1995). Absorption of malathion and parathion applied at different anatomical sites was also studied in man and found to be much higher from hairy skin like the scrotum and scalp than from other skin areas (**Table 1.3**).

REGION OF APPLICATION	% PARATHION ABSORBED IN 5 DAYS	% MALATHION ABSORBED IN 5 DAYS
Forearm	8.6	6.8
Palm	11.8	5.8
Abdomen	18.5	9.4
Hand, Dorsum	21	12.5
Scalp	32.2	
Scrotum	101.1	
Forehead	36.3	

Table 1.3 Summarises the effects of anatomical site on the percutaneous absorption of malathion and parathion (from Ballantyne *et al.*, 1992)**:** The percutaneous absorption of malathion and parathion applied at different anatomical sites was studied in man and found to be higher in hairy skin like the scrotum and scalp than in other skin areas. These data are delivered from analysis of plasma and urinary excretion and/or metabolic profiles as well as from tissue biopsies and sampling of suction blister fluid.

1.5.2 The cutaneous blood flow

Cutaneous blood flow is regulated by neural, endothelial, and humoral factors. The interaction between these mechanisms of blood flow is poorly defined (Joyner & Halliwill, 2000). Neural control is exerted in part by changes in the level of sympathetic vasoconstrictor nerve activity to the skin. Such nerves release noradrenaline when activated to induce vasoconstriction via α-adrenergic receptors (Pérgola *et al.*, 1993; Morris, 1999). Cutaneous vasodilatation occurs partly due to withdrawal of sympathetic vasoconstrictor tone and partly through the activation of an active vasodilator system (Johnson *et al.*, 1995; Joyner & Dietz, 1997). However, both the nerves involved and the substances that mediate the active vasodilatation are poorly understood. It has been suggested that sympathetic cholinergic nerves in the skin or a substance released from the sweat glands (e.g. ACh or bradykinin) following activation of the glands from the sympathetic nerves may cause vasodilatation. However, more recent studies argue against this idea and demonstrate that the neural pathway that mediates active cutaneous vasodilatation does not operate via muscarinic cholinergic receptors (Kellogg *et al.*, 1995; Shastry *et al.*, 2000). The best evidence suggests that an unknown substance is co-released from cholinergic nerves and is responsible for active cutaneous vasodilatation. Although the nature of this substance still remains to be elucidated, vasodilator peptides (CGRP, substance P) are possible candidates and may be released from sensory and possibly cholinergic nerves to cause cutaneous active vasodilatation (Joyner & Halliwill, 2000). Local vascular resistance and hence perfusion is also determined by the inherent tone of the smooth muscle cells of the small arteries and is affected by various vasoactive substances that are released from in response to different stimuli from the endothelium.

1.5.2a Factors that affect cutaneous perfusion: Activation of the endothelial cells, which surround the blood vessel wall may result from a number of factors such as the action of xenobiotics, disease and the environment (mainly temperature) and may lead to local or neurogenically mediated changes in cutaneous perfusion. Activation of the endothelial cells will cause the release of vasoactive substances with subsequent activation of a variety of cells such as mast cells, smooth muscle cells, keratinocytes and nerves as well as blood cells, lymphocytes and neutrophils. Consequently both adhesion molecules, for example integrins, E–selectin and ICAM–1, as well as various soluble products such as nitric oxide (NO), eicosanoids and leukotrienes are released from the active endothelium and result in changes in the cutaneous perfusion and permeability along with further

cellular recruitment and vascular remodelling. The present study investigates the effects of malathion on the cutaneous microcirculation via its inhibition of acetylcholinesterase activity and the subsequent increase in the tissue levels of ACh. Xenobiotics such as malathion that may result in the local increase in the levels of vasoactive mediators (e.g. ACh) and/or a neurogenically mediated response will alter local perfusion and may therefore affect their own disposition within the dermis and their subsequent systemic distribution. In addition increased levels of ACh in the tissue may result in the release of secondary mediators capable of producing an increase in cutaneous blood flow and/or neurogenic inflammation and may therefore potentiate the systemic distribution of malathion. The next few paragraphs will therefore focus on the effects of ACh on skin blood flow and the possible mechanisms underlying the ACh induced cutaneous responses.

1.5.2b Possible mechanisms underlying the cutaneous vasodilatation induced by ACh: Acetylcholine mediated increases in local skin blood flow have been demonstrated extensively both in animal models and in man. Animal studies where ACh was applied in blister bases showed that the vasodilator response to ACh comprises two parts **(i)** a local effect probably mediated via the generation of NO and/or other vasodilators that are released following direct stimulation of the microvascular endothelium and **(ii)** a neurogenic effect mediated through an excitatory action on peripheral nociceptive fibres with release of a sensory transmitter(s), which cause vasodilatation independently of NO (Ralevic *et al.*, 1992).

i) ACh induced local cutaneous vasodilatation: ACh-induced vasodilatation is probably mediated through the activation of muscarinic receptors found on endothelial cells and/or other non-neuronal cells. Muscarinic receptors predominantly of the M_1, M_3 and M_5 subtype activate phospholipase-C and can therefore result in the mobilisation of intracellular calcium and the release of NO that in turn will lead to an increase of cGMP in the smooth muscle and subsequent cutaneous relaxation **(see also section 1.2.2)**. Activation of phospholipase-C will also result in the production of prostaglandins and subsequent increase in the levels of cAMP **(Figure 1.5)**. The intracellular effects of cAMP involve activation of protein kinase A family, which causes smooth muscle relaxation by reducing intracellular calcium ions. Muscarinic receptors of the M_2 and M_4 subtypes are unlikely to be involved in the ACh evoked dilatation as these subtypes are coupled to an

inhibitory G-protein (G_i) and therefore activation of these receptors will result in the inhibition of cAMP formation.

Several studies have investigated the role of these mediators in the cutaneous vascular responses to ACh. Morris & Shore have demonstrated that inhibition of prostaglandin production by aspirin did not alter the increase in forearm skin blood flow stimulated by iontophoretically delivered ACh in healthy volunteers (Morris & Shore, 1996). Conversely other studies have suggested that the vasodilator response to iontophoretically delivered ACh may be in part or wholly mediated by prostaglandins (Khan *et al.*, 1997; Noon *et al.*, 1998). The dose-dependent increase in forearm skin blood flow to intradermal injection of ACh is also partially inhibited by the nitric oxide synthase inhibitor L-NMMA. These data suggest that both NO release and a possible involvement of prostaglandins mediate the local vasodilatation caused after ACh (Warren, 1994; Warren *et al.*, 1994).

More recent studies in isolated hamster arterioles as well as in conscious animals using intravital microscopy of hamster muscle suggest that the ACh–induced dilatation is predominantly mediated by a factor different from NO and prostaglandins, presumably an endothelium-derived hyperpolarizing factors (EDHF) (Bolz *et al.*, 1999; de Wit *et al.*, 1999). The chemical nature of EDHF is still unknown, but data support the possibility that EDHF is a product of the cytochrome P-450 pathway (de Wit *et al.*, 1999). EDHF has been demonstrated to activate potassium channels in vascular smooth muscle cells and to be active predominantly in the microcirculation (Hwa *et al.*, 1994). *In vitro* studies in hamster isolated arterioles demonstrate that mechanisms that induce vasodilatation to ACh depend on the duration of the stimulus. With brief stimuli and in the early phase of a sustained stimulus, NO–independent mechanisms appear to dominate both local and conducted responses. During the later phase of the response to a sustained stimulus a contribution of NO becomes apparent (Doyle & Duling, 1997).

ii) ACh induced stimulation of peripheral nerves: The neurogenic response to ACh is characterised by a widespread vasodilator (flare) response accompanied by sensation. These effects are probably mediated by a direct action of ACh on non–myelinated C–fibres as demonstrated in saphenous nerve (Douglas & Ritchie, 1960) and cutaneous afferent nerves of the cat (Fjallbrandt & Iggo, 1961). In man iontophoresed ACh can

stimulate peripheral nociceptive C–fibres to produce flare which is abolished by anaesthetic and is absent in denervated skin (Westerman *et al.*, 1987; Benarroch & Low, 1991; Morris & Shore, 1996). These nociceptive effects of ACh result from stimulation of nicotinic receptors present on perivascular nerve endings (Juan, 1982). More recent studies in man have demonstrated the flare response to ACh to be inhibited by hexamethonium, a specific antagonist of nicotinic receptors and are therefore consistent with the mediation of the response by nicotinic receptors found in nociceptive axon terminals (Benarroch & Low, 1991).

It is possible that the neurogenic effects of ACh (flare response and sensation) are a product of secondary mediators released in response to ACh stimulation and not due to direct action of ACh on the cholinergic receptors in nerve endings. For example NO in addition to its direct effects on the vascular smooth muscle can act as a "hormone" and may initiate the release of other vasoactive substances such as calcitonin gene related peptide (CGRP) from afferent nerve fibres (Holzer *et al.*, 1995). Prostaglandins released in response to ACh are known to sensitise nociceptive nerve endings and may therefore play a role in neurogenic inflammation. It has also been suggested that histamine, which can be released in response to stimulation of cholinergic receptors found on mast cells or by the action of neuropeptides such as substance P on mast cells may play a role in the neurogenic response to ACh (Rodger & Xiong, 1997a). This suggestion is supported by a recent study in humans in which the ACh-induced flare response was blocked by antihistamines (Cavanah *et al.*, 1991).

In conclusion cutaneous perfusion is a major factor that influences the disposition of topically applied substances within the dermis and their subsequent systemic distribution. Application of malathion on the skin may result in the inhibition of AChE and the increase of ACh in the tissue with subsequent vascular relaxation and increase in blood flow. The increase in cutaneous perfusion induced by ACh can be either a localised or a neurogenically mediated response, mediated via the stimulation of cholinergic receptors found in non-neuronal cells as well as on nerve endings in the skin. Several studies have demonstrated that endothelial cell-derived mediators such as NO, PG's and EDHF as well as mast cell derived histamine may be involved in the ACh-induced cutaneous vascular relaxation.

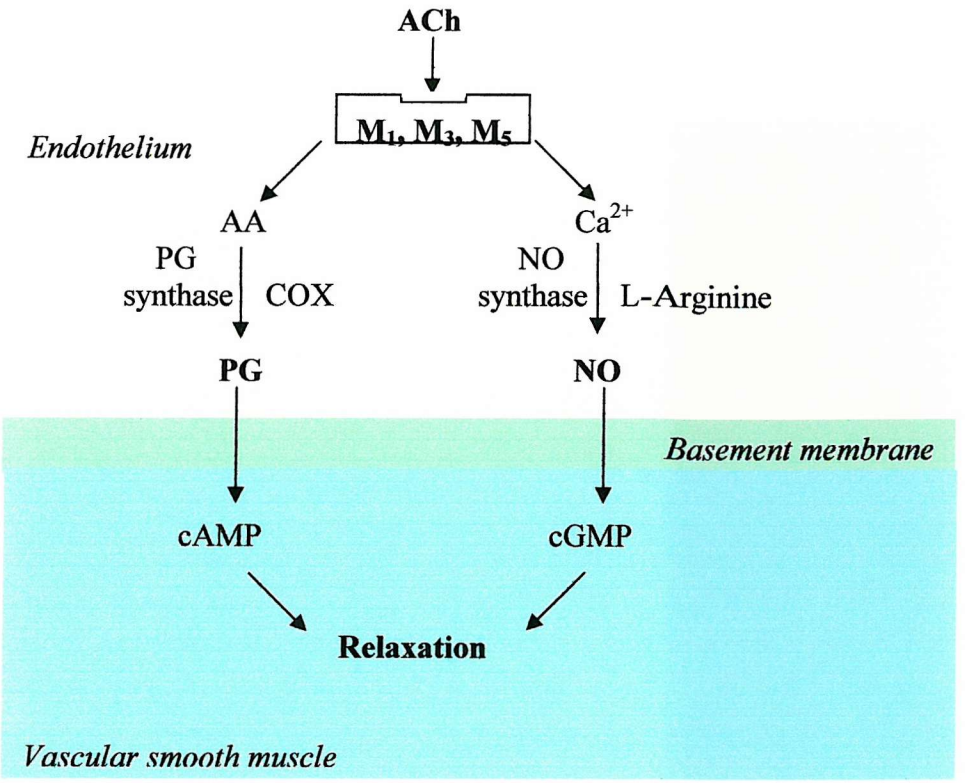

Figure 1.5 Potential mechanisms underlying the ACh-induced cutaneous relaxation. Stimulation of the M_1, M_3 and M_5 receptor subtypes by ACh results in the formation and release of nitric oxide (NO) and prostaglandins (PG). NO is formed after activation of nitric oxide synthase (NOS) by Ca^{2+} and calmodulin and in turn stimulates guanylyl cyclase to increase cGMP in the vascular smooth muscle with subsequent relaxation. Prostaglandins (PG) are formed from arachidonic acid (AA) by the action of cyclooxygenase (COX) and PG-synthase in the endothelium and elicit relaxation of the adjacent vascular smooth muscle via increase of cAMP

1.6 Experimental Techniques

Because of its relative accessibility a large number of techniques have been developed to study blood flow in the skin. The best are relatively a-traumatic and allow the study of skin physiology without significant perturbation of the normal function.

1.6.1 Microdialysis in percutaneous drug absorption

In humans the absorption of topically applied drugs has traditionally been assessed by kinetic analysis of plasma, urinary excretion and/or metabolic profiles (Schaefer and Redelmeir, 1996). Tissue biopsies and sampling of suction blister fluid have also been used to assess local drug concentrations (Averbeck *et al.*, 1989; Benfeld *et al.*, 1999). However these techniques yield information at only a single time point after topical drug exposure and are relatively traumatic. Cutaneous microdialysis has found important applications in the area of drug distribution and metabolism, as it enables continuous assessment of cutaneous drug delivery in the target tissue. Microdialysis is considered ideal for the present study as it allows repeat sampling of the tissue fluid during topical application of malathion to healthy human skin *in vivo.* In addition, microdialysis can be used to manipulate local blood flow by delivering vasoactive substances in the tissue space via the microdialysis probe. Thus a relationship between the changes in local vascular perfusion and the rate of the percutaneous absorption of malathion can be established.

Bito and colleagues were the first to implant dialysis sacs into the subcutaneous tissue of the neck and the parenchyma of the cerebral hemispheres of dogs to estimate the average concentration of amino acids in those tissues (Bito *et al.*, 1966; Kehr, 1993). The kinetics of paracetamol (oral dose) and theophylline (i.v. infusion) were measured in two different studies following single dose administration, in dialysates from subcutaneous tissue and muscle, saliva samples as well as cantharides induced skin blisters and compared to plasma concentrations. In both studies measurements in saliva overestimated the corresponding serum concentrations whereas results for both theophylline and paracetamol obtained using microdialysis correlated well to the calculated free plasma levels. Although data from skin blisters were closely related to the calculated serum concentrations for paracetamol, blister measurements for theophylline overestimated free plasma concentrations even more than saliva measurements (Brunner *et al.*, 1998; Müller *et al.*, 1998). Thus microdialysis yields to more accurate results in comparison to skin blisters and/or saliva measurements.

Measurements of endogenous compounds: Anderson *et al.*, and Petersen *et al.*, were the first to use microdialysis in human skin in 1992. They used different types of probes to measure endogenous histamine and glucose levels respectively in the forearm of healthy volunteers *in vivo* (Anderson *et al.*, 1992; Petersen *et al.*, 1992). Since then many studies have used microdialysis in human skin to measure different metabolites such as NO (Clough *et al.*, 1998a) histamine release (Petersen & Skov, 1995; Horsmanheimo *et al.*, 1996; Petersen *et al.*, 1996; Church, 1997; Petersen, 1997) and lactate (Jansson *et al.*, 1996). Currently microdialysis is the only technique that allows direct sampling of compounds within the dermis.

Measurements of exogenous compounds: The ability of this technique to continuously monitor drug concentrations *in vivo* was first demonstrated using 5–fluorouracil (5–FU). The dermal concentration of 5–FU following topical application to rat skin was approximately 40–fold higher than that in excised skin *in vitro* emphasising the effect of cutaneous blood flow (Ault *et al.*, 1994). Transdermal delivery of nicotine was studied in healthy volunteers, *in vivo* using microdialysis probes implanted intradermally in the thigh. After application of the nicotine patch above the microdialysis probes it was possible to monitor the time–course of nicotine concentration in human skin (Hegemann *et al.*, 1995). In a more recent study penetration of salicylic acid, topically applied on the volar surface of the forearm, was assessed using microdialysis in normal skin and skin in which the epidermis has been perturbed (Benfeldt *et al.*, 1999). These investigators were able to demonstrate a significant correlation between the extent of barrier perturbation and *in vivo* penetration of salicylic acid (Benfeldt *et al.*, 1999).

Delivery of substances in the tissue: Microdialysis has also been used to deliver substances within the tissue space. These include drugs such as theophylline, milrinone, and compound 48/80 delivered locally to the interstitial space of skeletal muscle and skin in healthy volunteers *in vivo* (Müller *et al.*, 1997). Responses of the target tissues to the drugs were assessed by means of changes in the levels of cAMP and histamine in the tissue measured by microdialysis. The results indicate that microdialysis can be used for the study of the effects of multiple drugs on the local release and degradation of mediator and metabolites *in vivo* in humans (Müller *et al.*, 1997).

1.6.1a Principles of microdialysis

Microdialysis sampling is accomplished by implanting a short length of thin hollow dialysis membrane at the site of interest, the dermis. This probe is perfused with a solution (perfusate), such as physiological saline and functionally resembles an artificial blood vessel in the skin. The basic principle of microdialysis is that of passive diffusion. If a concentration difference exists between the probe lumen and the surrounding tissue small hydrophilic molecules with a diameter smaller than that of the pores in the dialysis membrane, will diffuse across the membrane (Fick's law). Thus recovery or delivery of substances from and/or to the tissue is possible if the concentration of the compound is higher in the tissue than in the perfusate or higher in the perfusate than in the surrounding tissue respectively. The concentration of solute measured in the dialysate is thus a function of the actual tissue concentration. It has shown to be related to the flow rate and the size of the molecule. The fraction of the substance, which is collected in the dialysate, relative to the actual extracellular tissue concentration of unbound substance is termed relative recovery (RR) and is needed for quantitative measurements with microdialysis **(see Equation 1.1)**.

Several methods have been used to assess the relative recovery in microdialysis experiments in order to quantify the absolute concentration of a substance at a target tissue (Benveniste & Hüttemeier, 1990). While the *in vitro* recovery of a probe can be very easily estimated using solutions of known concentration in the external medium (C_{bath}) and measuring the resulting concentration in the dialysate ($C_{dialysate}$), it is not possible to directly determine recovery *in vivo* because the extracellular tissue concentration is not known.

$$RR = \frac{C_{perfusate} - C_{dialysate}}{C_{bath} - C_{perfusate}} \qquad \textbf{Equation 1.1}$$

In vitro recovery may not be a reliable indicator for the *in vivo* recovery because of factors in biological tissues that affect the diffusion of the analyte from the extracellular tissue to the probe and vice versa (Benveniste & Hüttemeier, 1990). However it provides a good indication for the ability of the microdialysis probes to sample the substance of interest at a constant rate.

Several approaches to the calibration of microdialysis probes *in vivo* have been described in order to avoid the error introduced by *in vitro* calibration. These methods are of great importance in studies if microdialysis is used to quantify the absolute concentration of the substance of interest in the tissue space. In this study, however, microdialysis was used to explore relative changes in the concentration of malathion in the dialysate samples under different skin blood flow conditions. Hence the methods for calibrating microdialysis probes *in vivo* are not going to be described in detail here. However the factors that could influence the recovery of malathion are of great importance and need to be considered to ensure constant sampling of malathion throughout the experimental procedure and are therefore described below.

1.6.1b: Factors that affect the efficiency of dialysis

The ability to dialyse a particular substance (i.e. recover it from or deliver it to the tissue) will therefore be determined by the physicochemical properties of the solute **(1)** & **(2)**, including its size and charge and by the nature of the dialysis membrane **(3)** (its composition, pore area and pore dimensions i.e. molecular mass cut off) across which it is diffusing. The concentration gradient of the solute across the membrane will be determined by the concentration of the solute in perfusate and that in the tissue. The latter will in turn be governed by the rate of removal of the solute in the dialysate **(4)** and its clearance from the tissue space by tissue-related factors such as local blood flow and metabolism **(5)**.

(1) Molecular weight: The relative recovery is inversely proportional to the molecular weight of the substance studied, with smaller molecules diffusing through the membrane much easier than large molecules. This could be explained if one considers that the diffusion coefficient is very low for substances with high molecular weight (Benveniste & Hüttemeier, 1990).

(2) Lipophilicity, electrical charge and the ability of the analyte to bind to proteins will affect the recovery of the compound in the dialysate.

(3) Nature of dialysis membrane: Recovery is directly proportional to temperature and the size of the dialysis membrane area and can also be affected by the dialysis membrane materials that are known to interact with transported substances (Hsiao *et al.*, 1990).

(4) Flow Rate: The recovery of a microdialysis probe increases when perfusion flow rates are kept low and changes with time. Initially recovery is high and then it decreases rapidly

although it never reaches a steady state. This has been attributed to a steep concentration gradient across the dialysis membrane when the probe is first inserted into the medium.

(5) Other factors: The tissue/medium where microdialysis measurements take place will also affect the recovery of the analyte. Factors such as blood flow in the tissue, tissue metabolism and the tortuosity factor (i.e. the interaction of the substances with cell membranes and other impermeable structures) can significantly alter the *in vivo* recovery.

Although mathematical models have been developed to describe the effects of these processes on the microdialysis measurements, the total impact and the influence of each individual factor are currently poorly explained and remain to be demonstrated *in vivo*.

1.6.1c Insertion trauma and limitations of microdialysis

Insertion Trauma: Microdialysis is a relatively non–invasive technique when compared to blood sampling and biopsies. However the insertion of the microdialysis probe usually via a guide needle, as in the present study, and the presence of the probe in the tissue could affect the local tissue status. As mentioned previously, changes in the environment around the microdialysis probe will affect the recovery and therefore the measurement of the substance in question. The effects of the microdialysis probe insertion may involve an increase in blood flow and erythema, wheal of the skin and histamine release. Insertion of the guide needle could also cause direct trauma to cells and tissue and initiate circulatory effects over a wider area by axon reflexes and other mechanisms. In a recent study it was demonstrated using laser Doppler perfusion imaging that increases in cutaneous circulation after probe insertion in humans centre around the point of insertion. These increases begin to subside at around 15 min after probe insertion and by 60 min the values are at near resting levels (Anderson *et al.*, 1994). Similar were the data obtained after insertion of microdialysis probes in hairless rats. In this study histamine release was also followed and found to increase after insertion of the probes. The increase in the levels of histamine declined to baseline 30 min after probe insertion (Anderson *et al.*, 1992; Petersen, 1997). Thus after implantation of the microdialysis probes and before any further experimental work a period of up to 1 h must be allowed for the insertion trauma to settle down and the tissue to recover.

Limitations: One of the limitations of microdialysis is that the volume of the dialysate is usually small and in aqueous phase. Thus very sensitive assays for the analysis of the

dialysates are required. Further method development is often essential for the preparation of the dialysate samples into a suitable solvent that can be used with ordinary assays such as gas chromatography and high performance liquid chromatography. Larger molecules can be sampled using membranes with larger pores, however this will also introduce extracellular proteins and other high molecular weight substances (e.g. enzymes) into the dialysate and additional preparations will be required for analysis of the samples. Very lipophilic drugs and heavily protein bound drugs are currently not very easily sampled by microdialysis. The aqueous nature of the perfusate is at the moment the major drawback for sampling of lipophilic drugs along with drug adherence to tubing and plastic vials. Addition of solvents, lipid emulsions or protein into the perfusate will enhance the recovery of lipophilic compounds although the tissue surrounding the microdialysis probe and its tolerance to the perfusate content should be considered.

1.6.2 Dermal drug delivery

Several methods may be used to deliver substances locally to the skin including microdialysis, topical application in the form of cream preparations and patches, topical intradermal injections and iontophoresis. Iontophoresis and local application of malathion in the form of an aqueous based gel together with microdialysis are the main methods used in the present study to deliver the substances of interest in the tissue and so will be considered in more detail below.

1.6.2a Iontophoresis: In one part of this study iontophoresis is used to deliver ACh to malathion and control treated sites to explore the mechanisms underlying the effects of malathion on the peripheral vasculature. This is mainly because iontophoresis can be easily combined with laser Doppler fluximetry that allows continuous measurements of blood flux during drug delivery. Furthermore iontophoresis does not involve the insertion of needles and is therefore less invasive than microdialysis leaving the skin surface intact for further experiments. Iontophoresis has been used clinically for delivering certain compounds to surface tissues for topical as well as systemic treatment. The applications of iontophoresis in the treatment or diagnosis of a variety of clinical conditions have been recently reviewed by Singh & Maibach (1994) and Costello & Jeske (1995). Therapeutic applications of iontophoresis include the local delivery of anti-inflammatory drugs in the treatment of painful rheumatic disease, pilocarpine sweat testing in the diagnosis of cystic fibrosis as well as other applications in ophthalmology and dentistry (Costello & Jeske, 1995).

In addition to its clinical uses iontophoresis is often used as a non-invasive delivery system to study the physiology of human skin. (Malger *et al.*, 1990; Morris & Shore, 1996; Noon *et al.*, 1998). Iontophoresis has been used to investigate the effects of exogenous vasoactive agents on cutaneous perfusion (Malger *et al.*, 1990; Morris & Shore, 1996; Noon *et al.*, 1998). As well as being used to deliver molecules to the skin a number of studies are now investigating the potential to use the technique to extract biologically important molecules from the cutaneous space, a process called reverse iontophoresis (Merino *et al.*, 1999). Amino acids, glucose and inflammatory mediators such as prostaglandin E_2 have been successfully monitored by reverse iontophoresis, both *in vitro* and *in vivo* in animal models and humans (Rao *et al.*, 1995; Mize *et al.*, 1997; Merino *et al.*, 1999). Iontophoresis can also be used in combination with dermal microdialysis to assess the pharmacokinetics of iontophoretically delivered drugs in the dermis and the release of endogenous mediators in response to external stimuli.

1.6.2b Principles of iontophoresis

The penetration of compounds across the skin is usually very slow due to its barrier properties. The rate of membrane penetration of drugs could be increased by means of an external energy source. The basic principle of iontophoresis is that an electrical potential difference will actively cause ions in solution to migrate according to their electrical charge **(Figure 1.6)**. The magnitude of an electrical charge (Q) is dependent on the length of time (t) a current (I) is passed through the skin ($Q = I \times t$). Hence by passing different amounts of current for different length of time is possible to construct dose-response curves for the substances of interest.

It has been suggested that the major route for iontophoretic transport is through sweat glands and hair follicles, although evidence exist for trans-epidermal transport (Singh & Maibach, 1994). Studies using pilocarpine and charged dyes demonstrate the opening of sweat glands during iontophoresis. Scanning electron microscopy has also been used to show that the iontophoretic transport of mercury chloride and ferric and ferrous ions occurs via sweat glands and hair follicles. Transport via a transepidermal pathway is supported from studies with Ni^{2+}, Na^{+} and Hg^{2+} ions, which can find their way between keratinised cells (Singh & Maibach, 1994). The evidence for the fate of the ions after iontophoretic delivery into the skin has been controversial. Several studies have proposed that the material delivered is removed by the subcutaneous circulation and distributed around the

body. However, other studies have demonstrated sufficient penetration of ions to produce deep cutaneous anaesthesia supporting the idea that after transport across the skin substances concentrate in the deeper tissues under the electrode (Costello & Jeske, 1995).

1.6.2c Factors that influence iontophoretic drug delivery

Some problems are associated with delivery of substances by iontophoresis. These include:

Iontophoresis of vehicle: Noon and colleagues showed that saline and tap water produced iontophoretic responses without addition of the drug. This was probably due to the release of vasoactive substances such as bradykinin and substance P after stimulation of nociceptive and thermal axon reflexes due to ions found in water and saline (Noon *et al.*, 1998). They therefore suggested the use of a 2 % methylcellulose gel, as a vehicle for the iontophoretic delivery of substances such as ACh and sodium nitroprusside. Two more studies have demonstrated non-specific vasodilator responses after iontophoresis of vehicle. Results from both studies suggest that there is a larger increase in skin microvascular blood perfusion at the cathodic site compared to the anodic site. The response is observed with high–resistance vehicles (e.g. deionised water) but not with low–resistance vehicles (for example 5 mol l^{-1} NaCl), possibly due to lower electrical potential over the skin (Morris & Shore, 1996; Asberg *et al.*, 1999).

Type of skin and cutaneous blood flow: Several studies have explored the effect of type of skin on the iontophoretic delivery of different substances. Results from these studies suggest that iontophoretic delivery may be independent of the type of skin and the site of application, although other factors such as age, race, thickness, degree of hydration and nature of the skin (normal or diseased) remain to be evaluated (Malger et al., 1990; Singh & Maibach, 1994). Dermal blood flux has, not unexpectedly, also been shown to affect transdermal iontophoresis (Singh & Maibach, 1994).

Taking these factors into account in the present study iontophoresis was used to deliver substances to the skin of the forearm of healthy volunteers. The iontophoresis chamber was placed on the volar surface of the forearm at acral sites. Deionised water was used as the vehicle and any non-specific vasodilator responses were quantified using laser Doppler fluximetry and scanning laser Doppler imaging. These responses were allowed for in further analysis of the results.

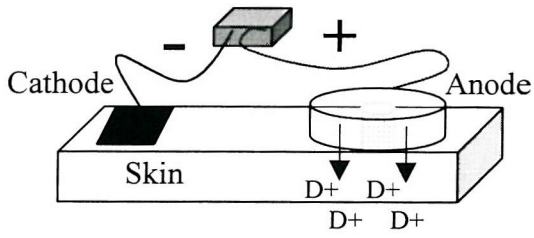

Figure 1.6 Iontophoresis applied for the delivery of drugs through the skin: The above figure illustrates a typical iontophoretic setup, used for the delivery of positive drug ions (D+) for example ACh. For the delivery of negatively charged ions (for example sodium nitroprusside) the electrode orientation is reversed.

1.6.3 Measurement of skin blood flow using Laser Doppler Imaging and Fluximetry

The present study considers both the effects of malathion on the microvasculature and the effects of changes in cutaneous blood flow on the absorption of malathion. In these experiments Scanning Laser Doppler Imaging (SLDI) and Laser Doppler Fluximetry (LDF) have been used to assess changes in cutaneous blood flow. They were chosen because they are non–invasive and have been shown to produce continuous and reproducible measurements of skin blood flux.

Previously superficial blood flow has been measured using plethysmography and calorimetry in skin or electromagnetic and ultra-sonic systems for evaluation of flow in exposed vessels. LDF has been widely used in clinical and research studies for cutaneous blood flow measurements, sometimes simultaneously with iontophoresis (Noon *et al.*, 1998). The technique provides continuous measurements of blood flux over any desired region of the skin and is specific to blood flow very near the surface of the skin (Saumet *et al.*, 1988). Studies comparing LDF with plethysmography and ^{133}Xenon clearance show a good correlation between the techniques (Johnson *et al.*, 1984). One of the major limitations of the LDF is that it consists of a static probe that provides information about blood flux over a very small area of tissue. Consequently a slight change in probe position often results in a substantially different reading on the instrument. Through the use of biopsies Braverman and others have demonstrated that the heterogeneity in normal skin perfusion measurements with LDF coincides with the anatomical microvascular segments (Braverman *et al.*, 1990; Rendell *et al.*, 1998).

The development of a high–resolution SLDI overcame the limitations of LDF by presenting tissue perfusion as an image rather than a single value recorded at one point only. With the help of a scanning mirror, the position of which is controlled by two stepping motors, the SLDI scans a low power laser beam in a raster pattern over the skin or other tissue surfaces. Because of its ability to scan larger areas, SLDI has been extensively used to map cutaneous vascular axon reflex responses induced after exposure to allergens or irritant stimuli in humans (Wårdell *et al.*, 1993a; Church & Clough, 1997; Clough *et al.*, 1998). In clinical practice it is applied in the assessment of psoriasis and burn depth as well as in the investigation of direct vascular damage that is caused after photodynamic treatment of non–melanoma skin tumours (Wang *et al.*, 1997).

1.6.3a Principles of SLDI and LDF

The techniques are based on the measurement of the Doppler frequency shift in monochromatic laser light, which is backscattered from moving red blood cells. In more detail, when a narrow monochromatic light beam illuminates a tissue surface, incident photons penetrate the tissue to a depth determined by its optical properties. In the presence of moving blood cells, the incident monochromatic light becomes distorted to a degree determined by the concentration and velocity of the moving red blood cells (Wårdell *et al.*, 1993). The reflected light from the static tissue and the frequency shifted light from moving blood is collected and mixed on a photodetector, and is then processed to produce indications of the flux, concentration and speed of the moving blood.

Both LDF and SLDI **(Figure 1.7 (A) and (B))** assess blood flux up to a depth of 1mm in the skin and are therefore accurate in monitoring both temporal and spatial changes in perfusion of the upper dermal plexus. Although the red helium/neon laser is the most commonly used laser source in LDF and SLDI, it is also possible to use the green and near infra–red laser to assess changes in tissue perfusion at different depths (Obeid *et al.*, 1988). There are a number of factors that will affect cutaneous blood flow. Hence LDF and SLDI measurements should be made under the same conditions of temperature, humidity and subject preparation. Movement between the probe and the tissue will also cause a Doppler shift and thus produce blood flux artefacts. In this study the position of the scanning probes for both the LDF and the SLDI were fixed to avoid any movement artefacts.

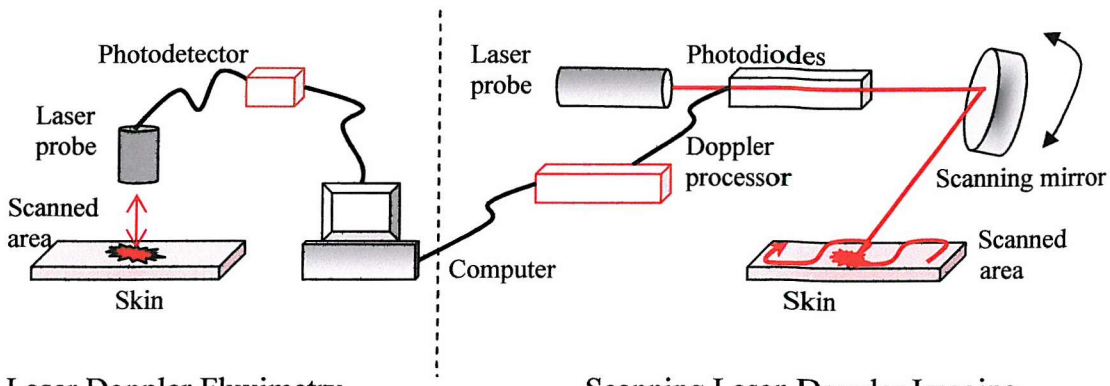

Figure 1.7 Application of Laser Doppler Fluximetry (LDF) (A) and Scanning Laser Doppler Imaging (SLDI) (B) in the measurement of cutaneous perfusion: The LDF probe in (A) is a stationary probe and provides measurements of blood flux over an area of few square millimeters. In contrast SLDI (B) with the aid of scanning mirrors allows measurements of blood flux over a larger area of tissue. Both techniques assess cutaneous blood flow up to 1 mm below the surface of the skin.

1.7 Aims and Objectives of the Study

The present study aims to assess the responses of the peripheral vasculature to a low-dose of malathion and elucidate the mechanisms underlying these responses. It is hypothesised that malathion if absorbed through the skin, will augment cutaneous perfusion via action on non-neuronal cells. The mechanisms underlying the effects of malathion on the skin vasculature will be the inhibition of AChE and the subsequent increase of ACh in the tissue. It is also hypothesised that changes in local skin blood flow will affect the levels of malathion in the tissue.

Thus the objectives of this study are:

(1) to measure the rate of percutaneous absorption of malathion in healthy volunteers *in vivo* and assess its effects on the cutaneous microvasculature.

(2) to establish a relationship between tissue levels of malathion and changes in local skin blood flow

(3) to investigate the role of acetycholinesterase and muscarinic receptors in the malathion-induced changes in vascular function.

To do this

(1) Dermal microdialysis was used to sample malathion within the tissue space during acute exposure of the skin to known doses of malathion. Dermal microdialysis has also been used to manipulate local blood flow by the delivery of vasoactive substances in the skin.

(2) Scanning laser Doppler imaging was used to quantify changes in skin blood flow and to relate tissue levels of malathion with the cutaneous vascular responses of the tissue

(3) Dermal iontophoresis was used to deliver vasoactive agonists and antagonists and in combination laser Doppler fluximetry to elucidate the possible mechanisms underlying the effects of malathion on the peripheral vasculature.

CHAPTER 2: GENERAL METHODS & VALIDATION

All *in vivo* experiments described in the present study were performed on the skin of the forearm in healthy human volunteers. Experimental procedures and general protocols used throughout this project are described in this chapter, along with the experiments performed to validate the techniques and explore their reproducibility. Materials and equipment used in the project are listed in Appendix 1 and specific modifications of protocols and/or techniques are described in further detail in the methods section of individual chapters.

2.1 Subjects

In total 70 volunteers, aged between 20 and 68 years participated in the present study. Of those 42 were females and 28 males. Some of the volunteers participated in more than one parts of this project. Informed written consent was obtained from all subjects and all studies were approved by the local ethics committee (LEC No: 301/98, 060/98, 137/01). Volunteers with dermatological problems, allergic disease, cardiovascular disorders or those on prescribed medication were excluded from the study. All subjects were asked to refrain from alcohol and caffeine 12 h prior to the study. On the study day subjects were acclimatised to 22-23 ^{o}C and experiments were performed with the subject lying in a supine position with their arms at heart level.

2.2 Drug preparation and application/delivery in the tissue

2.2.1 Malathion: Preparation, application and barrier perturbation

Preparation: Malathion 40 µl (99 % pure) was dissolved in 200 µl ethanol and then mixed with 5 g of aqueous based gel to give a concentration of 10 mg ml^{-1} malathion in the gel. The preparation was mixed for 5 min to ensure uniform spread of malathion in the gel. Saturation of the mixture was confirmed as the clear gel went cloudy after mixing with malathion in ethanol. The same procedure was followed to prepare a vehicle–control formulation, by adding 200 µl ethanol to 5 g of aqueous gel. The colour of the gel remained clear after the 5 min mixing period. The formulations were prepared immediately before each experiment. In experiments where commercial formulations containing malathion were to be tested they were used as prepared by the manufacturer.

Application: Different adhesive materials that could be used as drug wells to contain the formulations within a given area of the skin surface were tested at the beginning of this study. Comfeel® patches proved to be the most suitable as they caused minimum irritation when removed from the skin and the adhesive back prevented leakage of the drug.

Tegaderm® was used as the occlusive dressing of choice to cover the drug well and its contents. If subjects were sensitive to Tegaderm®, Comfeel® patches were used instead to occlude the drug well. At the end of each exposure time the drug wells were removed and the areas gently cleaned using damp cotton wool. They were then left for 10 min prior to measurement of blood flux.

Barrier perturbation: In some subjects the stratum corneum was removed prior to treatment by applying cellophane adhesive tape to the site and subsequently tearing it off ten times (Benfeldt *et al.*, 1999b). The sites were then left for 30 min before applying the formulations.

2.2.2 Vasoactive Drugs: Noradrenaline (NA), glyceryltrinitrite (GTN) and acetylcholine (ACh)

In experiments where the effects of skin blood flow on the absorption of malathion were to be investigated, local skin blood flow was manipulated using NA and GTN.

Noradrenaline (NA): NA was delivered in the skin via the microdialysis probes **(see section 2.3)** to reduce local skin blood flow. Levophed ampules (Levophed® Abbott Labs) (1 mg ml^{-1}) were used as the stock solution for NA, which was diluted to 0.005 mg ml^{-1} in sterile phosphate buffer solution (PBS) on the day of the experiment. NA was delivered to the tissue space via the microdialysis probes at 5 µl min^{-1} over the period of 5 h and 30 min and the total amount of NA delivered was 8.25 µg.

Glyceryltrinitrite (GTN): Where the effects of vasodilatation were to be investigated GTN was delivered in the skin either via the microdialysis probes or as a patch applied on the volar surface of the forearm. In studies where GTN was used as a patch (Transiderm-Nitro5 patches), it was applied to the skin 30 min before the start of the experiment and the period of exposure was no longer than 3 h. Over this time the total amount released was approximately 0.625 mg, well below the recommended daily dose (10 mg per day) for the treatment of angina. In studies where malathion was to be applied to the skin above the microdialysis probes and therefore precluding the application of a GTN patch, GTN was delivered in the tissue space via the microdialysis probe. Nitronal ambules (Nitronal® Lipha Pharmaceuticals Ltd) were used as stock solution (1 mg ml^{-1}), which was diluted down to 0.5 mg ml^{-1} in sterile PBS on the day of the experiment. GTN was delivered at 5 µl min^{-1} and the total amount delivered over the period of 5 h and 30 min was 0.825 mg.

Acetylcholine (ACh): ACh was used in two separate studies. In the first study ACh was delivered in the skin via iontophoresis. A solution of 20 mg ml^{-1} ACh was prepared in

distilled water on the day of the experiment, using acetylcholine chloride powder purchased from Sigma. In the second study ACh was delivered to the tissue space via the microdialysis probes. Acetylcholine chloride powder (0.182 g) were dissolved in 1 ml sterile PBS to give a 1 M stock solution of ACh. Test solutions of ACh ranging from 0.2 mM up to 50 mM were prepared in sterile PBS and delivered to the tissue at 5 μl min^{-1} for a period of 6 min. The total amount delivered using the highest dose (50 mM) may be estimated at a value of 40.5 μg.

2.3 Techniques used to recover and deliver substances from/to the tissue, to study the percutaneous absorption of malathion.

In the present study two techniques microdialysis and iontophoresis were used to deliver and/or recover vasoactive substances to the skin of the forearm. These well established techniques are considered ideal for this study as they are relatively a-traumatic and they can be easily combined with scanning laser Doppler imaging and fluximetry to allow simultaneous measurements of skin blood flow during drug delivery. In addition to microdialysis and iontophoresis, in one part of this study intradermal injections were used for the delivery of histamine in the tissue. The next few paragraphs describe the application of these techniques as used and the experiments performed to validate these techniques and explore their reproducibility.

2.3.1 Microdialysis: Manufacturing of probes, implantation and sampling

Microdialysis was used in the present study to sample the tissue space following application of malathion to the surface of the skin above the probe. Microdialysis was also used in some parts of this study to deliver vasoactive drugs such as noradrenaline (NA), glyceryltrinitrite (GTN) and acetylcholine (ACh) to the tissue, to study the effects of blood flow on the absorption of malathion through the skin and the mechanisms underlying the effects of malathion on cutaneous vasculature.

Manufacturing of the probes: Linear flow microdialysis probes were manufactured from Cuprophane membranes extracted from a renal dialysis capsule. The probe membrane had a 5 kDa molecular mass cut off, a wall thickness of 8 μm and an internal diameter of 200 μm. Part of the membranes was strengthened with an eight cm length of stainless steel wire (100 μm in diameter). Approximately 2 cm of the strengthened end of the microdialysis probe was then inserted in a length of Portex tubing (13 cm long, 0.28 mm internal diameter) leaving about 6 cm of strengthened membrane available to use during

the experiment. To ensure a firm connection the microdialysis membrane was glued into place in the Portex tubing using one drop of super glue. The probes were packaged in groups of 5 or 6 and sterilized in ethylene oxide.

Implantation of the probes: On the day of the experiment each probe was checked for leaks before insertion by perfusing the probe with sterile saline solution. A local anaesthetic cream (EMLA^{TM} cream 5 %, 25 mg g^{-1} Lignocaine and 25 mg g^{-1} Prilocaine) was applied at up to four different sites (2.5 g per site) on the volar surface of one forearm. The cream was applied for a period of 1.5 h maximum under occlusive dressing before the probe insertion. The cream was then gently removed using a damp cotton wool and the skin was dried gently. Probes were inserted into the dermis at the anaesthetised sites using a 23-gauge (30 mm long) guide needle. Two ink dots (20 or 25 mm apart) marked on the skin surface were used to indicate the point of insertion and the point of exit of the needle respectively. The needle was inserted horizontally between the two marks such that it was possible to see the colour of the needle under the surface of the skin. The probe was then threaded through the needle. The needle was then removed carefully, leaving 20-25 mm of membrane in the tissue and 40 mm membrane outside the tissue (outflow) **(Figure 2.1)**. A portion of this (20 mm) was cut before the start of the experiment. The position of the probe was then adjusted so that the junction between the membrane and the portex tube abated the skin to avoid evaporation or contamination of the dialysate.

The depth of the probes measured using ultrasonography was 0.58 ± 0.04 mm (mean ± sem, n = 40 probes in 15 subjects) below the skin surface **(see section 2.3.2 for details)**.

After insertion the microdialysis probes were covered using a sterile dressing held in place with a bandage to prevent dislocation or damage of the probes. A 2 h recovery period was allowed for the local anaesthetic to wear off and the insertion trauma to settle down (Anderson *et al.*, 1994; Clough *et al.*, 1998a). After removal of the dressing the free end of the Portex tubing was connected to the perfusion pump using a length (50 cm) of a sterile Portex tubing (0.58 mm internal diameter). The free end of the longer tubing was then inserted into a syringe adapter and connected to a 1 ml syringe mounted in a microinfusion pump (Univentor 801 syringe pump). The probes were then perfused at a rate of 5 µl min^{-1} with phosphate buffered saline solution (PBS) and/or saline solution containing a vasoactive drug.

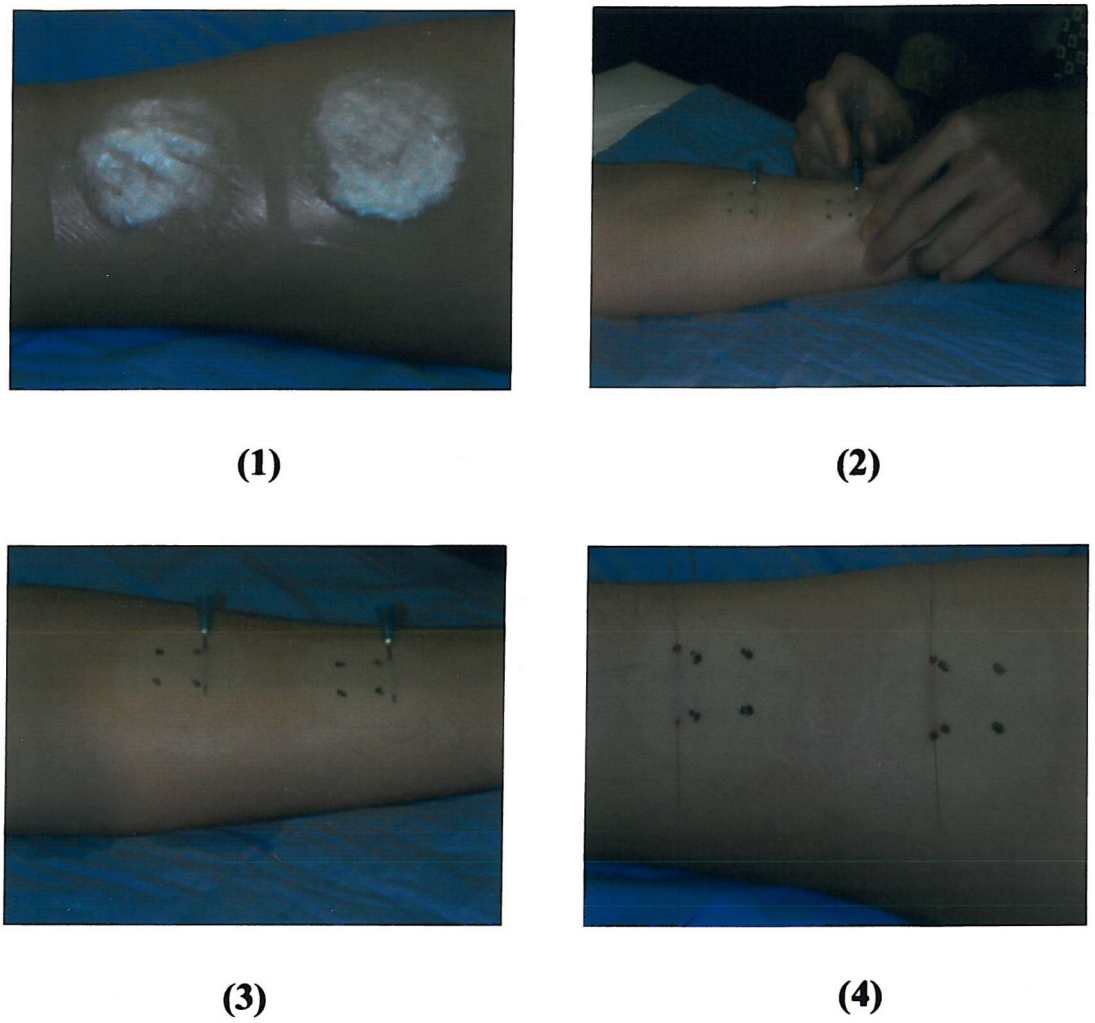

Figure 2.1 Implantation of microdialysis probes in human skin *in vivo*: Microdialysis probes were inserted under local anaesthetic in the skin of the volar surface of the forearm of healthy volunteers. The local anaesthetic cream was applied under occlusive dressing at up to 4 sites (2.5 g per site) on the forearm for a period of 1.5 hours **(1)**. The cream was then removed using a damp cotton wool and the sites were dried gently. Two black dots (20 mm or 25 mm) apart were marked on the skin surface to indicate the point of inlet and the point of outlet of the probe. A 23 gauge needle was inserted horizontally between the two marks such that it was possible to see the colour of the needle under the surface of the skin **(2)** and **(3)**. The probe was thread through the sharp end of the needle until the wire free end of the membrane reached the second black mark. The needle was then removed carefully, leaving the microdialysis probe in the tissue **(4)**. The length of each probe available for dialysis in the tissue was 20 or 25 mm depending on the study.

The "dead" space of the delivery tubing and the probe membrane was calculated using the equation: $\mathbf{V} = \pi \times \mathbf{r}^2 \times \mathbf{l}$, where **V** is the volume, π is a constant 3.14, **r** is the internal radius of the tubing and **l** is the length of the tube. The dead space from one end of the Portex tubing to the start of the membrane was approximately 6 µl and the dead space from one end of the microdialysis membrane to the other was 0.9 µl. In studies where the perfusate had to be changed (e.g. from PBS to ACh) a dead space volume of approximately 10 µl (approximately 2 min) was allowed before the first collection of the dialysate. Dialysate samples were collected into plastic vials (Eppendorfs, 500 µl) and stored at –20 °C for no more than fourteen days prior to assay. The collection periods of dialysates varied with the experiment performed.

The accuracy of the pumps to perfuse the microdialysis probes at a constant flow rate was assessed by collecting dialysate into weighed eppendorfs. The volume of dialysate was calculated assuming the density of the dialysate sample to be unity. The efficiency of the microinfusion pumps to deliver 150 µl over 30 min intervals at 5 µl min^{-1} was estimated as 99.8 ± 2 %.

2.3.2 Estimation of the depth of the microdialysis probes using ultrasonography

At the end of a number of microdialysis experiments the depth of the microdialysis probes and the distance between adjacent probes was measured using a 20 MHz Ultrasonograph (Dermascan C, Version 3). This operates under the basic principle that sound pulses are beamed into the skin and reflected at structural interfaces between or within the tissues, where fluctuations in either density or elasticity occur. Measurements of time, velocity and amplitude of each echo are converted into a spatial representation of the internal structure of the skin. The instrument operates at a frequency of 20 MHz and scans continuously in order to produce a cross-sectional image on the screen. The spatial resolution is about 60 µm axially and 360 µm laterally, sufficient to visualize macrocellular differences in the tissue. In this study during imaging subjects were sat with their arm resting on the arm of the chair. Contact gel was applied to the skin above the microdialysis probes to transduce the sound waves between the ultrasound probe and skin. The metal wire inserted into the microdialysis probes reflects the sound pulses beamed into the skin back to the ultrasound probe at a different density and elasticity that are then quantified and expressed in distance units (mm) **(Figure 2.2)**.

2.3.3 The efficiency of the microdialysis probes to recover malathion-*in vitro*

The *in vitro* recovery for malathion was assessed for a number of probes at intervals throughout this study to determine whether malathion could be recovered by microdialysis and to check for the reproducibility and uniformity of the probes. Although *in vivo* recovery can differ from *in vitro* recovery (Qiu *et al.*, 1996), the latter is a good indication that the type of probe used in this study was suitable for sampling of malathion. The dialysis efficiency of the 5kDa probes for malathion was estimated *in vitro* using the no-net flux method (Qiu *et al.*, 1996).

Experimental design: Dialysis probes were immersed in a bath (total volume 7 ml) containing 2.5 μg ml^{-1} malathion in PBS. Plastic petri dishes were used as containers for the bath solution. The probes were placed in the petri dishes through two small holes made using a needle at the two opposite sides of the petri dish. The holes were then sealed using super glue to prevent leakage of the bath solution. The length of the probe immersed in the bath solution available for dialysis was 30 mm. The probes were perfused at 5 μl min^{-1} with solutions containing malathion at concentrations of 0, 2.5 and 5 μg ml^{-1}, spanning the concentration in the bath (2.5 μg ml^{-1}). After a 30 min equilibration period two 30 min, 150 μl dialysates were collected for each perfusate concentration. Samples were taken from the bath and the perfusate solution at the beginning and the end of the experiment and assayed for malathion using gas chromatography.

The difference between the concentration of malathion in the dialysate (C_{dial}) and the perfusate (C_{perf}), (C_{dial}–C_{perf}) was plotted against the concentration of malathion in the perfusate (C_{perf}). The slope of the linear relationship is the fractional loss or gain of malathion from or into the bath and the intercept with the x–axis should represent the concentration in the bath **(Figure 2.3)**. The recovery of malathion, *in vitro*, was 51 ± 5 % (n= 6 probes) at 25°C over a dialysis length of 30 mm at a flow rate of 5 μl min^{-1}. At the point of no–net flux (1.23 μg ml^{-1} **Figure 2.3**) the apparent concentration in the bath was lower than that measured from samples taken from the bath (2.03 ± 0.24 μg ml^{-1}). The difference maybe explained by the lipophilic nature of malathion.

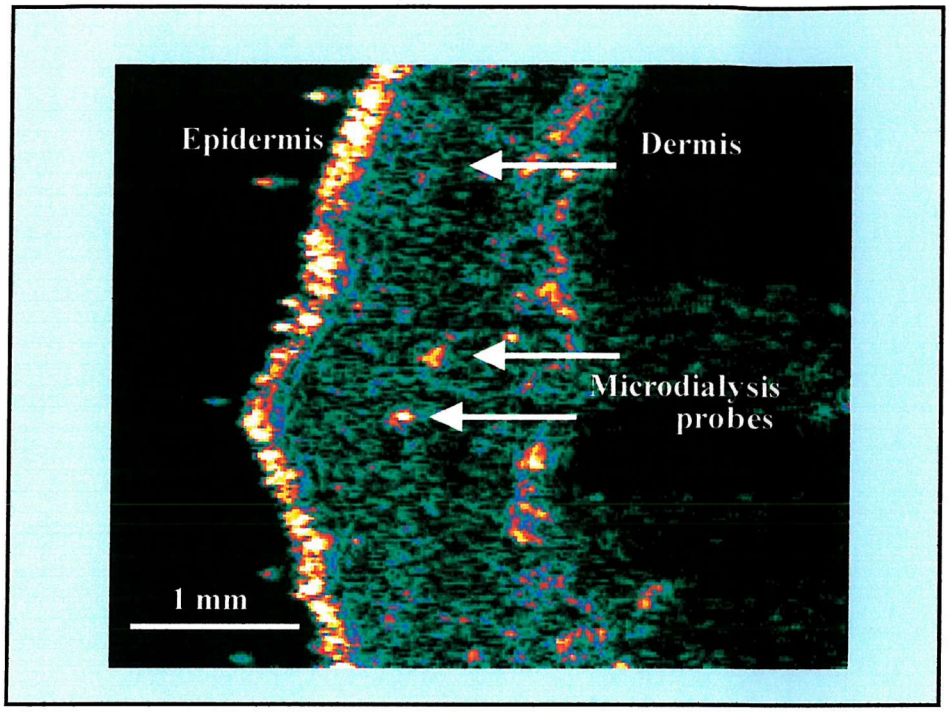

Figure 2.2 Application of ultrasonography to assess the location of the microdialysis probes in the tissue: Ultrasound images were obtained at the end of the microdialysis experiments to demonstrate the depth of the microdialysis probes in the tissue as well as the distance between the probes of the same pair. The microdialysis probes are represented on the image with brighter colours and the distance from the epidermis as well as the distance between the two probes may be calculated and expressed in distance units (mm). It is also possible to distinguish a small oedema represented as a slight rise of the epidermis at the site of insertion of the dialysis probes. This may be a result of the trauma or the effect of a vasoactive drug applied during the experimental procedure.

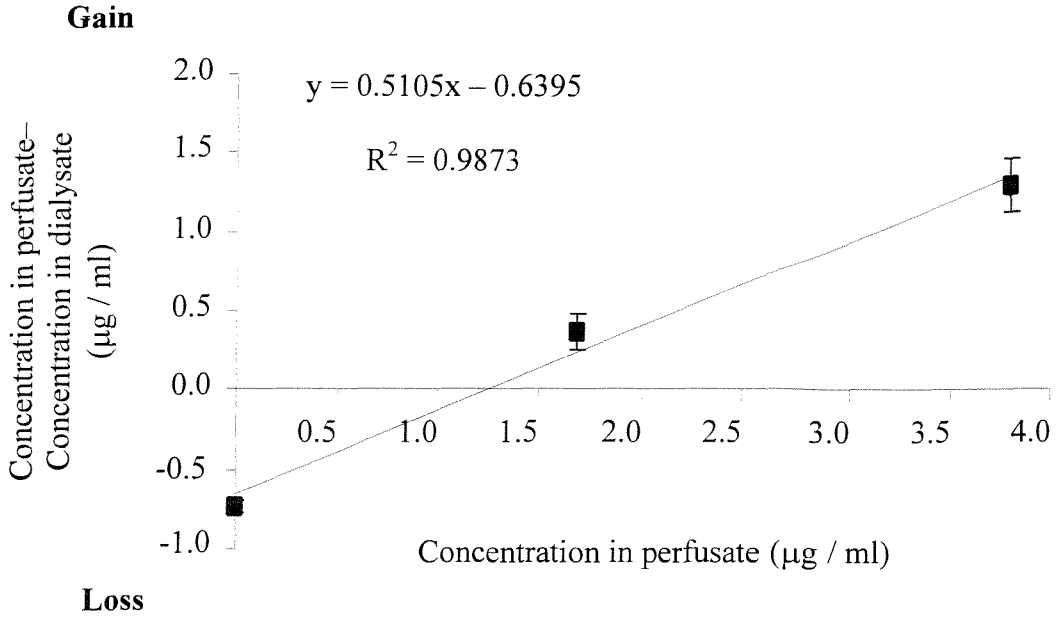

Figure 2.3 No-net flux experiments to estimate the efficiency of the probes to dialyse malathion *in vitro*: The difference between the concentration of malathion in the dialysate (C_{dial}) and the perfusate (C_{perf}) ($C_{dial} - C_{perf}$) is plotted against the concentration of malathion in the perfusate (C_{perf}). The slope of the linear relationship ($C_{perf} - C_{dial}/C_{perf}$) describes the *in vitro* fractional loss and/or gain of malathion from and/or into the microdialysis probes (51 ± 5 %, mean ± sem, n = 6). The intercept with the x–axis is the point of no-net flux and should be equal to the concentration in the bath (C_{bath}) surrounding the microdialysis probe.

Similar deviations have been observed before for other lipophilic drugs such as for example sodium fusidate (Qiu *et al.*, 1996) and make the interpretation of the results more difficult. However in this study *in vitro* efficiency is only used to test the reproducibility of the probes for *in vivo* sampling for malathion and therefore no further calculations were made to estimate the absolute *in vitro* efficiency for malathion as a constant relative recovery is assumed in these experiments (see below 2.3.4).

2.3.4 Experiments to investigate the effects of local skin blood flow on the ability to dialyse.

The ability to dialyse a molecule *in vivo* will by influenced by its concentration in the tissue space, which in turn will depend on the rate of delivery to and its removal from the tissue space. Removal from the tissue space will be determined by the local blood flux, metabolism and the process of dialysis itself **(Figure 3.5)**. The influence of local blood flow on the efficiency to dialyse a molecule can only be explored *in vivo,* in the presence of an intact microcirculation. Because of the toxicity of malathion it was not possible to estimate the effects of skin blood flow on the recovery of malathion by microdialysis *in vivo* in humans as this would require delivery of malathion in the tissue via the microdialysis probes. Hence sodium fluorescein was used as a non-toxic marker molecule as it is of similar molecular weight (318 Daltons) with malathion (330 Daltons). The effective loss of sodium fluorescein from the microdialysis probe was measured both *in vitro* and *in vivo* and was used as an indication of the ability of the 5kDa microdialysis probes to dialyse sodium fluorescein.

2.3.4a: *In vitro* efficiency of microdialysis probes for sodium fluorescein

As described for malathion in **section 2.3.3** prior to the *in vivo* experiments the microdialysis probes were calibrated *in vitro* for their efficiency to dialyse sodium fluorescein. Dialysis probes were immersed in a bath containing PBS and perfused at 5 µl min^{-1} with solution containing 1 mg ml^{-1} sodium fluorescein in PBS at 25°C over a dialysis length of 30 mm. The fractional loss of sodium fluorescein from the dialysis probe was calculated from the difference in the perfusate (C_{perf}) and dialysate (C_{dial}) concentration over the difference in the perfusate and the bath concentration ($C_{bath/tissue}$) at the beginning (t = 2 min) and the end of the experiment (t = 120 min) **(Equation 2.1)**.

$$\text{Fractional loss / gain (RR)} = (C_{perf} - C_{dial}) / (C_{perf} - C_{bath/tissue}) \quad \textbf{Equation 2.1}$$

At 2 min is valid to make the assumption that the concentration of sodium fluorescein in the bath (C_{bath}) is very close zero. Thus the calculated fractional loss of sodium fluorescein from the dialysis probes at 2 min of perfusion is 37.4 ± 4 % (n = 5). This falls to a value of 28.3 ± 3.5 % (n= 5 probes) at 120 min as the fluorescein is probably reabsorbed from the bath (C_{bath} = 0.035 mg ml^{-1} in 7 ml at 120 min) into the dialysis probe **(Figure 2.4)**.

2.3.4b *In vivo* efficiency of microdialysis probes for sodium fluorescein

To measure the *in vivo* efficiency microdialysis probes were inserted into the dermis of the volar surface of the forearm as described in **section 2.3.1**. The length of each probe available for dialysis was 20 mm and the probes were perfused with sodium fluorescein (1 mg ml^{-1} in PBS) at 5 µl min^{-1} for the period of 120 min. Dialysate samples were collected at 2 min intervals for the first ten minutes and at 10 min intervals over the rest of the 2 h period. The fractional loss for sodium fluorescein is calculated using **Equation 2.1** if we make the assumption that the initial concentration of sodium fluorescein in the tissue C_{tissue} will be very small and is taken to equal zero. Therefore the fractional loss of sodium fluorescein *in vivo* at t = 2 min is 38.5 ± 4 % (n = 5) over a 20 mm length of dialysis membrane and a constant flow rate of 5 µl min^{-1} **(Figure 2.5)**. This is very similar to that calculated *in vitro* after the first 2 min of perfusion (37.4 ± 4 %). The concentration of sodium fluorescein in the tissue space in the steady state (t = 100 min) is not known therefore only a relative value for fractional loss can be calculated at this time point for comparison with the initial loss of sodium fluorescein from the dialysis probe. Thus using **Equation 2.1** without taking into account the C_{tissue}, the apparent relative loss of sodium fluorescein at t = 100 min is estimated as 7.5 ± 3.3 % (n = 5).

2.3.4c The effects of blood flow on the *in vivo* efficiency of the dialysis probes for sodium fluorescein

As mentioned previously, it is probable that changes in blood flux will affect the ability of the microdialysis probes to dialyse a molecule *in vivo*. It was therefore necessary to estimate the relative recovery and loss from and into the tissue space for sodium fluorescein *in vivo* under different skin blood flow conditions. To achieve this up to three pairs of microdialysis probes were inserted into the dermis of the volar surface of the forearm as described in **2.3.1**. The distance between the pairs was 30 mm and the length of its probe available for dialysis was 20 mm. Ultrasound imaging showed the probes of the same pair to lie 1.26 ± 0.1 mm (mean ± sem, n = 19) apart.

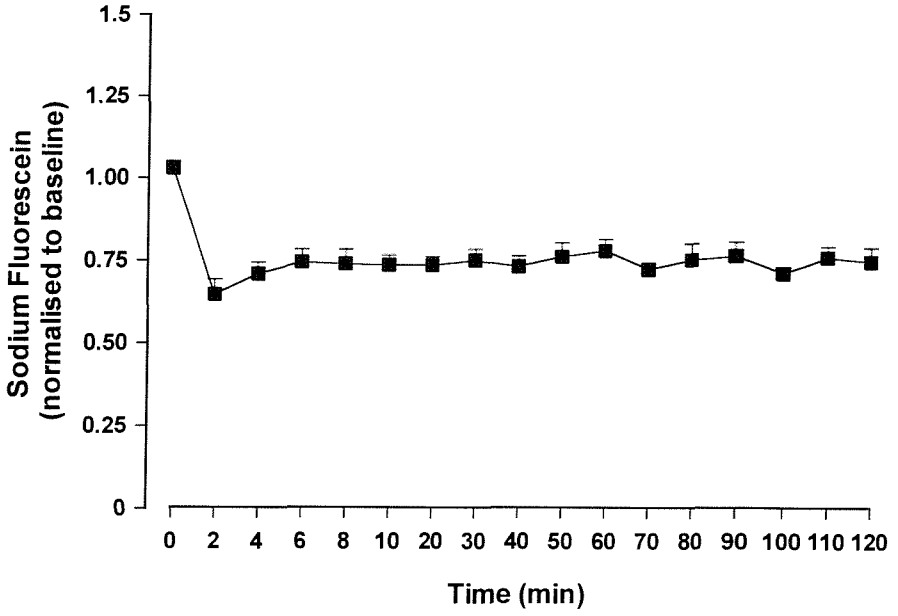

Figure 2.4 *In vitro* efficiency of the microdialysis probes for sodium fluorescein: The dialysis probes were immersed in a bath containing PBS and perfused at 5 μl min^{-1} with 1 mg ml^{-1} sodium fluorescein. The i*n vitro* efficiency of the microdialysis probes for sodium fluorescein is represented as the fractional loss of sodium fluorescein from the perfusate solution into the bath surrounding the probe. Data are normalised to baseline and expressed as mean ± sem, n = 5.

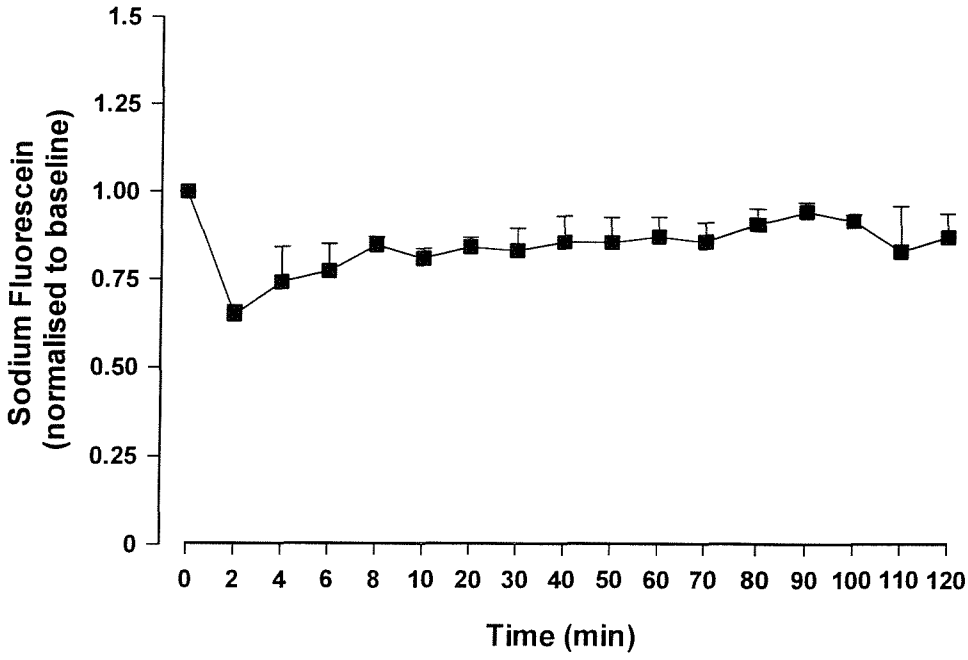

Figure 2.5 *In vivo* efficiency of the microdialysis probes for sodium fluorescein: Similar to the *in vitro* experiments microdialysis probes were perfused with 1 mg ml^{-1} sodium fluorescein *in vivo* at 5 µl min^{-1} over a period of 2 h. The i*n vivo* efficiency of the microdialysis probes for sodium fluorescein is represented as the fractional loss of sodium fluorescein from the perfusate solution into tissue space. Data are normalised to baseline and expressed as mean ± sem, n = 5.

Local blood flow was manipulated by perfusion of one of the probes in each pair with sterile 0.01 M PBS at pH 7.4 (control) or with a solution of noradrenaline (NA) (0.005 mg ml^{-1}) in PBS (vasoconstriction) for 30 min. Where the effects of vasodilatation were to be investigated a glyceryl trinitrate containing patch was applied above one pair of microdialysis probes 30 min before perfusion of sodium fluorescein. Addition of noradrenaline to the probe perfusate caused a significant reduction in resting blood flux, seen as an area of blanching extending up to 2.5 mm either side of the probe in the first 15 min of perfusion. In a separate study reduction of mean blood flux by noradrenaline was measured using laser Doppler imaging. Perfusion of microdialysis probes with NA for 30 min reduced local blood flux from a mean value of 232 ± 48 PU to one of 124 ± 29 PU. Increase of local skin blood flux was observed as an erythema that was restricted to the site of application of the GTN patch and did not extent beyond the patch margin. Previous studies have demonstrated that vascular perfusion beneath the patch to be increased from a resting value of 158 ± 21 to 433 ± 54 PU after 45 min application (Clough, 1999a). After the 30 min period the second probe in each pair was perfused with 1 mg ml^{-1} (n = 5) sodium fluorescein and samples were collected at 10 min intervals over the period of 2 h.

Loss from the probe to the tissue space: The total amount of sodium fluorescein delivered in the tissue space after perfusion of the microdialysis probes with PBS at 5 µl min^{-1} over the period of 120 min calculated from the area under the curve (AUC) of C_{perf}– C_{dial} and was 0.11 mg ± 0.02 (mean ± sem, n = 5). At sites treated with noradrenaline or GTN the total amount delivered in the tissue space was not significantly different from that at PBS sites (0.10 ± 0.03 for GTN and 0.09 ± 0.025 for NA) (mean ± sem, n = 5 ANOVA) **(Figure 2.6)**. The *in vivo* fractional loss of sodium fluorescein in the presence and absence of NA and GTN was calculated using **Equation 2.1**. At 2 min of perfusion the concentration of sodium fluorescein in the tissue was considered as zero (C_{tissue} = 0) and the fractional loss was 37.2 ± 4 % with NA and 33.2 ± 4 % with GTN. These values were not significantly different from the control site at resting blood flow (38.5 ± 4 %) (N.S., n = 5). A relative value for loss of sodium fluorescein in the tissue space was calculated in the steady state in the presence of NA and/or GTN. The values obtained were not significantly different from that at the control site (13 ± 2 % with NA and 11 ± 3.4 % with GTN compared with 7.5 ± 3.3 at control sites, N.S., n = 5). Thus addition of NA and/or GTN did not affect the delivery of sodium fluorescein to the tissue by the microdialysis probes.

Recovery from the tissue space to the probes: A fraction of sodium fluorescein available for dialysis in the tissue space was recovered in dialysate samples collected from the second probe that was placed next to the one delivering sodium fluorescein. Reducing skin blood flow by the addition of NA to the probe perfusate caused a significant increase in the amount of sodium fluorescein recovered in dermal dialysate. At 120 min the concentration of sodium fluorescein in the dialysate at sites treated with NA was 2.5 times greater than that at PBS sites **(Figure 2.7)**. The total amount of sodium fluorescein in the presence of NA was 1.250 ± 0.24 μg over the period of 120 min which was significantly greater than that recovered during perfusion with PBS (0.603 ± 0.26 μg, n = 5, P = 0.001, ANOVA). The concentration of sodium fluorescein in the dialysate at 120 min at sites treated with GTN appeared to be half the concentration of sodium fluorescein at PBS sites. However the total amount of sodium fluorescein recovered in the GTN treated sites (0.382 ± 0.12 μg over 120 min) did not differ significantly from that recovered in the PBS perfused probes in the same subjects (0.603 ± 0.26 μg) (N.S., ANOVA) **(Figure 2.7)**.

In summary changes in local vascular perfusion did not affect the total amount of sodium fluorescein delivered via the microdialysis probes in the tissue space. The fractional loss calculated for sodium fluorescein calculated either initial (2 min) or in the steady state (100 min) was remarkably similar *in vitro* and *in vivo* and was not altered in the presence of NA and/or GTN in the tissue. However changes in local skin blood flux did alter the total amount of sodium fluorescein recovered from the tissue space in the dialysates. Hence data from this study provide direct evidence that local skin blood flow plays an important role in the removal of substances from the tissue space and can therefore affect the ability to dialyse a molecule *in vivo* **(Figure 3.5)**.

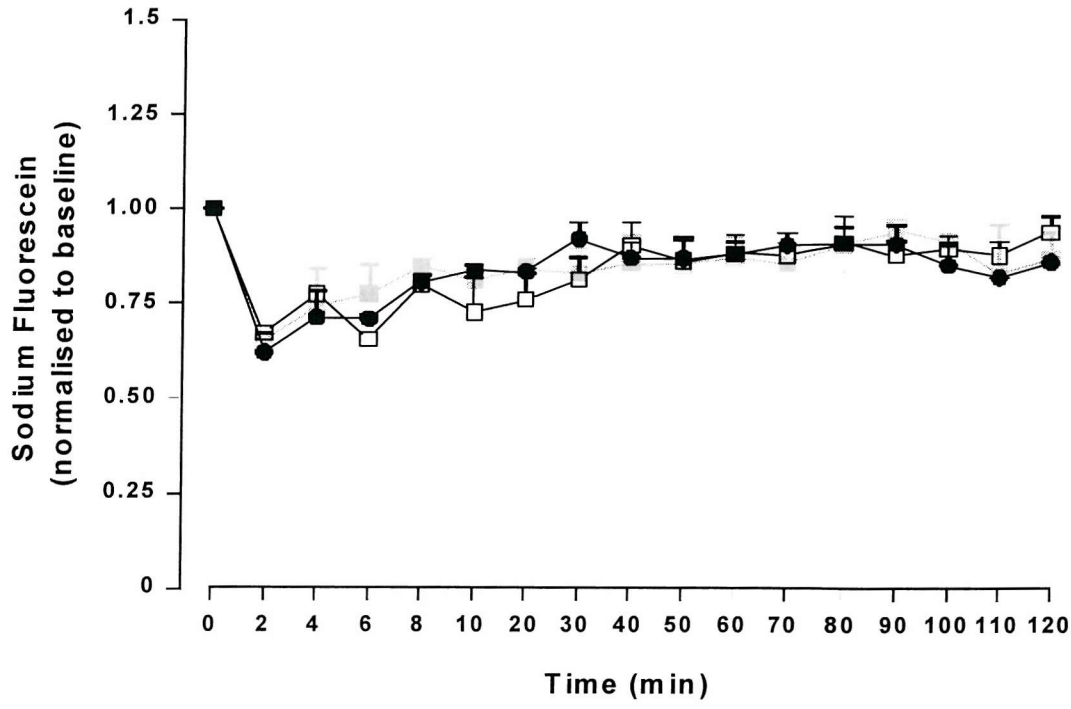

Figure 2.6 The effects of blood flow on the *in vivo* loss of sodium fluorescein: The effective loss of sodium fluorescein (1 mg ml^{-1}) from the dialysis probes to the tissue space was measured at resting blood flow (PBS) (grey solid squares) and in the presence of noradrenaline (0.005 mg ml^{-1}) (open squares) and glyceryltrinitrite (applied as a patch) (black solid squares). The data are normalised to baseline and expressed as mean ± sem (N.S., n = 5).

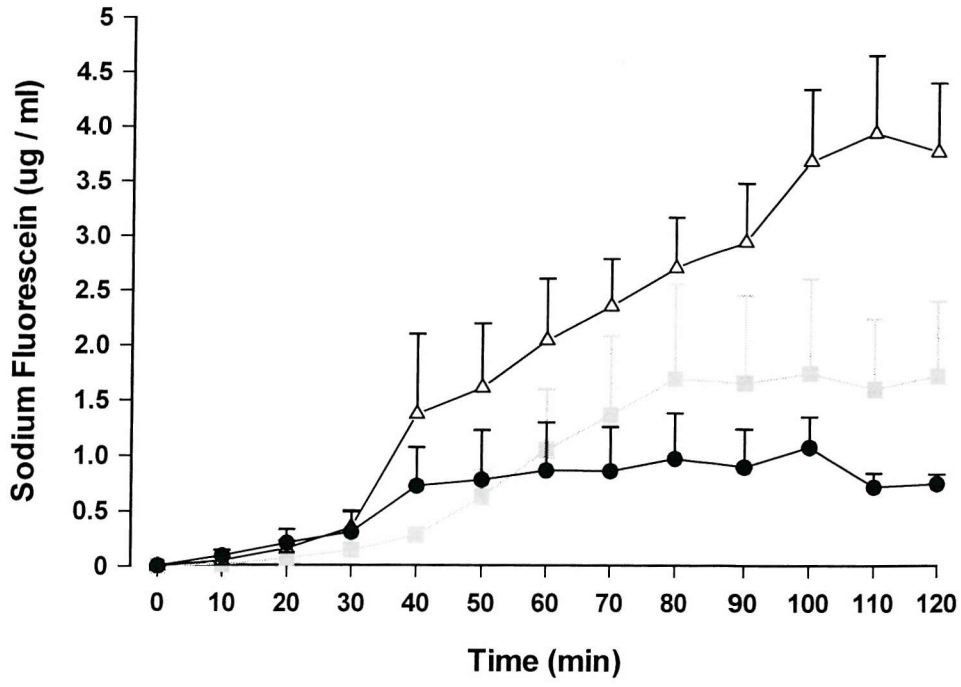

Figure 2.7 Effects of changes in blood flow on the ability of microdialysis probes to recover sodium fluorescein from the tissue space: The total amount of sodium fluorescein recovered in the dialysates over the period of 120 min was measured at resting blood flow (in the presence of PBS) (grey solid squares) and in the presence of noradrenaline (0.005 mg ml^{-1}) (open triangles) and glyceryltrinitrite (applied as a patch) (black solid circles). The data are expressed as mean ± sem (N = 5).

2.3.5 Iontophoretic drug delivery

Iontophoresis was used to deliver vasoactive substances such as ACh and sodium nitroprusside (SNP) as well as atropine to the skin of healthy volunteers *in vivo*. By increasing the amounts of current for different lengths of time it is possible to construct a dose-response curve for the substance of interest. In this study a Perspex direct electrode chamber (30 mm total diameter x 3 mm height, inner drug chamber 10 mm diameter) was used to deliver the drugs. The chamber was attached to the skin of the forearm by means of double–sided adhesive ring and an indifferent electrode was attached to the volar aspect of the wrist of the subject to complete the circuit **(Figure 2.8)**. The chamber was placed over the malathion or vehicle-control treated sites and filled with the solution under test (approx. 1 ml of 2 % ACh in distilled water, 1 % SNP, 10 mM Atropine and distilled water). The LDF probe was placed at the centre of the chamber approximately 1 mm above skin surface. To avoid contamination different iontophoresis chambers were used for different test substances. A battery powered iontophoresis controller was used to provide a direct current for drug iontophoresis. The protocol used in this study for the iontophoretic delivery of ACh (2 %) or vehicle-control was slightly modified from the one used in previous studies (Noon *et al.*, 1998a). Baseline flux was recorded over a period of 20 s before any current was delivered. Pulsed currents of increasing duration and intensity were then delivered allowing response periods of increasing duration between doses **(Figure 2.9)**. The resting periods were allowed for the blood flux to plateau prior to the next current delivery. A value for mean blood flux was calculated from the plateau of the response and is expressed in arbitrary flux units (AU). At the end of each protocol the iontophoresis chamber was removed and cleaned before repeating the procedure at a different site. Theoretically the dose (μg) of the drug delivered at each current dose may be estimated using the following equation:

$$\text{Dose (weight)} = \frac{\text{Q (coulombs) x MW}}{\text{Electron charge x N}} \qquad \textbf{Equation 2.2}$$

Where: **Q** is the charge delivered in coulombs (Q = I x t), **MW** is the molecular weight of the test substance, **Electron charge** = $1.6\ 10^{-19}$ coulombs and **N** = 6.02×10^{23} (Avogadro's constant).

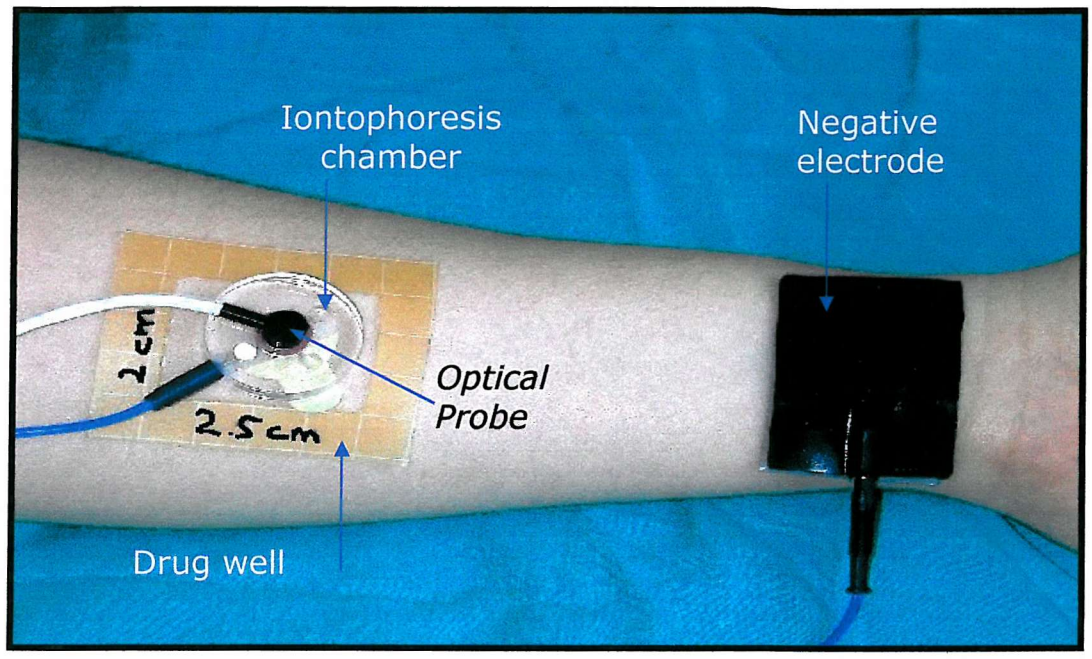

Figure 2.8 Iontophoretic drug delivery: Position of the iontophoresis chamber over malathion and/or control treated sites on the volar surface of the forearm. The laser Doppler fluximetry probe is placed in the middle of the iontophoresis chamber to continuously measure skin blood flux during iontophoretic drug delivery.

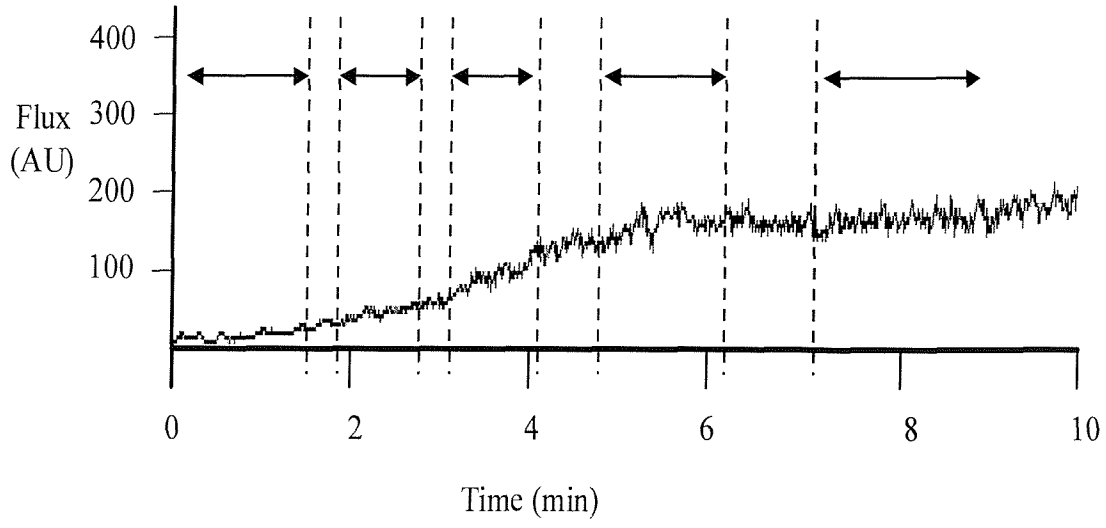

Figure 2.9 Dose-response to iontophoretically delivered ACh: Typical trace obtained using the laser Doppler fluximetry probe during the iontophoretic delivery of ACh. By passing different amounts of current (vertical dotted lines) for different lengths of time it is possible to construct a dose-response curve for the substance of interest. A resting period (horizontal arrows) was allowed before each dose for the skin to recover and for the response to reach a plateau. The protocol used in this study for the iontophoretic delivery of ACh, SNP and vehicle is shown in the table below.

Current I (μA)	**Duration t (sec)**	**Charge Q = I x t (mC)**	**Resting Period (sec)**
0	20	0	
100	10	1	60
200	10	2	60
200	20	4	90
200	40	8	120

2.4 Assessment of cutaneous blood flow

2.4.1 Scanning Laser Doppler Imaging (SLDI)

In this study the SLDI scanner was mounted 30 cm above the surface of the skin and a 5 x 5 cm^2 area scanned at each treatment site. Each scan comprised >16000 data points and took 2 min to collect. The images were stored for later analysis using the manufacturer's software (Moor SLDI version 3). Before scanning the site of interest two black dots 2 cm apart were marked on the surface of the forearm, and used to calibrate the images from a number of active pixels within a given region of interest. In this way the area of the flare produced after a stimulus could be calculated in cm^2 and therefore the size of the response could be related to the intensity of the sensation **(Figure 2.10)**. The number of pixels within the 2 cm is also an indication of repeatability of measurements and in this study was found to be 39 ± 1 (n = 57 sites in 31 volunteers).

Because of variations arising from tissue pigmentation, penetration depth and microvascular distribution within the tissue, it is not valid to calibrate the laser Doppler instrumentation in absolute units of flow. The scanning LDI was therefore calibrated to perfusion units (PU) and all measurements of mean blood flux in this project are expressed in PU. Due to residual interstitial movement, absence of blood flow does not lead to zero laser Doppler flux values, this is called the 'biological zero' effect. In order to establish the biological zero a sphygmomanometer cuff inflated to a pressure of 200 mmHg for a period of two minutes was used to occlude forearm blood flow. The residual signal was estimated to be approximately 40 PU.

Baseline blood flux can vary according to the age, sex and smoking habits of the subject as well as other factors such as skin temperature, physical condition and menstrual cycle. The mean baseline value calculated from SLDI scans taken from 36 volunteers (21 women and 15 men) and was 126 ± 5.2 PU. Baseline mean blood flux values varied between subjects, ranging from 75 PU to 233 PU. Baseline mean blood flux values measured in 21 young female (108 ± 5.4 PU) volunteers did not differ significantly from those measured in 15 male (112 ± 6.9 PU) volunteers. Furthermore no significant differences were observed between measurements at different sites along the length of the forearm (110 ± 5.8 PU elbow, 111 ± 7.1 PU middle and 113 ± 8.2 PU hand). Four of the volunteers were heavy smokers and their baseline flux (175 ± 9.1 PU) was slightly higher than those obtained from non-smoking volunteers, the small number of smokers however does not

allow statistical comparisons.

2.4.2 Laser Doppler Fluximetry (LDF)

In this study LDF was combined with iontophoresis to provide measurements of blood flux before and during drug administration **(section 2.3.5)**. The LDF probe was calibrated by the manufacturer and blood flux is expressed in arbitrary units (AU). The biological zero effect is also applicable to LDF measurements and in a different project in the department was estimated to be 4.3 ± 0.55 AU. The factors mentioned previously that influence SLDI measurements also affect LDF measurements and must be taken into account during the experiments and data analysis. A baseline value for mean blood flux in AU measured using the LDF probe in 11 volunteers (4 men and 7 women) was 17.2 ± 2.6 (AU). Two of these subjects were smokers and their baseline values were 34.8 AU and 43 AU respectively. During the experiment in which the LDF probe was placed at 4 different sites along the volar surface of the forearm no significant difference was observed between sites in the same subjects. However because the LDF probe provides measurements at a single point the placement of the probe is critical. For example in this study it was observed that when the LDF probe was placed directly above a larger blood vessel frequent and intense fluctuations of mean blood flux were seen during the baseline measurements.

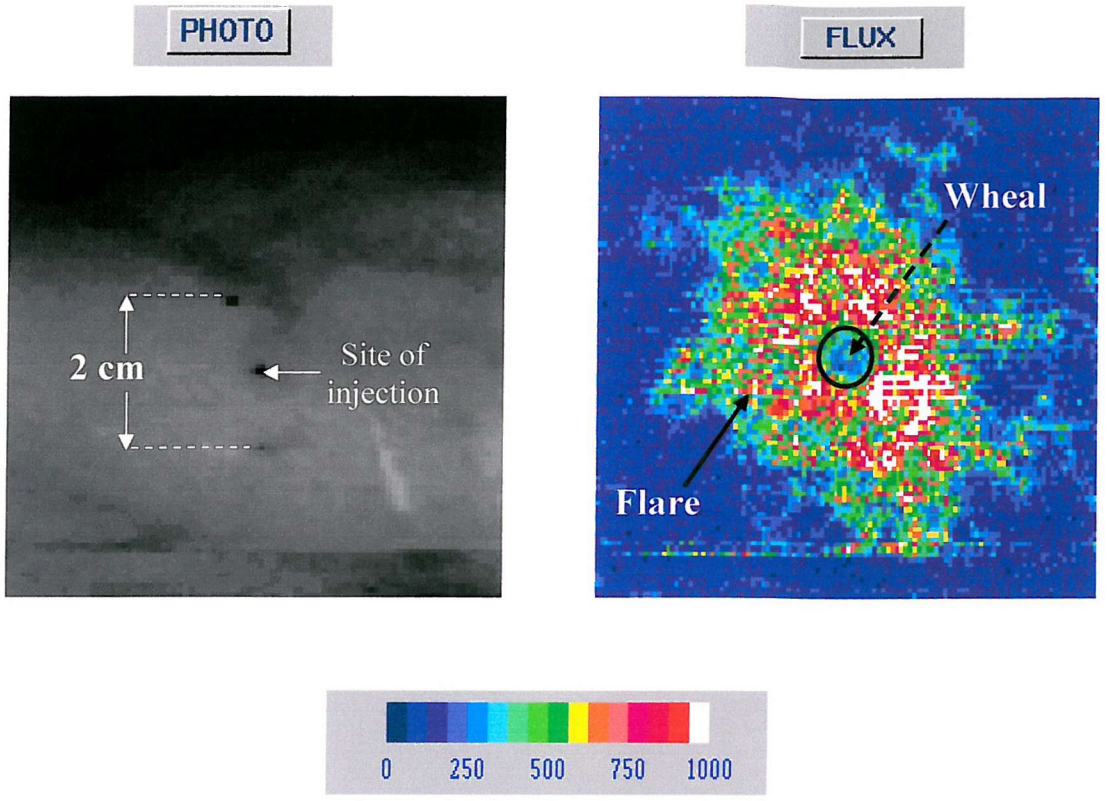

Figure 2.10 Application of scanning laser Doppler imaging (SLDI) to quantify changes in skin blood flux: Scanning laser Doppler image of a weal and flare response to the intradermal injection of histamine. The image was collected 10 min after the injection and comprises 128 x 128 pixels. The SLDI is calibrated in perfusion units (PU) (see scale 0-1000 PU) set by the scanner's software. A grey scale image can be used to calibrate the scans using two black dots 2 cm apart marked on the surface of the forearm (photo image).

2.5 Analysis of Dialysates

In the present study five different assays were performed to quantify the levels of malathion, malaoxon, sodium fluorescein, histamine and nitric oxide in dermal dialysate. These used gas chromatography for malathion and malaoxon, fluorescence assay for sodium fluorescein, enzymatic immunoassay for histamine and chemiluminescence for nitric oxide. A method was also developed for the assay of acetylcholine in the dialysate samples using mass spectrometry. This will be described in detail in **Chapter 4**.

2.5.1 Assay for Malathion

A number of methods such as high performance liquid chromatography (HPLC), and mass spectrometry (MS) combined with either liquid chromatography (LC) and/or gas chromatography (GC) have been developed to monitor the levels of OP's in food, soil and water (Hong *et al.*, 1993). Despite the good separation between different OP's obtained, most of these techniques require special preparation of the samples and are for qualitative purposes only. In this study gas chromatography was chosen as the most appropriate to quantify the levels of malathion in the dialysate samples as it provides reasonable sensitivity and a fairly short and not complicated extraction procedure before sample analysis.

The concentration of malathion in dermal dialysate was measured using a gas chromatograph equipped with a flame photometric detector and an auto sampler. Two microlitre samples were introduced to the capillary column through an on-column injector set at 95 ^{o}C. After the sample injection to obtain a better separation between malathion and malaoxon peaks the oven temperature was held at 90 ^{o}C for 2 min before increasing stepwise at 5 ^{o}C min^{-1} to 200 ^{o}C. The detector temperature was set at 260 ^{o}C. Hydrogen was used as the carrier gas and the total flow rate is 2 ml min^{-1}. The total run time for each sample was 25 min **(Figure 2.11)**.

After defrosting, 100 µl of dialysate sample and 10 µl of mecarbam that was used as the internal standard (600 ng in PBS) were mixed in a 10 ml glass tube along with 4 ml of hexane. Samples were shaken horizontally for 10 min and left to stand for 10 min. The hexane layer was then transferred into a clean tube and evaporated to dryness at 40 ^{o}C under a gentle stream of nitrogen. Samples were reconstituted in 40 µl of toluene and spiral mixed for 10 min. After a 10 min standing period the samples were transferred into

GC vials for analysis. Samples prepared following this extraction procedure were analysed in the GC and compared with samples prepared straight into toluene to evaluate the efficiency of the extraction procedure which was estimated at 90 ± 2 %. The retention times for malathion, mecarbam and malaoxon (the active metabolite of malathion) were 16.5, 19.4 and 15.1 min, respectively **(Figure 2.11)**.

The concentration of malathion in the samples was calculated from a calibration curve for malathion constructed for each experiment, using a series of solutions all containing 600 ng mecarbam and quantities of malathion varying between 10 ng and 600 ng. The concentration of malathion in the dialysate samples was then calculated as the ratio of peak areas for malathion and mecarbam (malathion/mecarbam) using the slope of the calibration curve to convert ratios to ng ml^{-1}. The lower limit of detection for malathion was 10 ng and the coefficient of variance of the assay 2.6 % and 2.4 % at 10 ng and 600 ng respectively.

2.5.2 Fluorescence assay

The concentration of sodium fluorescein in dermal dialysate (100 µl) was assayed in 96–well plates using a fluoresence plate reader (Cytofluor 4000 Microplate fluoresence reader). The excitation was set at 485/20 nm and emission at 530/25 nm specific for fluorescein. A gain of 40 gave the lowest background value (max 16 ± 2 FU) and the sensitivity of the assay at these settings was 5 ng ml^{-1} with a coefficient of variance at 0.08 %. Samples were diluted with PBS up to x200 as appropriate and fluorescein was quantified in 100 µl aliquots using a calibration curve constructed for each experiment, over the range of 5-1000 ng ml^{-1} **(Figure 2.12)**.

2.5.3 Histamine immunoassay

The enzyme immunoassay for histamine (Immunotech, A Beckman Coulter company, France) used in this study is based on the competition between the histamine to be assayed and its enzyme conjugate, histamine alkaline phosphatase, which is used as a tracer for binding to the antibody. To ensure complete binding of histamine to the enzyme conjugate has been modified. Therefore, the histamine in the sample must be derivatised in the same manner as the histamine of the conjugate. This is achieved with an acylating reagent at slightly alkaline pH.

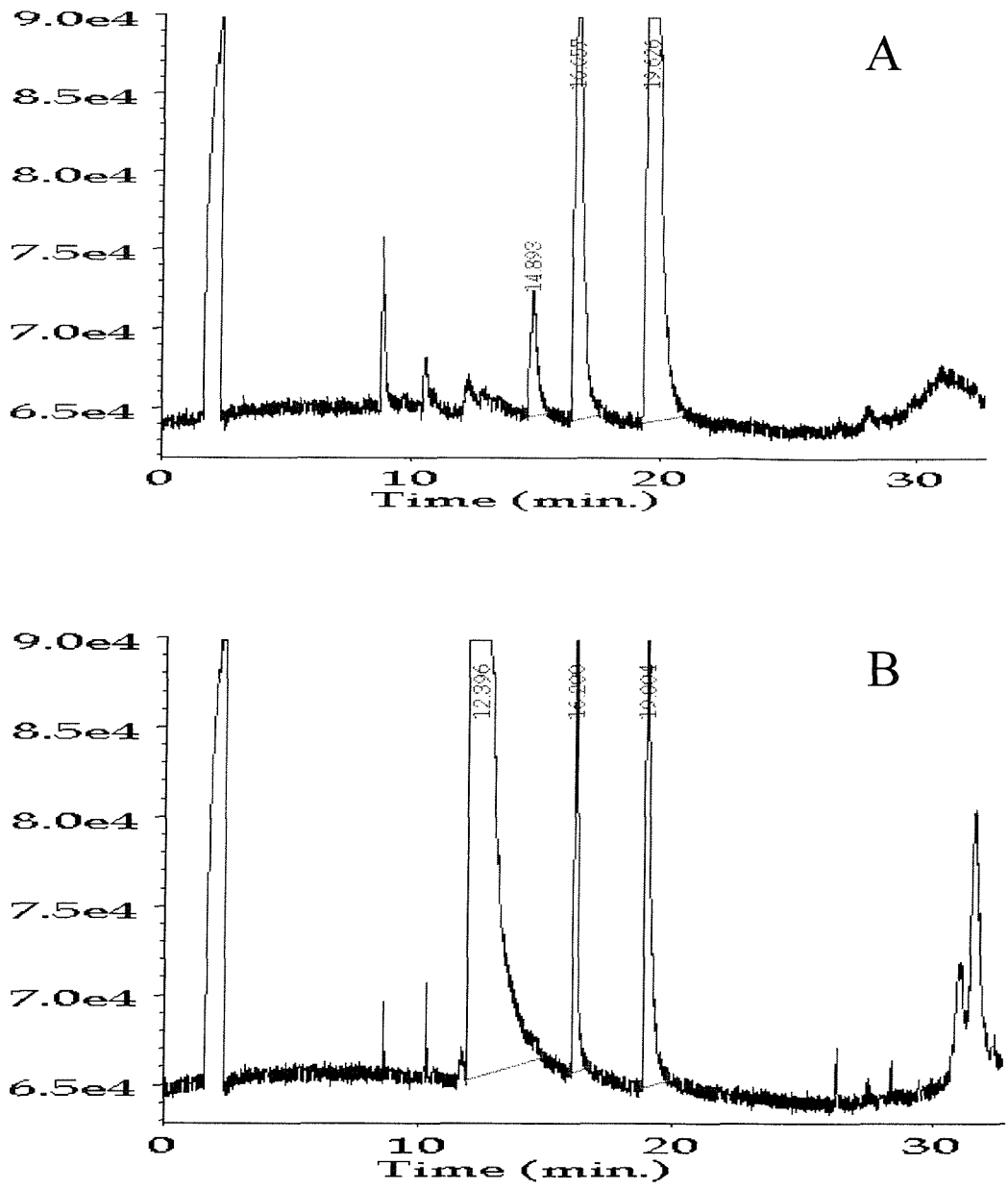

Figure 2.11 Analysis of malathion and malaoxon in the dialysates: Typical GC chromatographs obtained for malathion (16.6 min) and malaoxon (14.9 min) standards **(A)** as well as for *in vivo* dialysate samples **(B)**. Mecarbam was used as the internal standard (19.5 min) to ensure reproducibility of the assay. An unknown peak (12.4 min) appeared in all *in vivo* samples but was not detected in the standards. Malaoxon under the conditions used was not detected in the dialysate samples.

Figure 2.12 Calibration curve for the assay of sodium fluorescein: The concentration of sodium fluorescein in dermal dialysate was assayed in 96–well plates using a fluoresence plate reader (Cytofluor 4000 Microplate fluoresence reader).

The acylated histamine of the dialysate sample and the histamine alkaline phosphatase conjugate, when added to the 96-well microtiter plates, compete for binding to a limiting number of antibody sites. After incubation the wells are rinsed in order to remove non-bound components. The bound enzymatic activity is then measured by the addition of chromogenic substrate (para-nitrophenylphosphate). The intensity of the colour is inversely related to the concentration of histamine in the sample. The concentration is calculated from the standard curve obtained with the standards supplied with the kit.

Before the assay, all the components of the kit were equilibrated to room temperature. Three different immunoassay kits of the same batch (Lot: 25) and reference number (Ref: 2562) were used to assay dialysate samples from 6 healthy volunteers. Standards and samples were assayed at the same time and the standards were assayed in duplicate. Dialysate samples obtained from healthy volunteers before (25 µl), during and after (10 µl) challenge with different doses of acetylcholine were diluted with phosphate buffered saline solution (PBS) to give a total volume of 100 µl sample. For the acylation of standards and samples, 25 µl of acylation solution and 100 µl of standards (0-100 nM histamine) and samples were added in plastic tubes along with 25 µl of acylation buffer and vortex mixed immediately. The acylated standards and samples (50 µl) were then added onto antibody-coated wells at 23°C along with the enzymatic conjugate (200 µl). The plate was then incubated for 18 hours at 2-8 °C without shaking. At the end of the 18 hours the microtiter plate wells were washed twice using the washing solution provided. Two hundred microliters of substrate (200 µl) was then added to all wells and the plate was incubated for 30 min at 23 °C with constant shaking at 350 rpm on a microtiter plate shaker (Dynex technologies, AM89B, UK). After incubation the reaction was stopped by adding 50 µl of stop solution to all wells. A microplate spectrophotometer (SPECTRAmax® 340PC, Molecular Devices Corporation, California, 94089) set at 414 nm was then used to read the plate.

The sensitivity of the assay is 0.5 nM histamine and the coefficient of variance of the assay is 6.2 % for 3 nM histamine. Cross reactivities (%) for several endogenous analogues and pharmacologically active substances were calculated by the supplier (Cross reactivity (%) = Concentration of acylated histamine / concentration of analogue x 100) and ranged from 0.027 % for acylated 3-methylhistamine to $<4 \times 10^{-5}$ acylated serotonin. These indicate that the assay is specific for acylated histamine and that interference of

endogenous analogues that may be found in the dialysates with the assay is insignificant.

2.5.4 Nitric oxide assay

Nitric oxide (NO) was assayed in the dialysate samples using a nitric oxide analyser (NOA) with a high–sensitivity detector for measuring nitric oxide based on a gas–phase chemiluminescent reaction between nitric oxide and ozone:

$$NO + O_3 \longrightarrow NO_2^{\bullet} + O_2$$

$$NO_2^{\bullet} \longrightarrow NO_2^{-} + h\nu$$

Emission from electronically excited nitrogen dioxide ($NO_2^{\bullet}$) is in the red and near–infrared region of the spectrum, and is detected by a thermoelectrically cooled, red–sensitive photomultiplier tube. The sensitivity of the NOA for measurement of gas–phase NO is less than 1 part per billion by volume. The sensitivity for measurement of NO and its reaction products in liquid samples is ~1 pmole.

NO released in the tissue reacts with dissolved oxygen to form nitrite (NO_2^-). Nitrate may also be present in the dialysates and although it was not measured in the present study it was shown in a recent study that the proportion of nitrate relative to nitrite in the dialysate is very small (Clough, 1999a). It is therefore likely that the assay measures ongoing production of NO within the tissue rather than accumulation of NO converted to nitrate as the final oxidative step. Ten microlitre samples of dialysate were reduced using an acidic NaI solution (0.05g of NaI dissolved in 1 ml of PBS and mixed with 5 ml acetic acid) prepared in the vessel of the NOA apparatus and the concentration of NO generated from nitrite in the dialysate was measured:

$$I^- + NO_2^- + 2H^+ \longrightarrow NO + \tfrac{1}{2} I_2 + H_2O$$

A calibration curve was constructed before any sample analysis by stepwise additions of increasing concentrations of $NaNO_2$ prepared in PBS. The linear fit correlates the emission (mV) generated by the chemiluminescent reaction of NO with ozone, with the corresponding NO concentration. The slope of the curve was then used to calculate the concentration of NO measured in the dialysates. This is assumed to represent a significant fraction of NO / nitrite available for dialysis within the tissue space and thus to reflect dynamic changes in tissue NO.

CHAPTER 3: THE EFFECTS OF SKIN BLOOD FLOW ON THE PERCUTANEOUS ABSORPTION OF MALATHION IN HUMAN SKIN *IN VIVO*.

3.1 Introduction and Aims

The aim of this study was to measure the rate of percutaneous absorption of malathion in human skin, *in vivo*, and to explore the relationship between tissue levels of malathion and changes in local skin blood flow. The skin is an important route for the absorption of malathion. Several factors have been shown to influence its absorption following topical application, including the treatment regimen, the formulant and the skin site of application. There have been many attempts to model the kinetics of transdermal absorption (see for example Albery *et al.*, 1983; Guy & Hadgraft, 1984; Singh & Roberts, 1993) and to measure the rates of penetration of a wide range of agents both *in vitro* in isolated skin preparations (Cross *et al.*, 1998) as well as *in vivo* in animal models (Benfeldt & Serup, 1999) and in man (Benfeldt *et al.*, 1999) **(see section 1.3.2)**.

However, the factors that influence the disposition of topically applied solutes within the dermis and their subsequent systemic distribution, such as tissue composition, tissue metabolism and cutaneous perfusion can only be explored *in vivo,* in preparations where a viable dermis and dermal microcirculation are maintained (Riviere & Williams, 1992; Singh & Roberts, 1994). Such studies have demonstrated that clearance from the dermis, particularly the upper dermis, of small diffusible molecules is highly dependent upon local blood flow. Our findings using sodium fluorescein delivered in the tissue space, showed that a greater amount of sodium fluorescein is available in the tissue space for dialysis in the presence of the vasoconstrictor noradrenaline, compared with that measured under resting blood flux **(see section 2.3.3c)**. Thus it may be speculated that agents that themselves affect cutaneous blood flow will influence their own distribution within the tissue.

In this study microdialysis probes were implanted within the upper dermis of healthy human volunteers to follow the time course of the percutaneous penetration of topically applied malathion. Changes in the cutaneous perfusion after exposure to a low-dose of malathion were assessed using non-invasive scanning laser Doppler imaging. To establish a relationship between tissue levels of malathion and local skin blood flow cutaneous microcirculation was manipulated using the vasoconstrictor, noradrenaline and the vasodilator, nitric oxide donor, glyceryltrinitrate, delivered in the tissue via the microdialysis probes.

3.2 Materials and Methods

3.2.1 Subjects and experimental conditions

Thirty-three healthy volunteers (12 male and 21 female) aged between 18-45 years were recruited into the study, performed according to the declaration of Helsinki. The study was divided into three parts (i) absorption studies using microdialysis (n=10), (ii) effects of topically applied malathion on dermal perfusion (n=21), and (iii) effects of altered blood flow on percutaneous absorption (n=13). Some subjects participated in more than one part of the study. Informed consent was obtained from all subjects and the study was approved by the local ethics committee (JEC No: 301/98).

3.2.2 Drug preparation

Malathion 10 mg ml^{-1} in an aqueous based gel and vehicle-control were prepared on the day of use as described in **section 2.2**. An aqueous based, commercially available formulation of malathion (0.5 % w/w Derbac M, Seton Healthcare Group, Oldham, UK) was also used together with vehicle-control (Aquagel). Probe perfusate solutions of sterile 0.01M phosphate buffered saline (PBS) with a pH 7.4 at 25 °C and solutions of noradrenaline (NA, 0.005 mg ml^{-1}) and glyceryltrinitrate (GTN, 0.5 mg ml^{-1}) in PBS were also prepared on the morning of the experiment and stored on ice prior to use.

3.2.3 Microdialysis

Microdialysis probes were manufactured and implanted in the volar surface of the forearm as described in **section 2.3.1**. Where the effects of changes in skin blood flow on the percutaneous absorption of malathion were to be investigated, two of the six microdialysis probes were perfused with PBS containing the vasoconstrictor NA (0.005 mg ml^{-1}) and two with the nitric oxide donor (vasodilator) GTN (0.5 mg ml^{-1}). The remaining two control probes were perfused with PBS alone. In two subjects pralidoxime mesylate (0.1 mg ml^{-1} in sodium chloride) was added to the probe perfusate to allow the assay of malathion's active metabolite malaoxon in the dialysate. The dose (45 μg) of pralidoxime mesylate used in this study is well below the recommended dose for organophosphate poisoning (30 mg kg^{-1}). After an equilibration period of 30 min a baseline dialysate sample (30 min, 150 μl) was collected prior to the application of malathion. After malathion application, dialysate was collected over 30 min intervals (150 μl aliquots) for 5 hours and stored at –20°C prior to assay for malathion and NO.

3.2.4 Application of malathion

Malathion or vehicle-control (0.5 ml) was applied to a 2 cm x 1 cm area of skin above each dialysis probe in occluded drug wells made from adhesive dressing for 5.5 h. In a separate series of experiments, where the effects of malathion on skin blood flow were to be investigated, 0.5 ml of malathion, Derbac M or vehicle-control was applied for 30, 90, 150 or 300 min to 2 cm x 1 cm areas of the volar surface of the forearm under occlusive dressing. In some subjects the effects of disruption of the stratum corneum on drug penetration were investigated by applying cellophane adhesive tape prior to treatment with Derbac M **(see section 2.2.1)**.

3.2.5 Measurement of skin blood flux

Skin blood flux was measured using non-invasive scanning laser Doppler imaging (SLDI) as described previously in **section 2.4.1**. In experiments where the effects of malathion or Derbac M on skin blood flux were to be investigated, skin blood flux within the treatment area was measured before and after exposure to malathion or vehicle control and expressed as mean blood flux in SLDI perfusion units (PU). Changes in mean blood flux were expressed relative to baseline values. Where tape stripping was performed, baseline blood flux was measured 30 min after tape stripping, just prior to application of Derbac M. The area of the erythematous response to malathion or to vehicle-control was also calculated from the calibrated scans.

In experiments where skin blood flux was manipulated by addition of NA or GTN to the probe perfusate, mean blood flux in an area 2 cm x 0.2 cm above each dialysis probe was calculated from images taken before and at intervals up to 30 min after the start of perfusion but before the application of malathion. Measurements were also made at the end of malathion exposure after removal of the malathion-containing gel. No images were collected during malathion exposure, as the low power laser beam was unable to penetrate the gel preparation.

3.2.6 Statistical analysis

Where statistical comparisons were made a Student's t-test for paired data was used. Analysis of variance (ANOVA) was used were appropriate. A probability value of $P < 0.05$ has been taken as significant. All subjects acted as their own controls.

3.3 Results

3.3.1 Percutaneous absorption of malathion

Malathion was detected in dialysate collected from the PBS perfused probes within 30 min of application of 10 mg ml^{-1} malathion in Aquagel preparation to the skin surface **(Figure 3.1)**. The dialysate concentration of malathion increased with lengthening period of exposure to reach a steady state concentration of 50.5 ± 11.3 ng ml^{-1} at 3 h (9 probes in 6 subjects). There was little further increase in concentration up to 5 h continuous exposure. The total amount of malathion recovered was 71 ± 18 ng. The recovery of malathion in the dialysate showed marked inter-subject variability with the concentration of malathion in dialysate recovered after 5 h exposure ranging between 9–112 ng ml^{-1}. No malaoxon, the metabolite of malathion, could be detected in the dialysate samples at any time in the presence and absence of pralidoxime mesylate. No malathion was detected in dialysate collected for up to 5 h after application of Derbac M to intact skin (7 probes in 2 subjects).

3.3.2 Effects of malathion on skin blood flow

Malathion, when applied under occlusive dressing to the intact skin of the volar surface of the forearm for periods of up to 5 h, caused a marked and long lasting erythema **(Figure 3.2)**. The increase in mean blood flux at the malathion treated sites at 5 h (108 ± 44 %) was significantly greater than that at vehicle-control treated sites in the same subjects (18 ± 16 %) ($P < 0.002$, $n = 7$) **(Figure 3.3)**. No significant increase in blood flux over baseline was seen after 5 h treatment with vehicle-control. The area of the erythema was restricted to the site of application of malathion and did not extend beyond the margin of the drug well. In some subjects the erythema was still visible 1.5 h after removal of the malathion-containing gel. Derbac M had no measurable effect on skin blood flux when applied to intact skin, under occlusive dressing. Nor did it significantly increase mean blood flux following application to tape stripped skin when compared with similarly treated vehicle-control sites. At 5 h the increase in mean blood flux at tape-stripped Derbac M treated sites was 26 ± 19 % compared with 22 ± 17 % at tape stripped vehicle-control treated sites (N.S., $n = 7$).

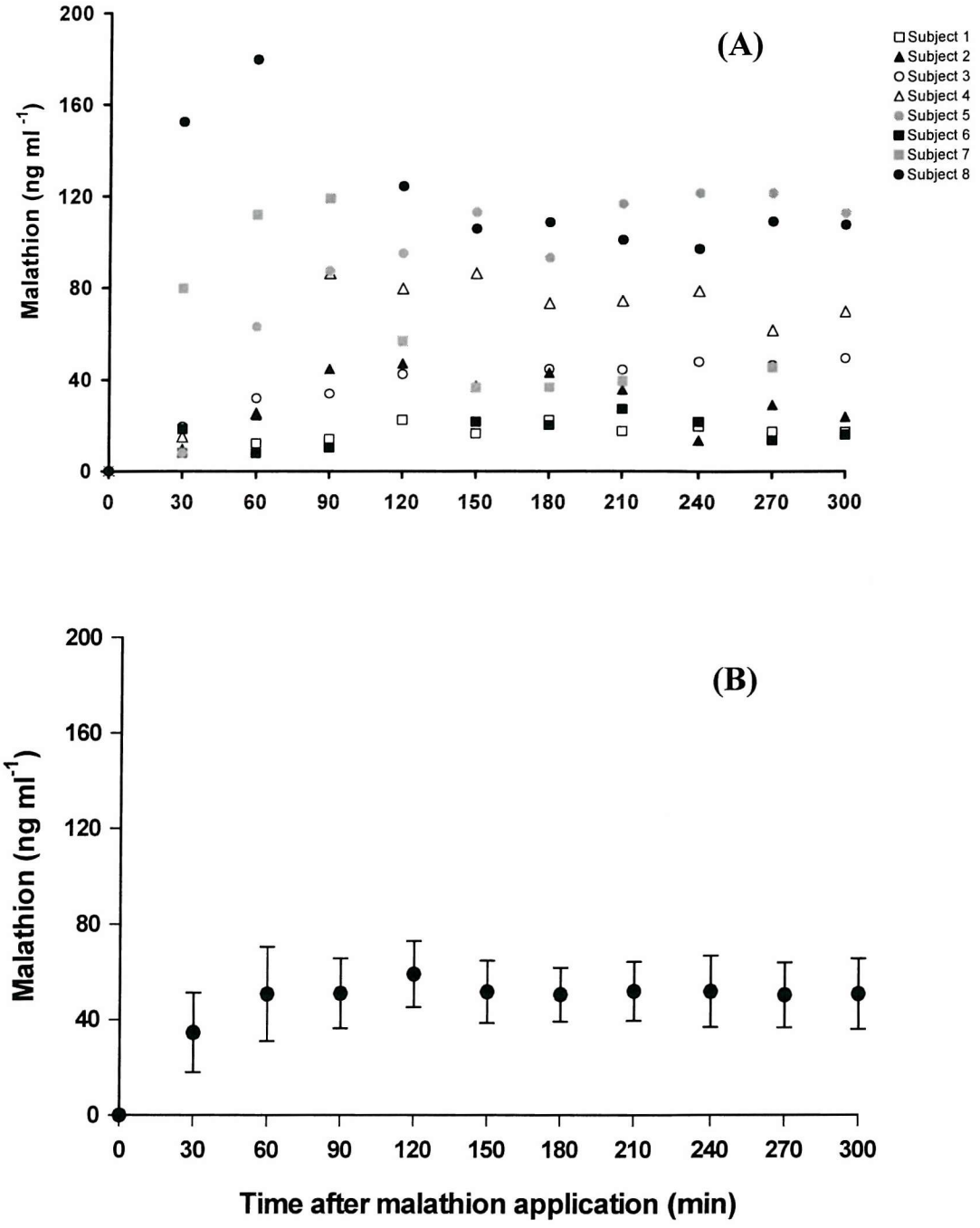

Figure 3.1 Percutaneous absorption of malathion: (A) Concentration of malathion in dialysate recovered from the skin of the forearm of eight subjects using 5 kDa microdialysis probes in perfused with phosphate buffered saline at a rate of 5 µl min^{-1}. Malathion (10 mg ml^{-1}, 0.5 ml) was applied topically to the surface of the skin above the probes under occlusive dressing. **(B)** shows mean ± sem of the data from the 8 subjects.

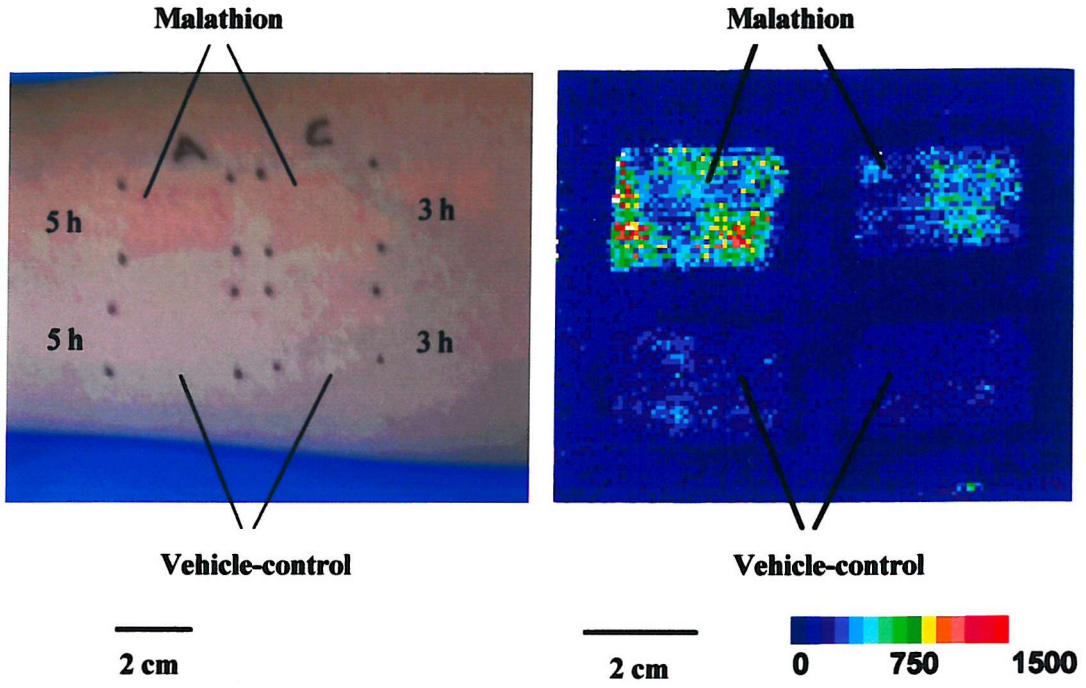

Figure 3.2 Effects of malathion on skin blood flow (A): The photograph (left) illustrates the malathion-induced erythema following topical application on the surface of the skin under occlusive dressing for 3 and 5 h. Changes in mean blood flux were measured using scanning laser Doppler imaging (right) at malathion and vehicle-control treated sites.

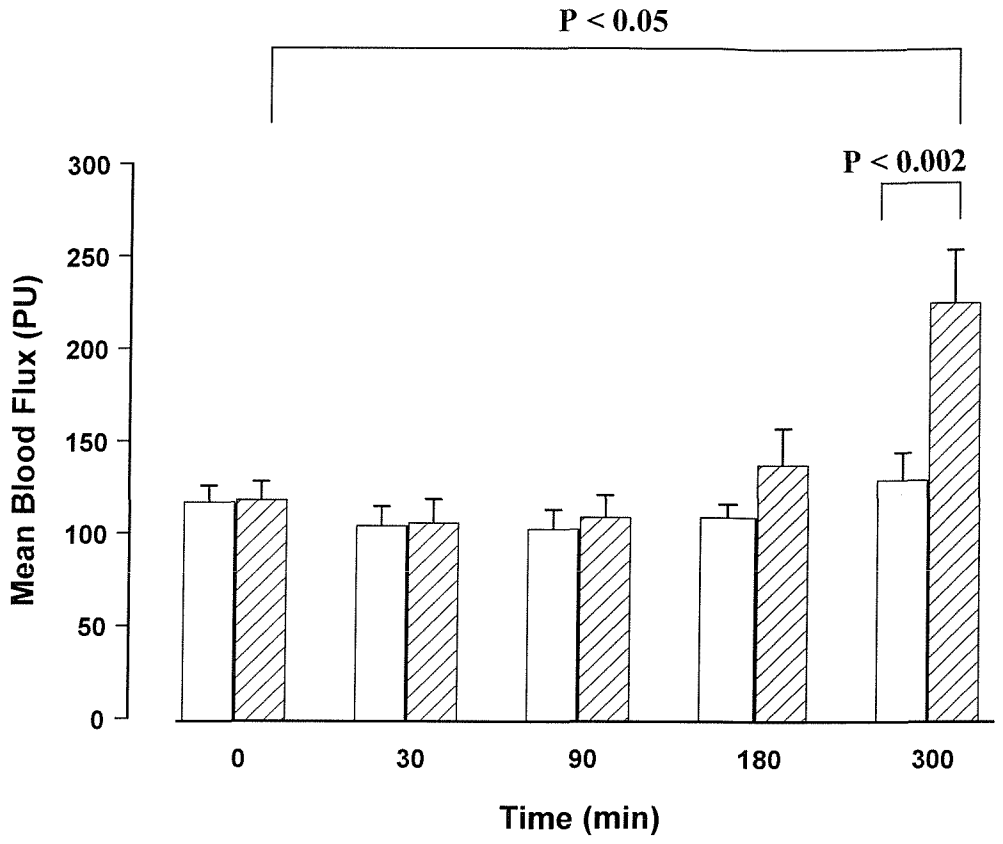

Figure 3.3 Effects of malathion on skin blood flow (B): Mean blood flux was measured within an area of 2 x 1 cm^2 using SLDI before and at intervals after topical application under occlusive dressing of vehicle (open bars) or malathion (10 mg ml^{-1}) containing gels (hatched bars). Gels were removed 10 min prior to measurement of blood flux. Data are mean ± sem from 7 subjects. The increase in mean blood flux caused by malathion at 5 h is significant when compared with baseline ($P < 0.05$, paired t-test) and the vehicle-control treated site at 5 h ($P < 0.002$, paired t-test).

3.3.3 Effects of NA and GTN on skin blood flow

Addition of noradrenaline to the probe perfusate caused a significant reduction in resting blood flux, seen as an area of blanching extending up to 2 mm either side of the probe. In four subjects the mean blood flux fell by up to 40 % in the first 10 min of perfusion with NA. At 30 min, just prior to the application of malathion, NA had reduced local blood flux from a mean value of 232 ± 48 PU to one of 124 ± 29 PU (4 probes in 4 subjects) **(Figure 3.4 & Figure 3.5)**. After removal of the malathion 5 h later, the effect of NA could still be seen as an area of blanching surrounded by the malathion-induced erythema. Perfusion with PBS also caused a decrease in skin blood flux of approximately 20 % at 10 min, which was maintained throughout the 30 min. At the time of application of malathion, 30 min after the start of perfusion, mean blood flux had fallen from a value of 264 ± 46 PU to one of 200 ± 71 PU (3 probes in 3 subjects) **(Figure 3.5)**.

By contrast, perfusion of the dialysis probes with GTN caused a rapid increase in skin blood flux of up to 25 %, 10 min after the start of perfusion **(Figure 3.4 & Figure 3.5)**. At 30 min this increase had fallen to approximately 10 %, to a value of mean blood flux measured over the probe of 255 ± 43 PU compared with one of 231 ± 37 PU (n = 4 probes in 4 subjects) before the start of perfusion. Thus, at the time of application of malathion or vehicle-control, the relative difference in blood flux between the NA and GTN perfused sites was of the order of 100 %. Because of the vasodilator effects of malathion itself on skin blood flow, the GTN-induced changes in blood flux could not be distinguished from those of malathion upon its removal at 5 h.

To investigate whether the effects of GTN were maintained for 5 h and that NO was continuously being generated from the GTN, we compared the concentration of NO in the GTN-containing perfusate with that of the dialysate at intervals during the experiment. The concentration of NO in the perfusate was 9.18 ± 1.34 μM (11 probes in 6 subjects) and was not significantly different from that in the dialysate, which at 5 h was 12.75 ± 0.82 μM (N.S.). For comparison, the concentration of NO in PBS was 0.03 ± 0.01μM (n = 11).

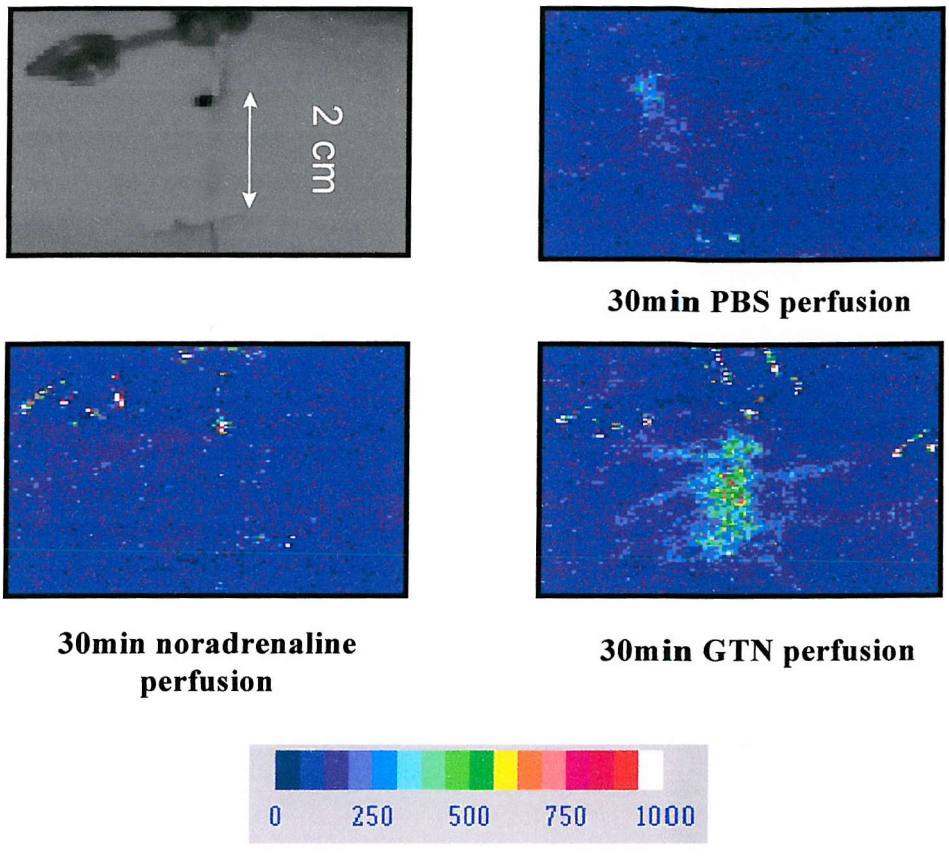

Figure 3.4 Effects of PBS, noradrenaline and glyceryltrinitrate on skin blood flow (A): The grey image on the top left corner was obtained using scanning laser Doppler imaging and represents a photograph of the forearm with the microdialysis probe in place. Microdialysis porbes were implanted under the surface of the skin of the forearm for a length of 2 cm. Scanning laser Doppler images were obtained before application of malathion (10 mg ml^{-1}, 0.5 ml) at sites treated with either PBS and/or PBS containing noradrenaline (0.005 mg ml^{-1}) or glyceryltrinitrite (GTN) (0.5 mg ml^{-1}) for 30 min.

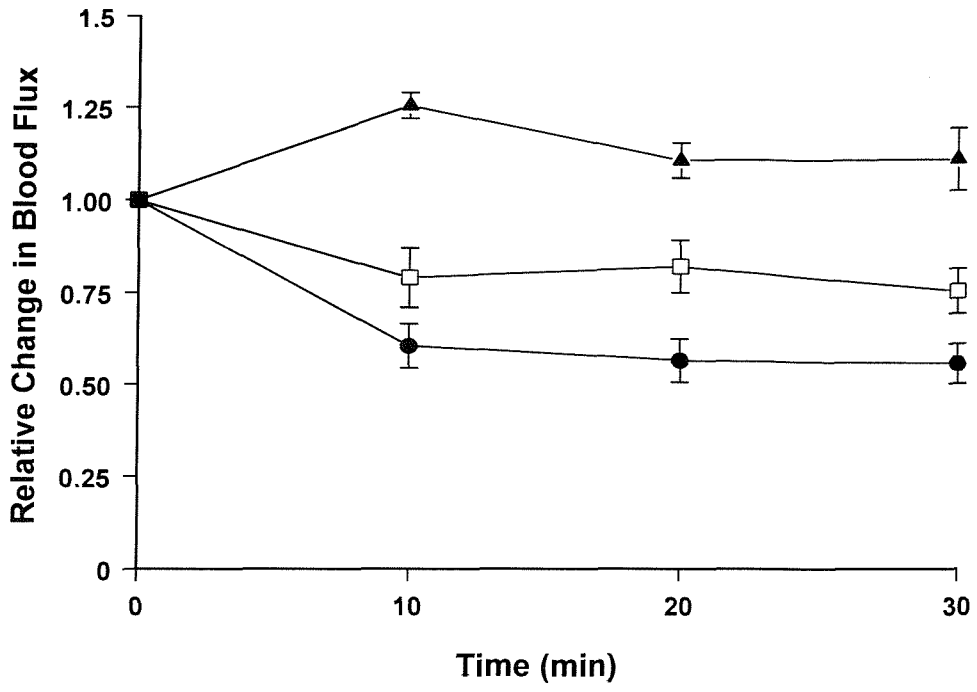

Figure 3.5 Effects of noradrenaline, glyceryltrinitrate on skin blood flow (B): Changes in mean blood flux relative to baseline values during probe perfusion with PBS (open squares), PBS containing noradrenaline (0.005 mg ml^{-1}, filled circles) or PBS containing glyceryltrinitrite (0.5 mg ml^{-1}, filled triangles). Values were calculated as a mean flux in an area 2 x 0.5 cm over the probe from scanning laser Doppler images. Data are mean ± sem (3 probes in 3 subjects for PBS and 4 probes in 4 subjects for both GTN and NA).

3.3.4 Effects of altered skin blood flow on the percutaneous absorption of malathion

Reducing skin blood flow by the addition of noradrenaline to the probe perfusate caused a significant increase in the amount of malathion recovered in dermal dialysate. At 4 h after application of malathion the concentration of malathion in dialysate increased to 600 ± 147 ng ml^{-1} (11 probes in 8 subjects) in the NA-perfused probes compared with a value of 71 ± 27 ng ml^{-1} (9 probes in 7 subjects) recovered from the PBS-perfused probes **(Figure 3.6)**. The total recovery of malathion in the presence of NA was 556 ± 140 ng over the 5 h experiment which was significantly greater than that recovered during perfusion with PBS (71 ± 18 ng, $P < 0.001$, ANOVA).

Addition of GTN to the probe perfusate appeared to have little effect on the concentration of malathion in the dialysate compared with that measured in the PBS-perfused probes. Four hours after application, the concentration in the GTN-perfused probes (60 ± 13 ng ml^{-1}, 6 probes in 5 subjects) was not significantly different from that in the PBS-perfused probes **(Figure 3.6)**. The total amount of malathion recovered in the GTN-perfused probes (55 ± 16 ng over 5 h) did not differ significantly from that recovered in the PBS perfused probes in the same subjects (N.S., ANOVA).

Interestingly, the slope of the initial rate of increase in the concentration of malathion in dialysate over the first 30 min was similar for all probes. However, whilst this rate of increase was not maintained in the GTN and PBS-perfused probes, it was maintained in the NA-containing probes.

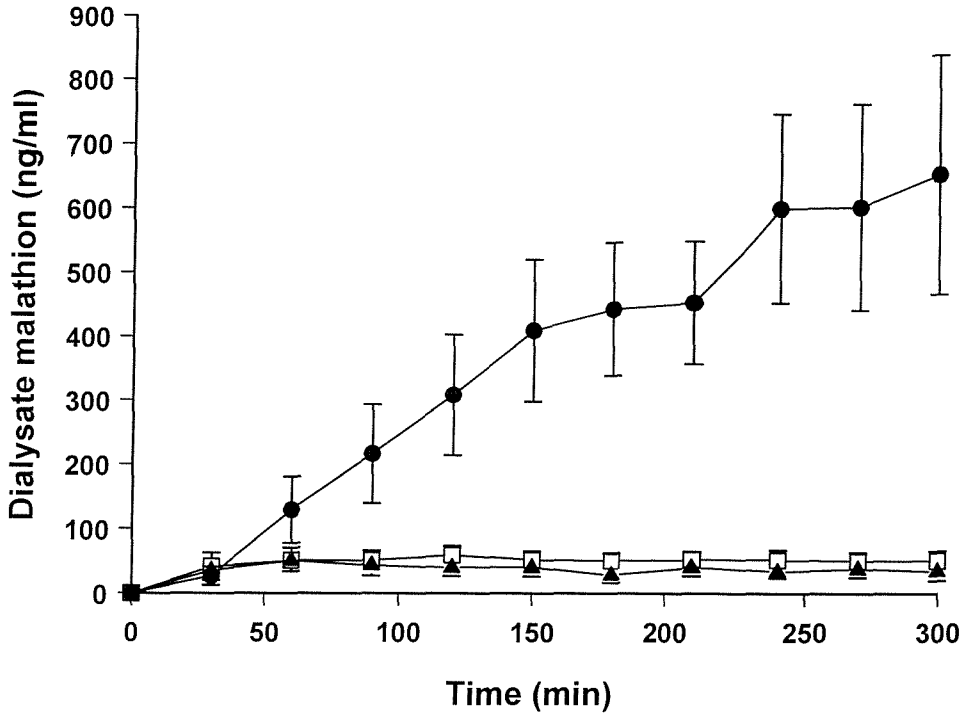

Figure 3.6 Effects of altered skin blood flow on the percutaneous absorption of malathion: Concentration of malathion in dialysate from microdialysis probes perfused with PBS (open squares), PBS containing noradrenaline (0.005 mg ml^{-1}, filled circles) or PBS containing glyceryltrinitrite (0.5 mg ml^{-1}, filled triangles). Probes were perfused for 30 min prior to the topical application of malathion (10 mg ml^{-1}) over the probes under occlusive dressing. Data are mean ± sem for PBS 9 probes in 6 subjects, NA 11 probes in 8 subjects and GTN 6 probes in 5 subjects. The amount of malathion recovered in the dialysate in the presence of noradrenaline was significantly greater compared to that in the presence of PBS ($P < 0.001$, ANOVA). No significant difference was observed between the GTN and PBS treated sites (N.S., ANOVA). Where error bars are not visible they lie within the symbol.

3.4 Discussion

This study shows that the organophosphorus compound malathion is absorbed through the skin of healthy human volunteers, *in vivo* and that the amounts absorbed are sufficient to cause a localised erythema. This study demonstrates that it is possible to follow the time course of the percutaneous absorption of malathion following topical application, using the technique of cutaneous microdialysis and that the concentration of malathion within the cutaneous tissue space, as determined by microdialysis, is dependent upon local tissue blood flow. It has also shown for the first time that the microdialysis technique may be used to manipulate the local tissue environment by addition of vasoactive agents to the probe perfusate.

3.4.1 The percutaneous absorption of malathion

The time course of the recovery of malathion in the dialysate demonstrates that malathion penetrates the skin relatively rapidly and that it is available for dialysis within the fluid phase of the tissue space within 30 min following application to the skin surface. Even though the *in vitro* efficiency of recovery of malathion (molecular mass 330 Daltons) was estimated to be more than 50 %, i.e. that approximately one half of the solute available for dialysis could be recovered under the conditions used, the recovery of malathion from the dermis over the 5 h of the experiment was very low (less than 0.002 % of the applied dose). This is not dissimilar to that reported by Benfeldt (Benfeldt *et al.*, 1999) for the recovery of salicylate and confirms that the intact epidermis presents a significant barrier to the percutaneous penetration of xenobiotics, including malathion. That none of the metabolite of malathion, malaoxon was detected in the dialysate is not surprising as the conversion of malathion to malaoxon has been shown to take as long as 4 h in human plasma (Mason *et al.*, 1992). Thus it is unlikely that it would be available in sufficient quantities for dialysis within the 5 h experimental period. Furthermore, malaoxon when available in the tissue will bind to AChE to inhibit the enzyme. The size of the AChE-malaoxon complex is such that it would be unable to enter the microdialysis membrane. To prevent this association and thus to facilitate recovery of malaoxon pralidoxime mesylate was used to release the AChE-bound malaoxon. However, no malaoxon was detected in the presence of pralidoxime mesylate and this is probably due to the very low-concentrations of the metabolite in the tissue.

3.4.2 Dermal vascular responses to malathion

Malathion, at the concentration measured within the dermis, caused a marked and long lasting erythema possibly through the inhibition of acetylcholineserase that leads to an increase in the levels of ACh in the tissue. That the vasodilatation is only evident 180 min after application of malathion may be due to the time taken to accumulate ACh within the tissue space in sufficient quantities to cause a visible erythema. Whether the cholinergic effects of malathion are restricted to the skin vasculature has yet to be investigated. There was no obvious oedema after 5 h exposure to malathion, nor did the subjects report any sensation of discomfort or itch during exposure. Thus, in this study, there is no evidence for malathion, in the aqueous preparation used, behaving as a contact sensitiser through activation of mast cells to release histamine (Sharma & Kaur, 1990; Rodgers & Xiong, 1997). In addition, the malathion-induced erythema did not extend beyond the area of treatment suggesting that under the conditions used in this study, malathion does not initiate a neurogenically mediated axon reflex flare. The concentration of malathion used was determined by the saturation limit of the aqueous vehicle but was similar to that in human miticide preparations. However, similar vasodilator responses were not seen with the commercial preparation tested, suggesting that the malathion in this formulation did not penetrate the skin in significant amounts, even when the barrier properties of the skin were disrupted by tape stripping. This is confirmed by our inability to detect malathion in dialysate from Derbac M treated skin, even after 5 h application, and is taken as evidence for a reduced bio-availability of malathion in this formulation, an important factor in its suitability for use to treat head lice in children.

3.4.3 Cutaneous blood flow and percutaneous absorption of malathion

Several factors have been shown to favour the systemic absorption of malathion following its use topically for the treatment of lice and scabies, including repeat application or taking a hot bath prior to application (Committee on Toxicity of Chemicals in Food, 1999). One of the aims in this study was to explore the contribution that the skin blood flow makes to the absorption of malathion. It has been previously demonstrated that the ability to dialyse a molecule is determined in part by its concentration within the extravascular fluid space and that this in turn will depend on the rate of delivery of the molecule to, and its removal from, the tissue space **(see section 2.3.3c)**. Removal from the tissue space will be determined by clearance by the

vasculature, by metabolism and also by the process of dialysis itself **(Figure 3.7)**. This is of particular significance for a small diffusible molecule for which the relative recovery by dialysis is high (Clough, 1999b). This study shows that reducing the vascular compartment by constriction of the arteriolar vascular bed with noradrenaline, results in an increase in the levels of malathion in the dialysis fluid and, by implication, the levels of malathion within the extravascular space. The finding that the concentration of malathion in dialysate under conditions of resting blood flux reached a steady state within 60 min suggests that under these conditions, malathion is being lost from the tissue space as rapidly as it enters it across the epidermal barrier. The continuing increase in the concentration of malathion in the dialysate from NA–perfused probes, where removal by the vasculature was significantly reduced, suggests that the epidermis remains the rate-limiting step in the systemic absorption of malathion in these experiments. However the eight-fold increase in dialysate malathion in the presence of NA confirms that the local vasculature does play a significant role in the removal of the OP from the dermis.

It was hypothesised that vasodilatation and hence expansion of the vascular compartment would increase the clearance of malathion from the tissue space into the systemic circulation, and that this would be seen as a reduction in the dialysate concentration of the OP. The failure to detect a significant reduction in recovery of malathion in the presence of GTN is most likely due to the fact that malathion itself causes a vasodilatation, such that the GTN-induced dilatation would have little additional effect. An alternative explanation for the failure to see an effect of GTN on tissue malathion concentration may be the development of tolerance to GTN during the 5.5 h perfusion period. A number of recent studies have suggested that, as well as being a NO donor through denitration and release of NO into the extravascular space, GTN may also have a direct effect on the endothelium to stimulate nitric oxide synthase (NOS) activity and that prolonged exposure to GTN may result in tolerance through depletion of L-arginine the substrate for NOS (Cheesman & Benjamin, 1994; Kodja *et al.*, 1998; Abou-Mohamed *et al.*, 2000). An attempt was made to study the effects of prolonged exposure to GTN by measuring the levels of NO/NO_2^- in the dialysate collected from the GTN-perfused probes. This was confounded by the unexpectedly high levels of NO in the GTN-containing perfusate. These high levels are most probably due to denitration of the GTN within the perfusion system that mask any changes in

dialysate NO due to tissue metabolism of GTN and NO generation. It is also possible that humoral mechanisms such as an increase in tissue levels of ACh may impair the biotransformation of GTN (Stewart *et al.*, 1986) and hence result in an attenuation of its vasodilator effects.

3.5 Summary

In summary, the present study demonstrates that following topical application malathion is absorbed into the dermal compartment and that changes in vascular perfusion of the tissue space have profound effects on the tissue levels of malathion. Thus it is concluded that substances such as malathion, which themselves increase dermal vascular perfusion can enhance their own systemic uptake and subsequent toxicity through a direct effect on the local vasculature. In addition this study has shown that exposure of healthy human skin to a single low-dose of malathion results in an intense long-lasting erythema, possibly due to accumulation of ACh in the tissue. The mechanisms underlying the increase in vascular perfusion after exposure to malathion are explored in the following chapters, along with the mechanisms involved in the responses of the vasculature to exogenous ACh.

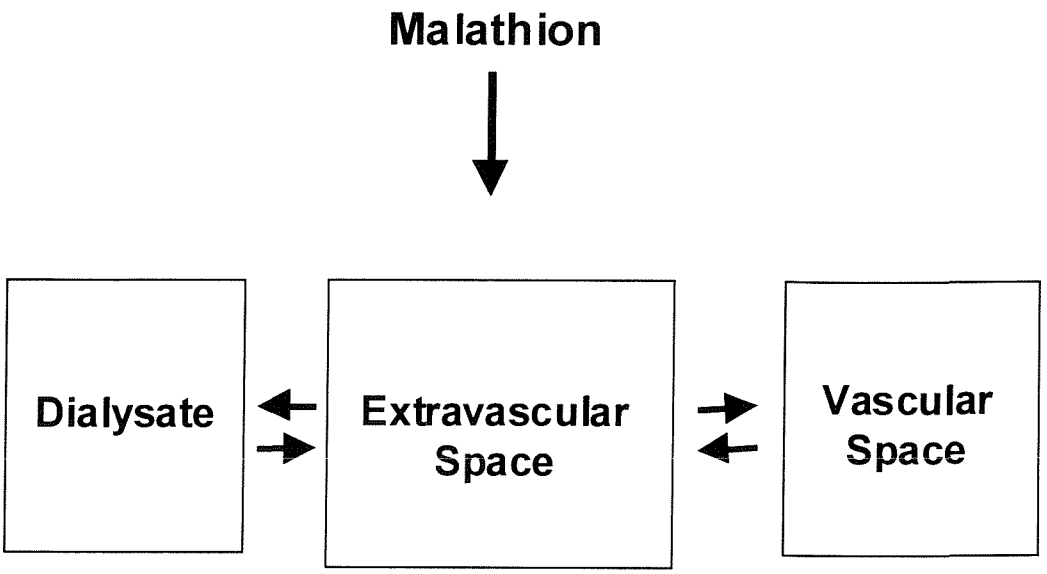

Figure 3.7 The distribution of malathion in the skin: Schematic representation of the distribution of malathion between compartments within the dermal space.

CHAPTER 4: THE ROLE OF ENDOGENOUS ACETYLCHOLINE AND NITRIC OXIDE IN THE MALATHION INDUCED ERYTHEMA- DIRECT MEASUREMENTS

4.1 Introduction and Aims

The results described in chapter 3 lead to the hypothesis that malathion inhibits acetylcholinesterase (AChE) in healthy human skin *in vivo* which results in the increase in the levels of acetylcholine (ACh) in the tissue. It is further hypothesised that the increase in endogenous ACh will result in vasorelaxation of the skin microcirculation, manifest as an erythemateous response to dermal application of malathion. Furthermore, it is known that the vasodilatation induced by exogenous ACh is mediated by the release of secondary mediators from the endothelium such as NO (Morris & Shore, 1996; Doyle & Duling, 1997), prostanoids (Noon *et al.*, 1998; Khan *et al.*, 1997) and endothelial derived hyperpolarizing factor (EDHF) (Bolz *et al.*, 1999; de Wit *et al.*, 1999). Therefore, this chapter describes experiments in which tissue levels of ACh and NO were assessed at malathion and control treated sites in human skin *in vivo*.

The aim of this study was to quantify changes in tissue levels of ACh and NO in the presence and absence of malathion in human skin *in vivo*. Microdialysis was used to continuously monitor ACh and NO released in the tissue before and during application of malathion over a period of 5 hours. Liquid chromatography combined with mass spectrometry was used to detect and quantify ACh in dermal dialysate. A chemiluminescence method was used to quantify the levels of NO in the dialysate samples. In this way the possible role of endogenous ACh and NO in the erythemateous response induced by malathion may be elucidated in human skin *in vivo*.

4.2 Materials and Methods

Two separate studies were performed to investigate:

1) Differences in the ACh levels in dialysate samples obtained at malathion and control treated sites.
2) Differences in the NO levels in the dialysate samples in the presence and absence of malathion.

4.2.1 Subjects

1) ACh release was measured in dialysate samples collected from the skin of the forearm of 2 female volunteers. The study was approved by the local ethics committee (JEC No: 301/98) and both subjects gave written informed consent.

2) Nitric oxide release was measured in dialysate samples collected from the skin of the forearm of nine healthy volunteers (4 men and 5 women) aged between 18–45 years. The study was approved by the local ethics committee (JEC No: 301/98) and all subjects signed informed consent form the day before the experiment.

4.2.2 Microdialysis

The characteristics of the microdialysis probes and the experimental procedures are described in detail in **chapter 2**. In both parts of the study up to six microdialysis probes were inserted in the volar surface of the forearm of the healthy volunteers as described in **sections 2.3.1**. The probes were perfused with phosphate buffered saline (PBS) for an initial equilibration period of 30 min before application of malathion and/or control above the microdialysis probes in occluded drug wells **(see section 3.2.3)**. The probes were perfused at 5 μl min^{-1} and dialysate samples were collected continuously for a period of 5 h over 30 min intervals. These were then stored at –20°C and up to 50 μl of each sample used for the assay of ACh and NO in study **(1)** and **(2)** respectively.

4.2.3 Assay of Acetylcholine in the dialysates

The method by Zhu *et al* (Zhu *et al.*, 2000) was modified to estimate the levels of ACh in dermal dialysates. The LC/MS system used in this study is an Agilent 1100 series LC/MSD equipped with an electronspray ionisation source. The analytical column was a Phenomenex Luna C18 100 mm long and with a 4.6 mm diameter. Thirty microlitre of standards and samples were injected using an autosampler. The mass spectrometer was operated in an API-ES (atmospheric pressure ionization-electronspray) positive mode.

Nitrogen was used as the auxiliary gas at a flow of 6 L min^{-1} and pressure of 30 psig. The capillary voltage was set at 3000 volts and the drying gas temperature was set at 300 °C. For the identification of ACh the mobile phase used consists of 10 % methanol (Aldrich), 20 mM ammonium acetate (Sigma) and 20 mM trifluoroacetic acid (TFA) (Aldrich, Lot: EI00641BI). The flow rate was set at 0.4 ml min^{-1}. For the first 3 min of analysis the effluent was diverted to the waste in order to reduce the amount of salt entering the mass spectrometer. Acetylcholine was monitored using selected ion monitoring (SIM) mode at m/z 146.1 to increase the sensitivity of the assay. The lowest standard of ACh detected using this method was 10 ng ml^{-1}. For the detection of the different components present in the dialysate samples the effluent was directed straight into the mass spectrometer without a delay. Positive ion scan mode was used for the detection of all m/z values present. The mobile phase used consists of water and acetonitrile (Aldrich). The flow rate was now set at 1 ml min^{-1} and 10 % of the mobile phase entered the mass spectrometer in a time dependent generic gradient. UV detection was set at 210 and 254 nm.

4.2.4 Assay of NO in the dialysates

The levels of NO in the dialysate were quantified using the chemiluminescence method described in chapter 2 **(see section 2.5.3)**. Dialysates (10 µl) were injected in the acidic sodium iodide (NaI) solution prepared in the vessel of the nitric oxide apparatus. Two injections were performed for each dialysate sample to account for pippeting errors. Extra PBS injections were performed at the start of each run to establish interference of noise and background levels of NO/nitrite. A calibration curve was constructed before the assay of the dialysates and was used to quantify the levels of NO/nitrite in the samples. This is expressed in concentration units (µM).

4.3 Results

4.3.1 Identification of acetylcholine in dialysate samples.

Different acids (heptafluorobutyric acid), formic acid and trifluoroacetic acid) were tested as volatile ion pairing reagents for the identification of ACh in the microdialysis samples. Heptafluorobutyric acid resulted in strong ion peaks in the mass spectrum that interfered with the ACh peak and reduced the sensitivity of the assay, whereas formic acid gave very broad chromatographic peaks. Therefore, trifluoroacetic acid was used as the ion-pairing reagent in the subsequent experiments.

Under these conditions acetylcholine (m/z 146.1) was eluted at 5.8 ± 1.2 min (n = 30, mean ± sem) in the LC/MS spectrum and was detected in all microdialysate samples (6 microdialysis probes in 2 volunteers) tested **(Figure 4.1)**. Using the conditions developed for the detection of the different components in the microdialysis samples five peaks were consistently observed in addition to the ACh peak at m/z 236 (2.1 ± 0.8 min), m/z 221 (5.2 ± 1 min), m/z 235 (6.2 ± 1.3 min), m/z 184 (7.5 ± 0.9 min), and m/z 214 (8 ± 0.3 min) (n = 30, mean ± sem) **(Figure 4.2)**. Identification of these peaks requires tandem mass spectrometry experiments, which cannot be carried out with the instrument used. Although ACh was successfully detected in the dialysate samples the construction of a calibration curve was extremely difficult because the shape of the ACh peak was broad and not reproducible. Hence it was not possible to quantify changes in the levels of ACh detected at malathion (n= 3 lines in 2 volunteers) and control treated sites (n=3 lines in 2 volunteers).

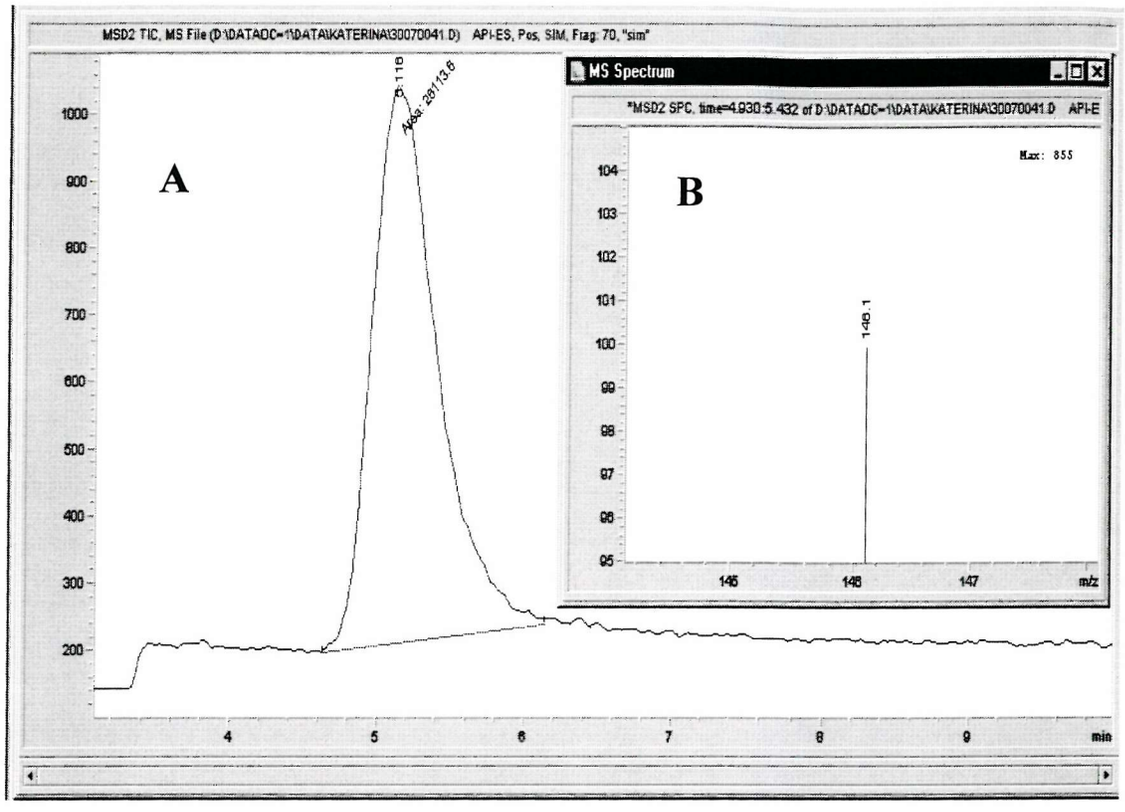

Figure 4.1 ACh levels in dialysate samples: Single ion monitoring of m/z 146.1. The chromatogram (**A**) shows a peak for ACh at 5.1 min and the MS spectrum (**B**) confirms the target mass.

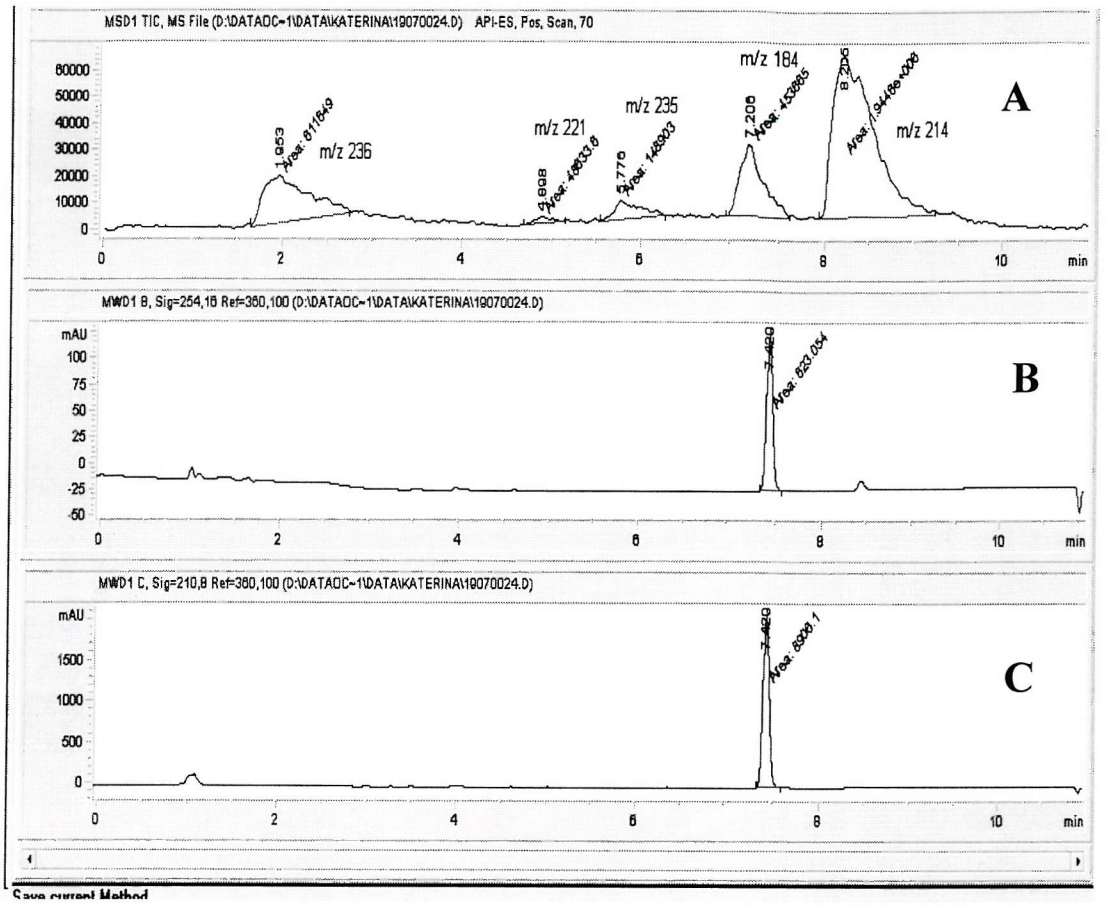

Figure 4.2 Dialysate components detected using LC/MS: Total ion chromatogram (TIC) (**A**) and UV spectra (254 nm, **B**) and (210 nm, **C**) of one dialysate sample. The above 5 peaks appeared consistently in the dialysate samples in the presence and absence of malathion. The UV chromatogram indicates the presence of an aromatic component that it is not observed on the TIC, due to the lack of ionisation sites. The absence of any other peaks on the UV chromatograms (both at 254 nm and 210 nm) suggests that the components detected by MS are aliphatic with low degree of conjugation (no chromophore).

4.3.2 NO measurements in the dialysates in the presence and absence of malathion.
The levels of NO in the dialysates were measured before and during the 5 h application of malathion over the microdialysis probes. The concentration of NO measured in the dialysates 5 h after malathion application (0.96 ± 0.2 μM) was not significantly different compared to the baseline samples (1.53 ± 0.24 μM) collected 30 min before malathion was applied on skin surface (N.S., n = 9) **(Figure 4.3)**.

A steep drop in the levels of NO in the dialysate (from 1.53 ± 0.24 μM to 0.6 ± 0.11 μM) was observed in the first 30 min of perfusion that is probably due to the depletion of the NO levels in the tissue surrounding the dialysis probe. These data are consistent with a previous study (Clough, 1999) where NO levels in the dialysate fell from a basal value of 1.24 ± 0.19 μM to one of 0.63 ± 0.09 μM after perfusion for 30 min. In the present study when perfusion was stopped at 120 min for less than 2 min to refill the perfusate in the syringe the levels of NO in the subsequent dialysate sample (1.72 ± 0.83 μM) increased towards its value in the initial dialysate sample (1.53 ± 0.24 μM) before falling for a second time over the next 30 min of perfusion (0.72 ± 0.14 μM) (n = 9).

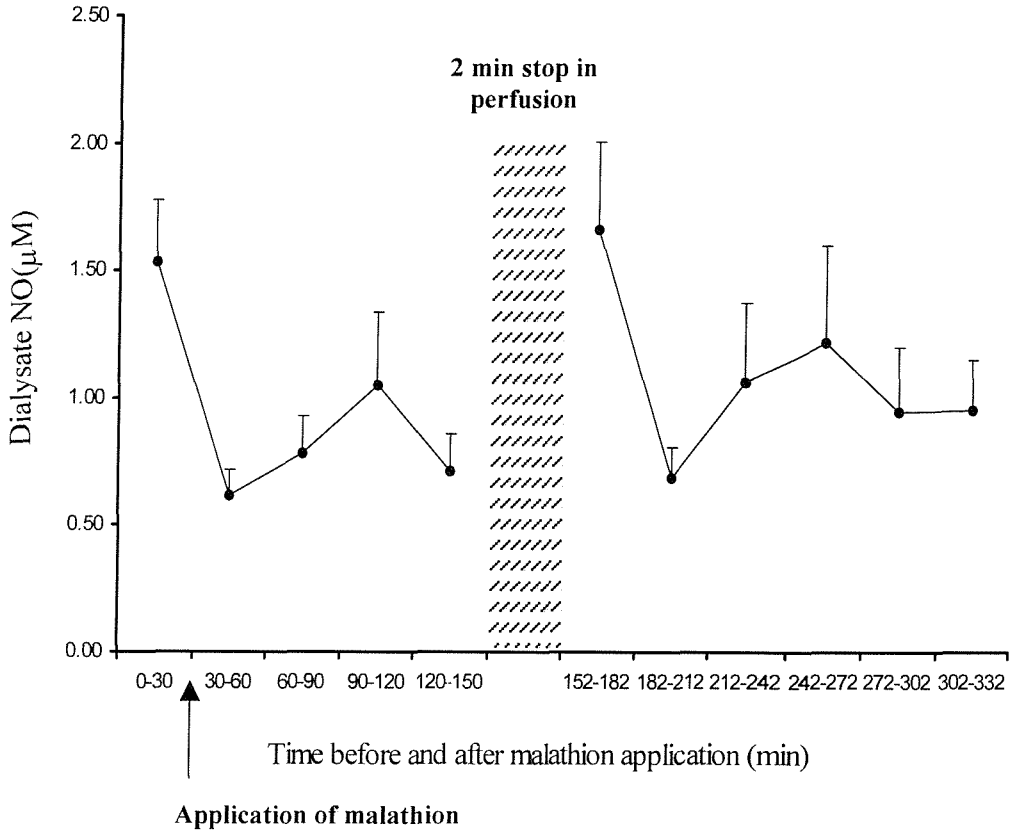

Figure 4.3 Dialysate levels of NO (μM) before and after application of malathion: NO levels were measured using a chemiluminescent method in the dialysate samples collected before and during application of malathion (10 mg ml^{-1}). Samples were collected continuously from the start of the experiment (0 min) up to 150 min of perfusion over 30 min intervals. At this point (150 min) perfusion of the probes was stopped for 2 min to refill the syringes. Perfusion was then continued up to 332 min and dialysate samples were collected as previously at 30 min intervals to the end of the experiment. Data are mean ± sem from nine subjects.

4.4 Discussion

It was the aim of the studies described in the present chapter to quantify malathion-induced changes in the levels of ACh and NO in the dialysate obtained from human skin *in vivo*, in order to elucidate the role of these mediators in the erythemateous response to malathion.

4.4.1 Acetylcholine levels in human skin *in vivo*

Acetylcholine was detected in dialysate samples obtained from human skin *in vivo* both at malathion and control treated sites using LC/MS. However, quantification of ACh levels in dermal dialysates was not possible as the construction of a calibration curve under the conditions used was extremely difficult as the ACh peaks were not consistently reproducible. However it will be possible to use a tandem mass spectrometer and the modified method developed in this study to identify compounds found in the microdialysis samples obtained from human skin *in vivo*. This will lead to a better understanding of the potential secondary mediators involved in the malathion–induced erythemateous response in human skin.

The ACh recovered by dialysis in the skin probably originates from non-neuronal cells such as keratinocytes, endothelial cells and fibroblasts (Wessler *et al.*, 1998; Wessler *et al.*, 1999) but could also derive from nerves. Acetylcholine has been detected previously in the skin using biopsy material taken from the superficial portion of human dermis. More recently the acetylcholine content of surface epithelial from human skin obtained from surgery was quantified using high performance liquid chromatography (HPLC) and estimated to be 1000 ± 300 pmol/g (Klapproth *et al.*, 1997). However, these techniques are invasive and in contrast to microdialysis do not allow continuous sampling of the tissue space. Furthermore the analytical method used is specific for the detection of ACh and the assay of different mediators is not possible.

4.4.2: The role of NO in the responses of the microvasculature to malathion

It was hypothesised that the malathion-induced erythema is a result of the increased levels of ACh and the subsequent increase in secondary mediators such as NO in the tissue space. Results from the present study demonstrate that the erythemateous response to malathion was not accompanied by an increase in the levels of NO in the dialysates. Previous studies have demonstrated that ACh when administered in the skin

induces vasorelaxation of the microcirculation, which is mediated partly by the release of NO (Morris & Shore, 1996; Doyle & Duling, 1997) as well as prostanoids (Noon *et al.*, 1998; Khan *et al.*, 1997), and EDHF (Bolz *et al.*, 1999; de Wit *et al.*, 1999). Alternatively it is possible that the increase in blood flow washes away the NO and limits the amount available for dialysis. The results from the present study may indicate that mediators other than NO are involved in the malathion-induced erythema in human skin.

In vitro experiments in rat brain have reported that malathion through its interaction with calcium/calmodulin inhibits nitric oxide synthase activity in a concentration dependent manner (Rao *et al.*, 1999). It is therefore possible that through its inhibitory action on acetylcholinesterase malathion results in the accumulation of ACh but that release of NO is prevented by its additional actions on NOS activity in the tissue.

4.5 Summary

The results presented in this chapter demonstrate that it is technically difficult to directly relate changes in the tissue levels of ACh to the malathion-induced erythema using microdialysis in human skin *in vivo*. They demonstrate that NO does not appear to play an important role as a secondary mediator in the malathion-induced vasodilatation. This however may be a result of an inhibitory action of malathion on NOS and does not preclude the release of other mediators in response to increased levels of ACh in the tissue. Therefore the initial hypothesis that the malathion-induced erythema is a result of the inhibition of AChE by malathion and the subsequent increase in the levels of ACh in the tissue is still valid and will be tested in the following chapters using indirect methods.

CHAPTER 5: A COMPARISON OF THE MALATHION-INDUCED ERYTHEMA AND THE DERMAL VASCULAR RESPONSES TO ACETYLCHOLINE

5.1 Introduction and Aims

As initial attempts to quantify changes in tissue levels of ACh in malathion exposed skin proved to be technically difficult, it was decided to investigate the modulatory effects of malathion on the AChE activity, indirectly, by comparing the vascular responses to ACh in the presence and absence of malathion. Prior to doing this it was necessary to characterise the cutaneous responses to ACh. As mentioned previously ACh may stimulate the release of NO (Morris & Shore, 1996; Doyle & Duling, 1997), prostanoids (Khan *et al.*, 1997; Noon *et al.*, 1998) and/or endothelial derived hyperpolarizing factor (EDHF) (Bolz *et al.*, 1999; de Wit *et al.*, 1999) from the endothelium, which then act upon the vascular smooth muscle cells to elicit changes in the vascular tone. In addition to its endothelial dependent effects, ACh can also induce vasodilatation through the stimulation of local sensory nerves (local axon reflex) (Benarroch & Low, 1991; Ralevic *et al.*, 1992; Berghoff *et al.*, 2002) or through stimulation of receptors on mast cells and subsequent histamine release (Cavanah *et al.*, 1991). Therefore, the dermal vascular responses to ACh along with the possible role of secondary mediators such as histamine and nitric oxide (NO) in these responses are measured in this chapter.

The objectives of this study were to quantify the responses of the skin microvasculature to exogenous ACh and to explore the possible role of histamine and NO in these responses. These findings were then related to the erythemateous response induced by malathion applied to healthy human skin *in vivo*. Microdialysis was used to deliver increasing doses of ACh to the dermis and to measure histamine and NO release in response to ACh challenge. The changes in the concentration of histamine and NO recovered in the dialysate were related to the changes in dermal blood flux measured using scanning laser Doppler imaging (SLDI) and to dermal sensation recorded using a visual analogue scale (VAS).

5.2 Materials and Methods

5.2.1 Subjects

Dermal vascular responses to increasing doses of ACh delivered by microdialysis were measured in 17 subjects (3 men and 14 women) aged between 18–48 years. Histamine release in response to ACh delivered to the dermis by microdialysis was measured in six (3 men and 3 women) of the volunteers. Seven of the female volunteers participated in the study to measure NO release in response to ACh and assess the effects of the nitric oxide synthase inhibitor (L-NAME) on the dermal vascular responses to ACh. The remaining four volunteers were excluded from the study due to hypersensitivity to the anaesthetic cream. Informed consent form was obtained from all subjects and the study was approved by the local ethics committee (JEC No: 138/01).

5.2.2 Microdialysis

The characteristics of the microdialysis probes and the experimental procedures are described in detail in **Chapter 2**. Up to 4 probes were inserted in the skin of one forearm and perfused for an initial 20 min equilibration period with PBS at 5 μl min^{-1}. The probe perfusate was then switched to one containing either 0.2 mM, 0.8 mM, 6.25 mM, 25 mM and 50 mM ACh and perfusion continued for a period of 6 min before switching back to PBS for a further 30 min recovery period. The probes were perfused randomly and sequentially to allow time for recovery between each provocation. Allowance was made at the start and the end of the ACh perfusion period for the dead space of the perfusion tubing connecting the probe to the pump (10 μl). The total volume of ACh delivered over the 6 min was 30 μl. If an approximate value of 30 % is allowed for the efficiency of microdialysis probes to dialyse ACh then the total amount of ACh delivered using the highest concentration of ACh (50 mM) tested may be estimated as 40.5 μg ACh.

Where the effects of inhibition of nitric oxide synthase (NOS) were to be investigated, L–NAME was added to the probe perfusate at a concentration of 5 mM (Clough, 1999) for a period of 40 min before perfusion of ACh (50 mM). Dialysate samples were initially collected over 5 min periods during the first 20 min of PBS perfusion and then over 2 min intervals during ACh challenge and for the remainder of the experiment. Samples were stored at –20 °C prior to assay for histamine and NO release.

5.2.3 Assessment of cutaneous blood flow

Skin blood flux was measured using scanning laser Doppler imaging at the beginning and the end of both the 20 and 40 min baseline perfusion periods, 2 and 5 min after the start of ACh perfusion and at 10 and 30 min during the recovery period as described previously in **section 2.4.1**. The direct effects of ACh on skin blood flux were assessed within a region of interest (ROI) of 2 x 0.5 cm^2 above each dialysis probe and expressed as mean blood flux in perfusion units (PU) calculated using the manufacturer's software. The area of the wider spread (neurogenic flare) response to ACh was also calculated. The distance that the flare spread either side of the microdialysis probe was also measured from the laser Doppler images.

5.2.4 Dermal sensation

Dermal sensation in response to the increasing doses of ACh was scored at 20 sec intervals during probe perfusion with ACh using a 10 cm visual analogue scale (VAS). The total itch response was calculated as a fraction of the maximum possible VAS score over the 6 min stimulation period (190 cm).

5.2.5 Assay of NO and histamine in dermal dialysate

NO in dermal dialysate was assayed using the chemiluminescensce method described in detail in **section 2.5.4**. The concentration of NO/NO_2^- in PBS and PBS-containing L-NAME was also measured.

The concentration of histamine in the dialysate samples was quantified using an enzymatic immunoassay as described previously in **section 2.5.3.** Baseline dialysate samples (50 μl) were diluted to 100 μl with PBS (50 μl PBS) prior to the assay. Similarly the dialysate samples collected during and after the challenge with ACh (10 μl) were diluted with PBS (90 μl PBS added in 10 μl dialysate sample) before the assay.

5.2.6 Statistical analysis

Where statistical comparisons were made a Student's t-test for paired data and/or analysis of variance (ANOVA) was used as appropriate. A probability value of $P < 0.05$ has been taken as significant. All subjects acted as their own controls.

5.3 Results

5.3.1 Dermal vascular responses to exogenous acetylcholine.

Baseline values of mean skin blood flux measured in the ROI (2 x 0.5 cm^2) above the probe varied between subjects and sites with values ranging from 88 PU to 360 PU (212 ± 42 PU). Mean blood flux values measured at 2 and 5 min during challenge with increasing concentrations of ACh (0.2 mM up to 50 mM) were at all times significantly greater than the baseline value measured at the same site **(Table 5.1)**. Mean blood flux increased linearly with increasing doses of ACh **(Figure 5.1)**. The peak response to ACh at highest dose was approximately 700 PU that was lower compared to the highest signal recorded (1068 PU) using the LDI. The ACh-induced increase in blood flux was maintained throughout the 6 min ACh perfusion period and then fell rapidly to return towards baseline levels by the end of the 30 min recovery period.

In addition to the direct dose-dependent increase in skin blood flux over the microdialysis probe, ACh also caused a dose-dependent neurogenic flare response surrounding the dialysis probe at perfusate concentration of ACh greater than 6.25 mM ($P < 0.001$) ($n = 6$ for 6.25 mM and 25 mM and $n = 7$ for 50 mM). No significant flare response was observed during challenge with the two lower concentrations (0.2 mM and 0.8 mM) of ACh **(Figure 5.2).** A reduction in the response by, 42 ± 9 %, 25.5 ± 6 % and 19 ± 8 % respectively was observed at 5 min challenge with 6.25 mM, 25 mM and 50 mM ACh respectively. The response was still visible 10 min after the end of ACh perfusion but had returned towards baseline by 30 min.

	MEAN BLOOD FLUX (PU)		
	Baseline before ACh	**2 min ACh perfusion**	**5 min ACh perfusion**
50 mM ACh	138 ± 16	703 ± 56 **	711 ± 39 **
25 mM ACh	219 ± 33	813 ± 56 **	883 ± 52 **
6.25 mM ACh	255 ± 40	714 ± 28 **	705 ± 34 **
0.8 mM ACh	229 ± 77	566 ± 69 *	502 ± 51 *
0.2 mM ACh	221 ± 42	352 ± 37 *	356 ± 55 *

Table 5.1 Mean blood flux measurements before and after challenge with ACh: Local vascular responses to ACh given via a dialysis probe. Mean blood flux was measured within an area of 2 x 0.5 cm^2 above the probe before and at 2 and 5 min during challenge (**P<0.001 and *P<0.01 challenge vs baseline). At all concentrations of ACh the increase in mean blood flux at 5 min was not significantly greater than that at 2 min. Data are presented as mean ± sem (n = 6 for 0.2 mM up to 25 mM and n = 7 for 50 mM) and expressed in perfusion units (PU)

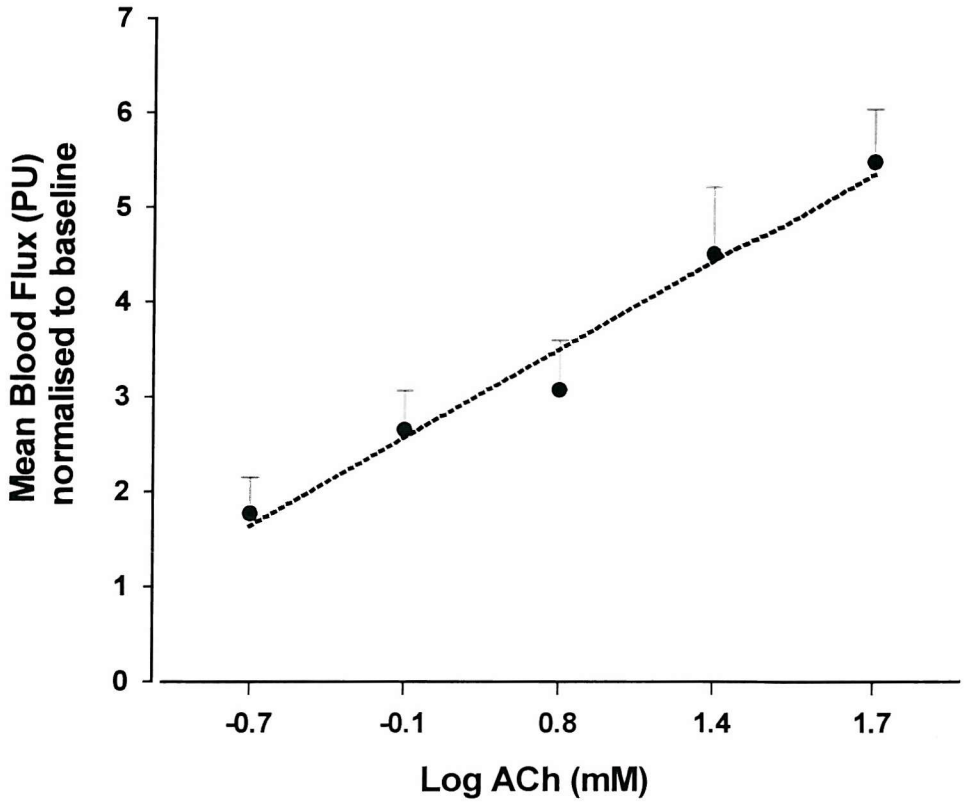

Figure 5.1 Dose-response to ACh: Mean blood flux measured directly over the probe after 5 min perfusion with ACh increased linearly to the logarithm of increasing doses of ACh used (0.2 mM, 0.8 mM, 6.25 mM, 25 mM and 50 mM). Data from 6 (0.2 up to 25 mM ACh) and 7 subjects (50 mM) are presented as mean ± sem and expressed in perfusion units (PU).

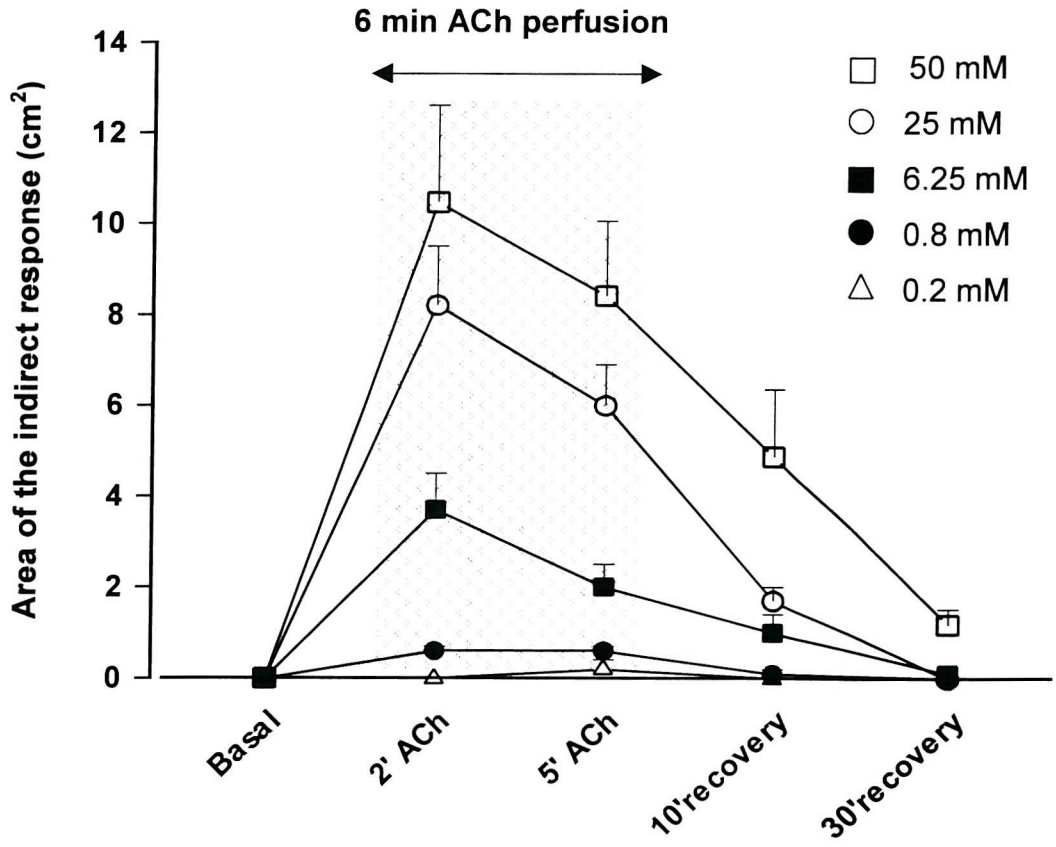

Figure 5.2 ACh-induced neurogenic responses: The area of the ACh-induced indirect response was calculated from the scanning laser Doppler images obtained at 2 and 5 min during perfusion (shaded area) with different doses of ACh and at 10 and 30 min after challenge (recovery). Data are mean ± sem (n = 6 for 0.2-25 mM and n = 7 for 50 mM).

5.3.2 The effects of L-NAME on the vascular responses to exogenous ACh

Addition of L–NAME to the PBS perfusate caused a small but not significant fall in basal mean blood flux in the area of the probe in resting skin **(Figure 5.3)**. It significantly reduced the increase in mean blood flux following perfusion with ACh (50 mM) by more than 27 % ($P < 0.007$, $n = 7$) as well as the time taken to return to baseline **(Figure 5.3)**.

L–NAME had little effect on either the area of the indirect response, which was not significantly different from that measured in PBS perfused probes (8.6 ± 1.2 cm^2 at 2 min falling to 8 ± 0.9 cm^2 by the end of 6 min perfusion with ACh, $n = 7$), nor the distance the response extended either side of the probe (total width: 3.2 ± 0.4 cm with PBS and 3.7 ± 0.4 cm with PBS+L–NAME).

5.3.3 Dermal Sensation to ACh

Immediately after the start of perfusion with ACh all volunteers reported the sensation of burning itch in the area surrounding the probe. The intensity of the sensation increased with increasing concentrations of ACh, and was minimal in the presence of the lowest concentration of ACh (0.2 mM) tested. However, no significant differences were observed in the total itch (maximum 190 over the 6 min perfusion) scored after perfusion with 6.25 mM, 25 mM and 50 mM ACh which was calculated as 18 ± 6 cm, 29 ± 8 cm and 23 ± 5 cm respectively. In contrast the total itch score after challenge with 0.2 mM and 0.8 mM ACh was significantly lower compared to the values reported for the higher concentrations of ACh (0 and 4.1 ± 2.6 respectively, $P < 0.01$, $n = 6$). The time course of the VAS scoring during ACh perfusion showed dermal sensation to peak at approximately 1 min after the start of perfusion for the different concentrations of ACh and to have returned towards baseline by the end of perfusion period (6 min). All subjects reported that the sensation was cyclical, with a frequency of about 2 min. L–NAME had no significant effect on the total itch score, which was calculated as 14 ± 2 cm with L–NAME pre–treatment and 23 ± 5 with PBS (N.S.) **(Figure 5.4)**.

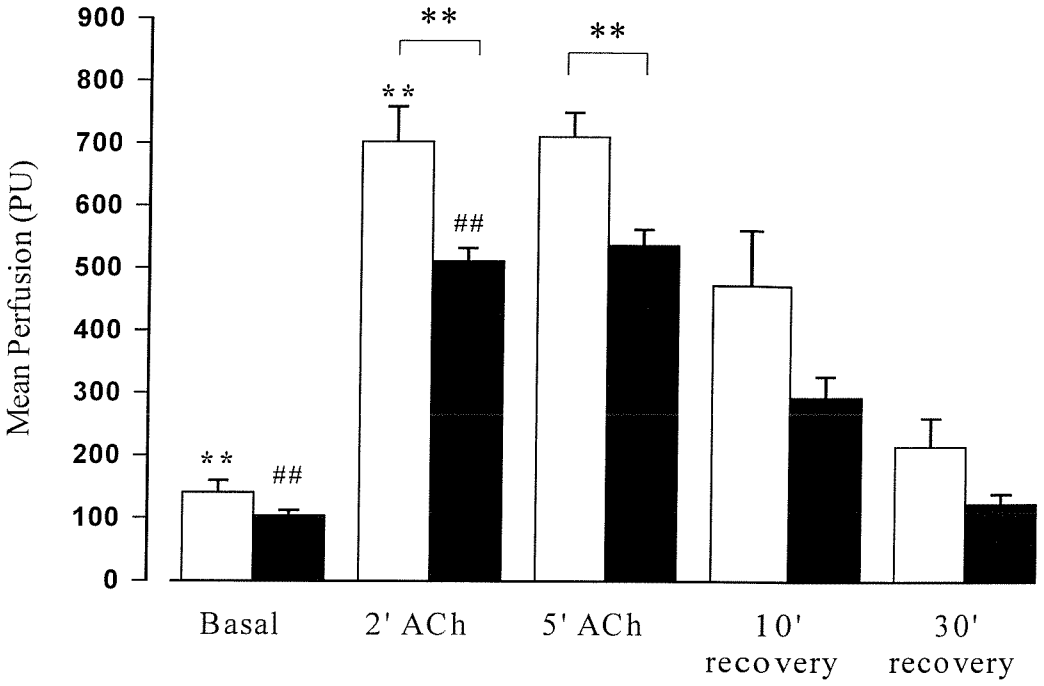

Figure 5.3 Effects of L–NAME on the direct local vascular response to ACh: Mean blood flux values (PU) were measured within an area of 2 x 0.5 cm^2 above the dialysis probe before, during and after perfusion with 50 mM ACh in the absence (open bars) and presence (hatched bars) of L-NAME (5 mM). The ACh–induced increases in blood flux at 2 and 5 min after ACh perfusion both in the presence and absence of L–NAME are significantly different when compared to basal values (** $P < 0.01$ and ## $P < 0.01$, $n = 7$, paired t-test) and are significantly attenuated by L–NAME (** $P < 0.01$, $n = 7$, paired t-test).

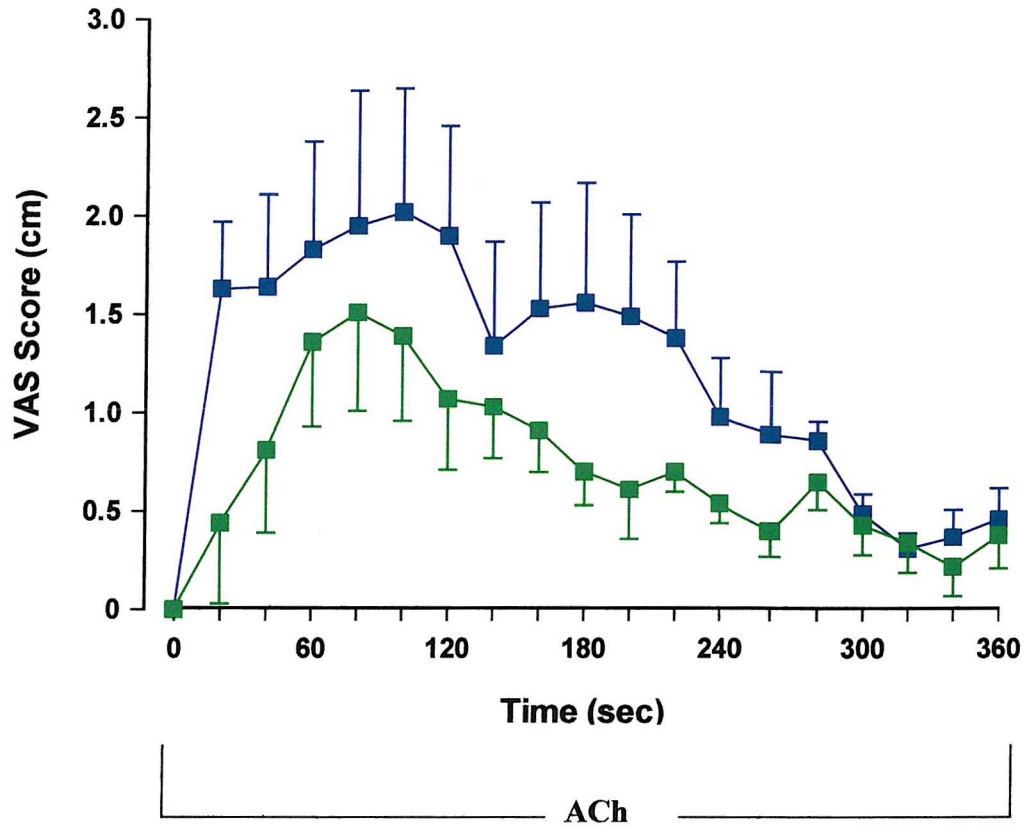

Figure 5.4 Effects of L–NAME on the dermal sensation induced by 50 mM ACh: Dermal sensation was scored in a 10 cm visual analogue scale (VAS) at 20 sec intervals during perfusion of the microdialysis probes with ACh (50 mM, 5 µl min^{-1} for 6 min) in the absence (blue squares) and presence of L–NAME (green squares). Data are mean ± sem from 7 volunteers (N.S., ANOVA).

5.3.4 Release of histamine in the dialysate in response to acetylcholine stimulation

Basal levels of histamine measured in the dialysates before challenge with ACh were estimated at (4.3 nM) but values varied between subjects ranging from 1.7 nM up to 240 nM. ACh-induced increase in the levels of histamine in the dialysate was independent of the dose of ACh used. The total amount of histamine recovered in the dialysate before challenge (1.1 ± 0.3 pg) was not different from that measured in dialysate obtained during the 6 min challenge with ACh (0.7 ± 0.5 pg for 0.2 mM, 1.1 ± 0.5 pg for 0.8 mM, 0.7 ± 0.4 pg for 6.25 mM, and 0.8 ± 0.4 pg for 25 mM).

5.3.5 Release of nitric oxide in the dialysates in the presence and absence of L-NAME

ACh (50 mM) caused a two–fold increase in the dialysate concentration of NO during the first 2 min of perfusion, levels increasing from a baseline value of 0.27 ± 0.05 μM to a peak of 0.60 ± 0.12 μM ($P < 0.03$, $n = 7$). As perfusion with ACh continued, the concentration of NO in dialysate fell to a mean value of 0.33 ± 0.08 μM most probably due to the maintained increase in cutaneous blood flow in the area of the probe and subsequent clearance of NO from the tissue space (Clough, 1999). L-NAME did not cause a significant change in the basal levels of NO in the dialysate (0.27 ± 0.05 μM without L-NAME compared with 0.61 ± 0.1 with L-NAME). However, the initial increase in dialysate NO concentration during ACh perfusion was totally abolished in the presence of L–NAME added to the probe perfusate **(Figure 5.5)**.

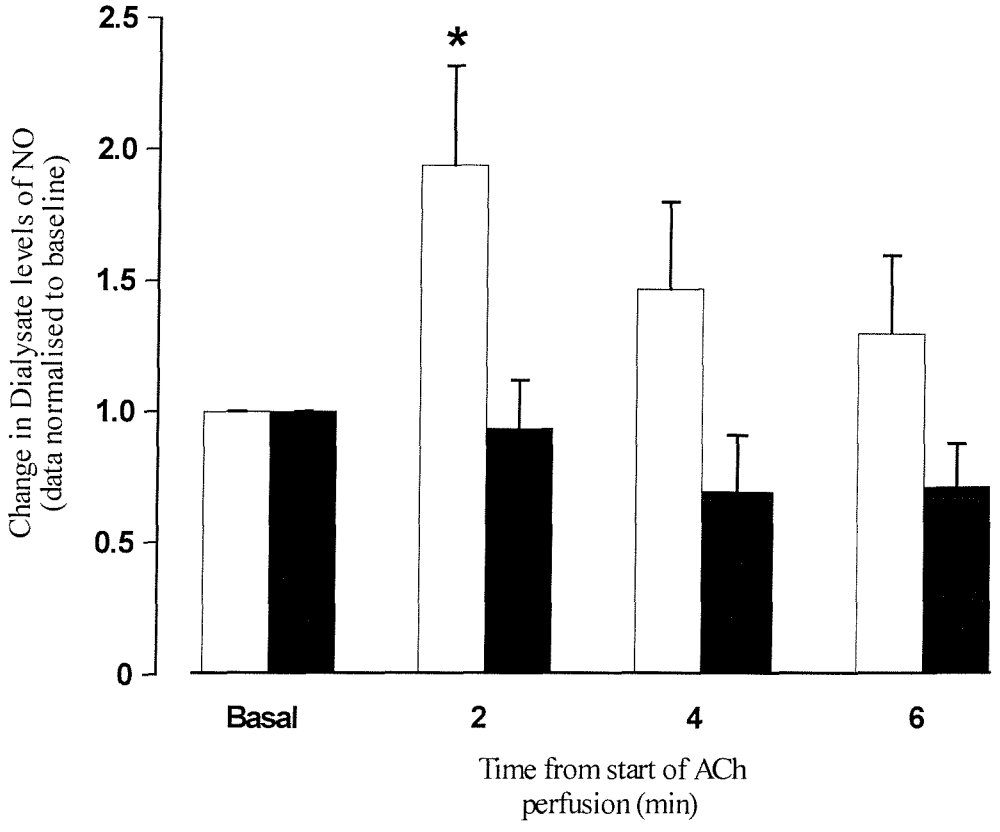

Figure 5.5 Effects of L–NAME on the ACh-induced NO release in the tissue: Changes in the dialysate levels of NO were measured before and during perfusion with ACh in the absence (open bars) and presence (hatched bars) of L–NAME (5 mM). Basal measurements were made 40 min after the start of perfusion of the probes with either PBS or L–NAME. Because of inter-subject variability in basal NO values for ACh-induced NO release are normalised to baseline. Data are mean ± sem from 7 subjects (*$P < 0.05$, paired t-test).

5.4 Discussion

In this study it has been demonstrated that exogenous ACh delivered to the skin via microdialysis results in a dose-dependent increase in blood flow that is accompanied at the higher doses by a widespread area of vasodilatation and the sensation of burning pruritus. Furthermore data from the present study provide direct evidence that ACh induces the release of NO in human skin but that the vasodilator response to ACh is only in part mediated by NO. It is also evident that neurogenically mediated changes in cutaneous blood flow in response to ACh involve mediators other than NO and histamine and that their release is not secondary to the generation of NO.

5.4.1 Dermal vascular responses to exogenous ACh

This study demonstrates that ACh delivered to the skin of healthy human volunteers via the microdialysis probe causes an intense short–lived erythema, which is accompanied by the sensation of burning pruritus. These findings are similar to previous studies where ACh caused a dose-dependent increase in skin blood flow after intradermal injection in the forearm and pain when applied to blister bases in man and rat skin (Ralevic *et al.*, 1992; Warren, 1994; Warren *et al.*, 1994; Berghoff *et al.*, 2002). The erythema runs along the whole length of the dialysis probe and is surrounded by a more widespread area of vasodilatation extending up to 5 cm either side of the probe.

Furthermore, the results demonstrate that all three components (local erythema, sensation and wide-spread vasodilatation) of the dermal vascular responses to ACh are dose-dependent and that the sensation and the widespread area of vasodilatation are only present when high concentrations of ACh are delivered to the tissue. This suggests that the mechanisms involved in modulating the dermal vascular responses to ACh may be different and that they are dependent on the concentration of ACh present in the tissue. It is well established that cholinergic vasodilatation is dependent on a functioning vascular endothelium and may be mediated by generation of nitric oxide (Morris & Shore, 1996), dilator prostanoids (Noon *et al.*, 1998) or EDHF (Bolz *et al.*, 1999). The ACh-induced indirect response has been previously reported in man and is thought to be mediated via stimulation of nicotinic receptors found on nociceptive axon terminals (Benarroch & Low, 1991) and/or mast cell degranulation and subsequent histamine release (Cavanah *et al.*, 1991).

5.4.2 The role of histamine in the vascular responses to ACh

In this study histamine levels in dermal dialysate collected before, during and after perfusion with ACh were measured using an enzymatic immunoassay. Baseline levels of histamine correlate well with the ones measured in dialysate samples from human skin by a sensitive radioimmunoassay (Petersen *et al.*, 1995; Clough *et al.*, 1998). However, the ACh-induced erythema was not accompanied by a significant increase in the concentration of histamine in the dialysate. These data suggest that histamine does not play a significant role in the dermal vascular responses to ACh and suggest that the widespread area of vasodilatation, as well as the sensation of burning pruritus that accompanied the ACh response, are not mediated via stimulation of cholinergic receptors on mast cells. Data from the present study are in contrast with previous studies performed mainly on isolated mast cells, which suggest that ACh and/or AChE inhibitors result in mast cell degranulation and subsequent histamine release (Fantozzi *et al.*, 1978; Cavanah *et al.*, 1991; Rodgers & Xiong, 1997).

Alternative mechanisms, such as direct stimulation of cholinergic receptors on local sensory nerves (Ralevic *et al.*, 1991) and subsequent release of vasodilator peptides for example calcitonin gene related peptide (CGRP) and substance P (Holzer, 1998), may be involved in the dermal vascular responses to exogenous ACh. Although a direct stimulation of local sensory nerves by ACh is possible, there is also evidence that secondary mediators such as nitric oxide and prostaglandins are associated with neurogenic vasodilatation in human skin and may result in the release of neuropeptides (Berghoff *et al.*, 2002).

5.4.3 The role of NO in the vascular responses to ACh

The dermal vascular response to ACh in this study was associated with an increase in the concentration of NO in the dialysate samples during ACh perfusion that was totally abolished by L-NAME. These data indicate that NO is produced in the tissue as a result of stimulation of the endothelium by ACh and are confirmatory of a role for NO in the vasodilator response of the microvasculature to ACh. In the present study L-NAME failed to reduce the basal levels of NO measured in the dialysates which is in contrast with previous studies by Clough where L-NAME caused a significant reduction in basal levels of NO (Clough, 1999). This may be a result of the low levels of NO measured in the dialysates in the absence of L-NAME or to a difference in the characteristics of the

study group e.g. age and sex. Thus the detection of a further reduction in the basal levels of NO in the dialysate would be difficult.

NO release is probably mediated through stimulation of cholinergic receptors on the surface of the endothelial cells by ACh and subsequent activation of specific G-proteins which in turn results in the production of NO from L–arginine, catalysed by NO synthase (NOS). NO may then diffuse out of the cell through the basement membrane and bind to the cytosolic guanylate cyclase of the smooth muscle cells. This induces a rise in cGMP and consequently smooth muscle relaxation **(Figure 1.5)**.

5.4.4 Effects of L-NAME on the ACh induced local erythema

Pre–treatment with L-NAME only partially decreased the ACh induced vasodilatation in the present study. The dose of L-NAME used in the present study was sufficient to abolish the ACh-induced release of NO in the tissue. Thus the data from this study suggest that mediators other than NO, such as prostaglandins and EDHF are involved in the response. These data are in agreement with data from different studies suggesting that more than one mediators are involved in the ACh-induced vasorelaxation of the cutaneous microcirculation (Morris & Shore, 1996; Noon *et al.*, 1998; Bolz *et al.*, 1999).

5.4.5 Effects of L-NAME on the ACh-induced indirect response and sensation of itch

As L-NAME failed to attenuate either the ACh-induced flare or itch, it is likely that the neurogenic response to ACh is mediated, independently of NO, via direct activation of sensory nerves by ACh. These data are in agreement with those from a study by Ralevic, who demonstrated that, in anaesthetised rats one component of the vasodilator response to ACh involves a direct action on the microvascular endothelium with subsequent generation of NO, while an additional component was elicited via the activation of sensory nerves and is largely independent of NO (Ralevic *et al.*, 1992). It is not possible to identify from the present data the mediator released by the action of ACh on sensory nerves. However Ralevic and colleagues suggested that CGRP was involved both because it can be localised to and released from sensory nerves and the vasodilator response of the microvasculature to CGRP was independent of NO (Ralevic *et al.*, 1992).

Other mechanisms may also be involved in the skin blood flow response to ACh. For example the spread of the vasodilator response to ACh may be attributed to the electronic spread of altered membrane potential via gap junctions on blood vessels. This conducted vasodilatation is a result of the spread of membrane hyperpolarization, which may be initiated after synthesis of EDHF and activation of K^+ channels. Doyle and Duling have demonstrated in the isolated arteriole, that sustained ACh stimuli induce local and conducted vasodilator responses. They have also shown that addition of L–NAME diminishes the local response and late phase of conducted response. However the early phase of the conducted response remains unaffected by L-NAME, suggesting that, both NO–dependent and NO–independent components are involved in the conducted response induced by ACh (Doyle & Duling, 1997).

5.5 Summary

Findings from the present study demonstrate the dermal vascular responses to exogenous ACh are dependent upon the concentration of ACh delivered to the tissue. It was not possible to elucidate all the mediators involved in the vascular responses to ACh but data from this study indicate that histamine does not play a role and NO only in part mediates the direct responses to ACh. The erythemateous response observed after application of malathion on human skin is not accompanied by any sensation and/or a widespread area of vasodilatation outside the site of application and therefore correlates well with the short-lived erythema observed when low-doses of ACh are delivered in the tissue. This suggests that similar mechanisms may underlie the two responses. Data from the present study also support the findings described in the previous chapter where the erythemateous response induced by malathion was not accompanied by NO but may still be mediated by the increased levels of ACh in the tissue with subsequent release of different secondary mediators **(see section 4.4.2)**.

CHAPTER 6: POTENTIAL MECHANISMS UNDERLYING THE MALATHION-INDUCED ERYTHEMA. I) THE ROLE OF ACETYLCHOLINESTERASE

6.1 Introduction and Aims

In previous chapters it was demonstrated that the responses of the vasculature to low-doses of exogenous ACh are similar to those induced by malathion. Unfortunately due to the increased levels of salt in the dialysate and the low-levels of ACh in the tissue, it was not possible to measure ACh directly in the dialysate and confirm its role in the malathion-induced erythema. Therefore, the next two chapters investigate the mechanisms underlying the malathion-induced erythema via an indirect method. In this chapter the hypothesis that the increase in cutaneous perfusion observed after application of malathion on healthy human skin *in vivo* is due to the inhibition of AChE and the subsequent accumulation of ACh is tested by investigating whether malathion enhances the duration of the responses of the microvasculature to exogenous ACh.

Although cases of non-specific skin rash (Schanker *et al.*, 1992) and other irritant responses (Sharma & Kaur, 1990) after exposure to malathion and other OP's have been previously reported, there are no epidemiological or other studies in which the mechanisms underlying these responses have been explored. This is mainly due to the lack of an experimental protocol using which direct evidence that these symptoms are unique to low-level OP exposure can be obtained. The experimental protocol developed in this chapter is used to quantify malathion-induced changes in the microvascular responses to exogenous ACh and other vasodilators.

It is the aim of the present study to explore and quantify differences in the responses of the microvasculature to exogenous ACh at malathion and vehicle-control treated sites. To do this a single dose of malathion and vehicle-control was applied on the skin of the forearm for 5 h. ACh was then delivered at both malathion and vehicle-control treated sites using iontophoresis and changes in skin blood flux assessed using LDF and SLDI. The combination of the two techniques is ideal for this study as LDF allows direct measurements of blood flux during iontophoretic delivery of ACh and SLDI provides quantitative data of any neurogenic responses around the area of drug application.

6.2. Materials and Methods

6.2.1 Subjects and experimental conditions

The study was in two parts. In the first part the responses of the microvasculature to iontophoretically delivered ACh and sodium nitroprusside at malathion and vehicle-control treated sites were investigated in 12 healthy volunteers (3 men and 9 women, average age 27 ± 2). For the second part of the study five of the volunteers (1 man and 4 women) returned 24 hours after removal of malathion and vehicle-control from the skin and the responses of the microvasculature to exogenous ACh were reassessed. The study was approved by the local ethics committee and all subjects signed informed consent forms the day before the experiment. Results from one subject who responded strongly to iontophoresis of vehicle and occlusive dressing application were excluded from the study.

6.2.2 Drug Application / delivery

Malathion: Malathion (1%) or vehicle-control were prepared, as described previously in **Chapter 2**, in an aqueous based gel and applied to areas of 2 x 2.5 cm^2 of the ventral surface of the forearm under occlusive dressing. After 5 h the formulations and drug wells were gently removed from the skin surface using a wet cotton wool and a period of 10 min was allowed for any irritation to settle down.

Acetylcholine: Iontophoresis was used to deliver ACh (2%, in distilled water) at malathion and vehicle-control treated sites both at less than an hour and 24 hours after removal from the skin. Distilled water was also iontophoresed at all of these sites to explore any non–specific responses of the microvasculature to current. Sodium nitroprusside (1%, in distilled water) was used as a nitric oxide donor to investigate for the non-endothelium dependent responses of the micro-vasculature. The protocol used in this study for the iontophoretic delivery of ACh and distilled water is described in detail in **section 2.3.5**.

6.2.3 Assessment of cutaneous blood flow

Scanning laser Doppler images were obtained before and after 5 h malathion or aqua gel application as described in **Chapter 2**. LDF was used in combination with iontophoresis to produce dose response curves to ACh, sodium nitroprusside and distilled water

during the iontophoretic protocol **(see section 2.4.2)**. At the end of the iontophoresis protocol the iontophoresis chamber was removed and the sites were gently dried using cotton wool. SLDI images were obtained 2-3 min after removal of the chamber as well as at 10 min, 20 min and 30 min after the end of iontophoresis **(see section 2.4.1)**. Both the iontophoretic protocol and the SLDI measurements were repeated 24 h after removal of malathion and vehicle-control from the surface of the skin.

Mean blood flux was calculated from SLDI images within a region of interest (ROI) 2 x 2.5 cm^2 consistent with the area of malathion or vehicle-control application **(Figure 6.1 A)**. The responses of the microvasculature to iontophoresis of ACh and/or distilled water at malathion and vehicle-control treated sites were classified as direct responses limited at the area of iontophoresis and indirect (neurogenic) responses that spread outside the area of ACh and/or distilled water iontophoresis **(Figure 6.1 B and C)**. Direct responses to ACh were measured within a ROI now set as a circle of 1 cm in diameter, matching the size of the iontophoresis chamber **(Figure 6.1 B)**. The change in blood flux in response to the iontophoreti delivery of ACh, SNP or distilled water was obtained by subtraction of the mean value for basal blood flux measured within the area of malathion and/or vehicle application. Indirect responses to ACh and/or distilled water were measured by selecting the response that spread outside the area of iontophoresis **(Figure 6.1 C)** following subtraction of the malathion induced response **(Figure 6.1 A)**. Two black dots (2 cm apart) were marked on the arm of the volunteer at the start of the experiment and used to convert the number of pixels within this area to cm^2.

6.2.4 Statistical analysis

Where statistical comparisons were made a Student's t-test for paired data and/or analysis of variance (ANOVA) was used as appropriate. A probability value of $P < 0.05$ has been taken as significant. All subjects acted as their own controls.

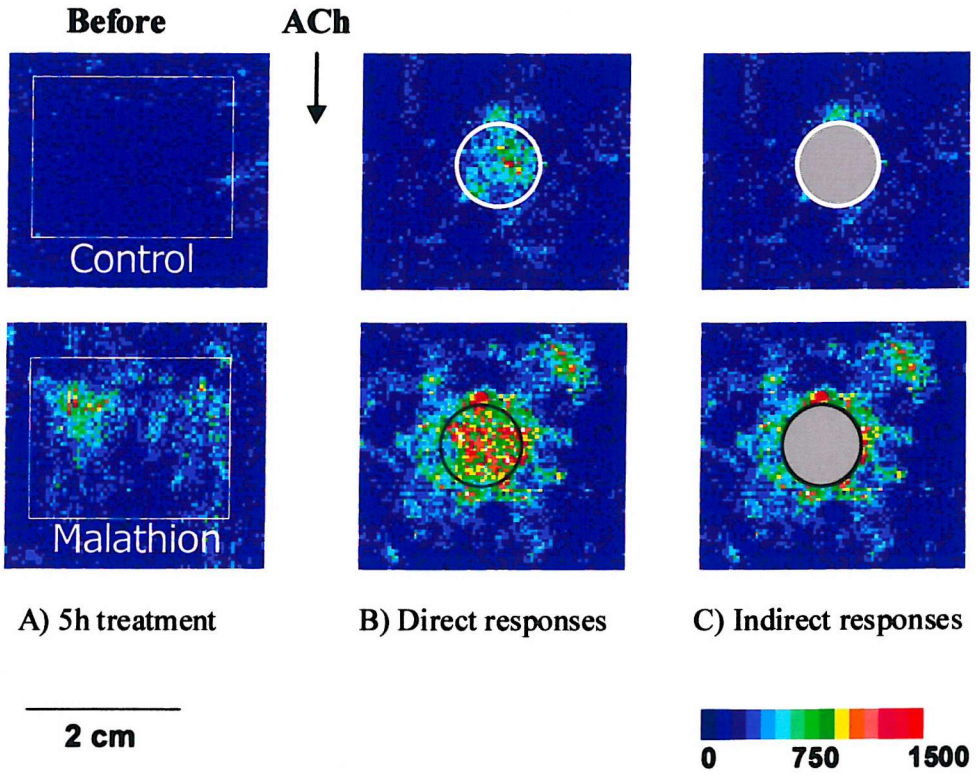

Figure 6.1 Scanning laser Doppler measurements: Mean blood flux (PU) was measured before and after 5h treatment with malathion and/or vehicle-control **(A)** within a region of 2 x 2.5 cm^2 (white square). Scanning laser Doppler images were also obtained after ACh iontophoresis at malathion and vehicle-control treated sites. Mean blood flux was measured directly over the area of iontophoresis **(B: within circle)** as well as outside the area of iontophoresis **(C: surrounding the circle)**.

6.3 Results

6.3.1a Effects of malathion on the dose response to ACh and SNP: Laser Doppler Fluximetry measurements during the iontophoretic protocol

Mean blood flux measured before the iontophoretic delivery of ACh at malathion treated sites was significantly greater than that at vehicle-control sites (37 ± 8.0 AU compared with 18 ± 3.5 AU, $P < 0.05$, n = 11). Iontophoretic administration of ACh in the skin caused a dose–dependent increase in mean blood flux both at malathion and vehicle-control treated sites. The ACh-induced increase in mean blood flux at vehicle-control treated sites was linearly related to the logarithm of the dose (μA x sec) of ACh delivered. Pre-treatment with malathion caused a shift in the ACh-induced dose response curve **(Figure 6.2)**. Immediately after the final dose of ACh mean blood flux had reach a value of 148 ± 28 AU (from a value of 18 ± 3.5 AU) at vehicle-control treated sites and a value of 153 ± 17 AU (from a value of 37 ± 8.0 AU) at malathion treated. The ACh-induced increase in mean blood flux from baseline vehicle-control treated sites (84 ± 4.8 %) and (73 ± 5.4 % AU) at malathion treated sites (N.S., n = 11).

The responses of the microvasculature to iontophoretic delivery of sodium nitroprusside also showed a dose–dependent increase in mean blood flux **(Figure 6.3)**. Malathion did not alter the linear relationship of the response. The sodium nitroprusside-induced increase in mean blood flux from baseline flux was not significantly different at vehicle-control (from 44 ± 16 before iontophoresis to 122 ± 29 AU) and malathion (96 ± 29 before iontophoresis to 171 ± 23 AU) treated sites (60 ± 10 % increase compared to 50 ± 10 % respectively) (N.S., n = 5).

Iontophoresis of distilled water did not cause any significant increase of mean blood flux over that measured before the iontophoretic delivery of distilled water at either vehicle-control (26 ± 5 before iontophoresis to 37 ± 8 AU, N.S., n = 6) or malathion (43 ± 15 before to 58 ± 17 AU, N.S., n = 6) treated sites **(Figure 6.3)**.

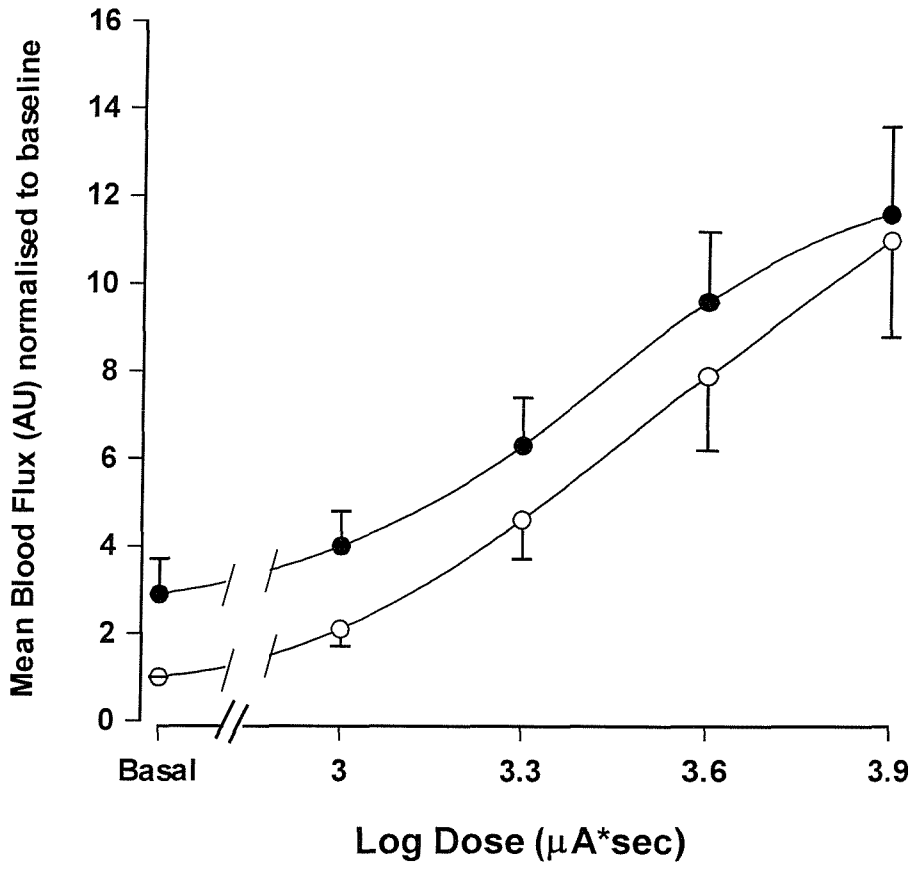

Figure 6.2 Effects of malathion on the dose-response to ACh: ACh (1%) was delivered at malathion (closed circles) and vehicle-control (open circles) treated sites using iontophoresis and changes in mean blood flux were measured using the laser Doppler fluximetry probe. Basal mean blood flux values measured before the iontophoresis of ACh were significantly different at malathion (37 ± 8.0 AU) and vehicle-control treated sites (18 ± 3.5 AU) ($P < 0.05$, $n = 11$). Thus the data are normalised to one baseline and are plotted against the log of the dose (μA*sec) of ACh delivered. Data are mean ± sem (n = 11).

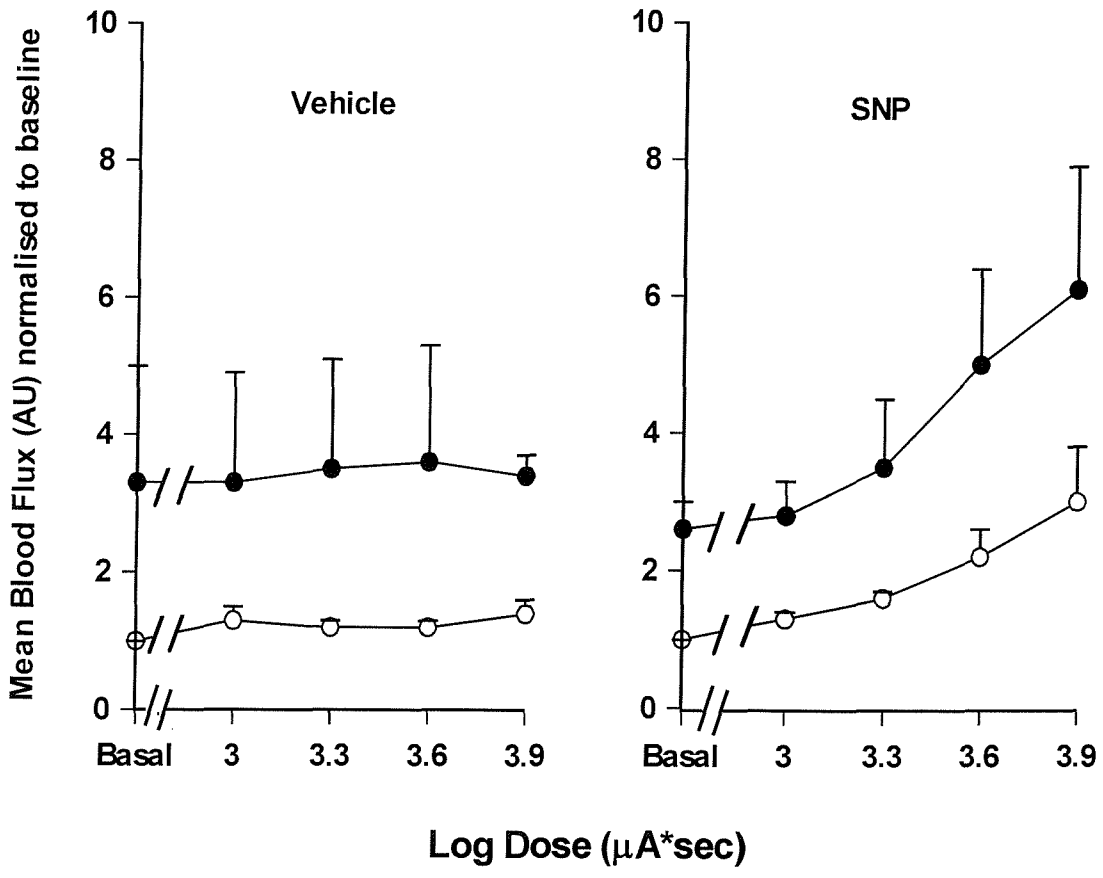

Figure 6.3 Effects of malathion on the dose-response to vehicle and sodium nitroprusside: Similarly dose-response curves were constructed for sodium nitroprusside (SNP, 2 %) and distilled water delivered at malathion (closed circles) and vehicle-control (open circles) treated sites. Mean blood flux values (AU) are normalised to baseline and plotted against the log of the dose (μA*sec) of ACh delivered. Data are mean ± sem (n = 5).

6.3.1b Effects of malathion on the duration and intensity of the responses of the microvasculature to ACh: Scanning Laser Doppler Imaging measurements

i) Direct Responses: The direct effect of ACh on the microvasculature at vehicle-control and malathion treated sites was measured immediately after the end of the iontophoresis protocol, using scanning LDI. The results are summarized in **Table 6.1** and indicate that ACh causes a significant increase in mean blood flux over the value obtained after 5 h treatment at both malathion and vehicle-control treated sites ($P < 0.01$ and $P < 0.001$ respectively, $n = 11$). Application of malathion did not significantly alter the intensity of the ACh induced increase in mean blood flux compared to the vehicle-control treated sites (590 ± 40 PU compared with 583 ± 58 PU) (N.S., $n = 11$). These findings are in agreement with the data obtained using the LDF probe **(see section 6.3.1a)**.

At all times the responses of the microvasculature to ACh were significantly greater than the responses to distilled water at both malathion and vehicle-control treated sites ($P < 0.01$, $n = 11$) **(Table 6.1)**. Iontophoretic delivery of distilled water did not cause a significant increase in mean blood flux above that caused by treatment with malathion or vehicle-control. No significant difference was observed when responses to distilled water iontophoresis at malathion sites are compared with those at vehicle-control treated sites (N.S., $n = 6$).

Pre-treatment of the skin with malathion prolonged the duration of the ACh-induced increase in mean blood flux compared with that at vehicle-control treated sites, which decreased rapidly towards baseline. The mean blood flux measured at malathion treated sites fell more slowly and at both 20 and 30 min after ACh iontophoresis and was significantly greater than that at vehicle-control treated sites ($P < 0.01$ at 20 min and $P < 0.001$ at 30 min, $n = 11$) **(Figure 6.4)**. The slopes of the recovery were calculated at malathion and vehicle-control treated sites for each individual from data normalised to the maximum increase in mean blood flux. The slope of the decay of the response at malathion treated sites (-0.11 ± 0.04 cm^2 min^{-1}) was significantly less compared to that at vehicle-control treated sites (-0.24 ± 0.03 cm^2 min^{-1}) ($P < 0.001$, $n = 11$) **(Figure 6.4)**.

MEAN BLOOD FLUX (PU) MEASURED USING SCANNING LDI DIRECTLY OVER THE AREA OF IONTOPHORESIS				
	Malathion Distilled water	**Control Distilled water**	**Malathion ACh**	**Control ACh**
Baseline	109 ± 5.9	106 ± 5	107 ± 6.7	104 ± 6.5
5h treatment	298 ± 48.8	134 ± 7.9	281 ± 39.1	129 ± 7.8
End of iontophoresis	235 ± 60	248 ± 86	590 ± 40	583 ± 58

Table 6.1 Mean blood flux measurements (direct) at malathion and vehicle-control treated sites before and after iontophoresis of vehicle and/or ACh: Mean blood flux (PU) values were measured at baseline, 5 h after malathion or vehicle-control treatment and immediately after the last dose of vehicle or ACh. Exposure to malathion for 5 h significantly increased skin blood flux when compared to baseline ($P < 0.001$) and 5 h vehicle-control treated sites ($P < 0.01$) ($n = 11$, mean ± sem). Vehicle-control treatment for 5 h resulted in a small increase in mean blood flux over baseline ($P < 0.01$). ACh significantly increased mean blood flux over 5 h treatment at both malathion and vehicle-control treated sites ($P < 0.01$ and $P < 0.001$ respectively, $n = 11$).

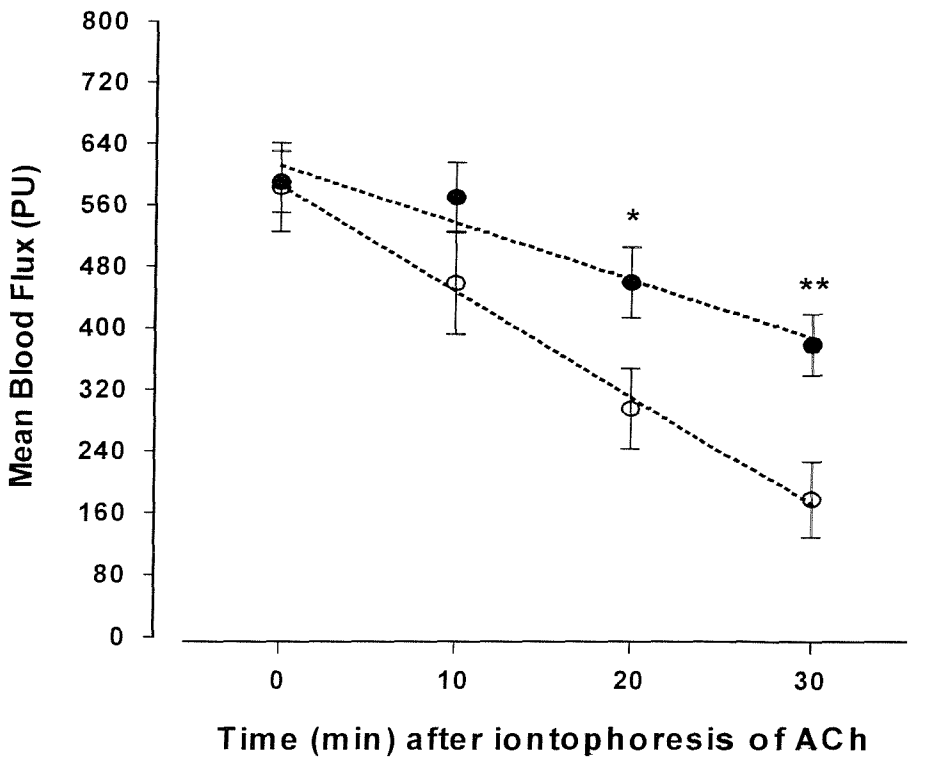

Figure 6.4 Effects of malathion on the responses of the microvasculature to ACh-i) Direct responses: Mean blood flux values (PU) at malathion (closed circles) and vehicle–control treated sites (open circles) were measured within a circle of 1 cm in diameter over the area of iontophoresis using scanning laser Doppler imaging. Data are mean ± sem (* $P < 0.01$ and ** $P < 0.001$, $n = 11$).

ii) Indirect Responses: Iontophoretic delivery of ACh caused an increase in skin blood flux that spread outside the area of iontophoresis (1 cm^2) at both malathion and vehicle–control treated sites. Application of malathion was found to augment the spread of the ACh-induced response that was twice as large as that at vehicle-control treated sites (2.4 ± 0.4 cm^2 compared with 1.2 ± 0.3 cm^2, $P < 0.001$, $n = 11$) **(Figure 6.5)**. Mean blood flux measured within that area outside the direct effect was also significantly greater at malathion treated sites compared to vehicle-control treated sites (434 ± 21 PU and 360 ± 29 PU respectively) ($P < 0.03$, $n = 11$).

Malathion also prolonged the duration of the ACh-induced indirect response compared to vehicle-control treated sites. The area of the flare response to ACh at malathion treated sites remained significantly greater compared to that at vehicle–control treated sites up to the 30 min time point **(Figure 6.5)**. The slope of the recovery of the response at malathion treated sites (-0.2 ± 0.03 cm^2 min^{-1}) was significantly smaller compared to that at vehicle-control treated sites (-0.33 ± 0.02 cm^2 min^{-1}) ($P = 0.02$, $n = 11$). Mean blood flux measured within this area was significantly greater at malathion treated sites compared to vehicle-control treated sites at all times after the end of the iontophoresis protocol. Hence 30 min after the end of the iontophoretic protocol mean blood flux within the flare area at malathion treated sites was 335 ± 20 PU and was significantly greater compared to 62 ± 37 PU at vehicle-control treated sites ($P < 0.001$, $n = 11$). In some subjects ($n = 4$) scanning laser Doppler images were taken at intervals for up to 60 min after the end of the iontophoresis protocol. At that point both the direct and the indirect ACh-induced responses at malathion treated sites had returned to baseline levels.

While the process of iontophoresis itself causes a minimal neurogenically mediated erythema (0.2 ± 0.06 cm^2 at malathion and 0.4 ± 0.2 cm^2 at vehicle-control treated sites), this is far smaller than that induced by ACh and does not significantly alter the interpretation of the results.

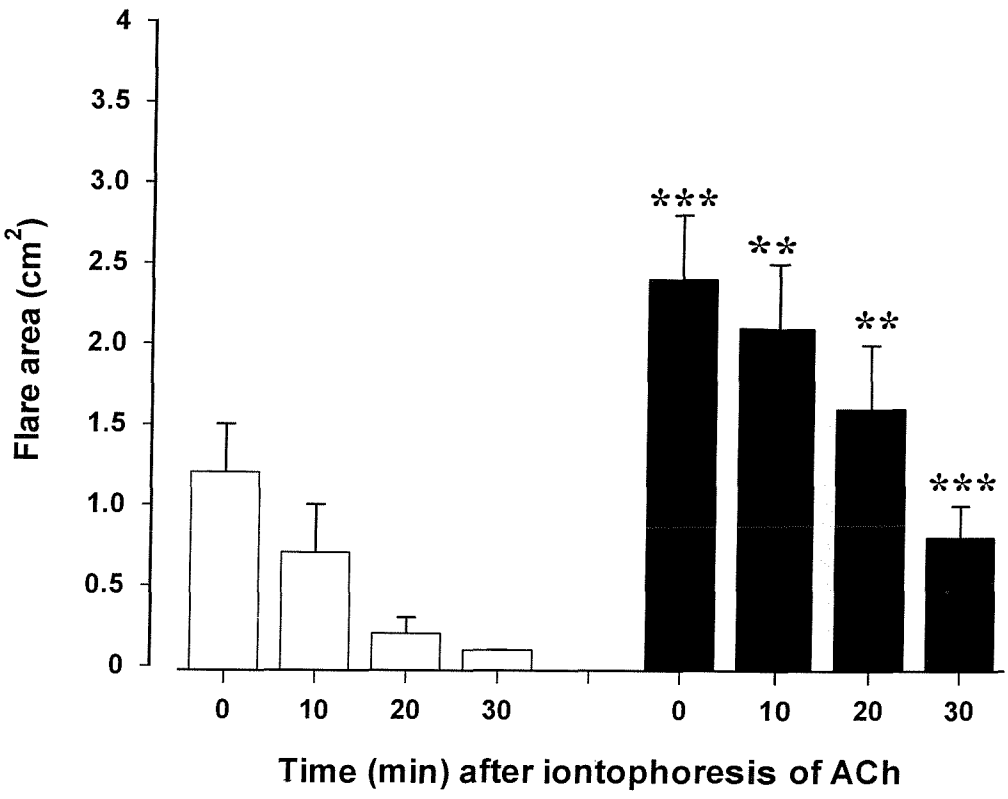

Figure 6.5 Effects of malathion on the responses of the microvasculature to ACh-ii) Indirect responses: The area of the ACh-induced vasodilatation outside the site of iontophoresis was measured at malathion (solid bars) and vehicle-control treated sites (open bars) using scanning laser Doppler imaging **(see pages 124 and 125)**. Data are mean ± sem from eleven healthy volunteers (** $P < 0.01$ and *** $P < 0.001$, malathion vs control, paired t-test).

6.3.2 Prolonged effects of malathion on the microvascular responses to ACh

Iontophoresis of ACh and vehicle was repeated 24 h after removal of malathion and vehicle-control from the skin in order to explore the prolonged effects of acute low-dose exposure to malathion on the responses of the microvasculature to ACh. As previously scanning laser Doppler images were obtained before and at 10 min intervals after the end of the iontophoretic protocol, and mean blood flux was measured both within (direct) and outside the area of iontophoresis (indirect).

a) Direct responses: ACh delivered to malathion and vehicle-control treated sites 24 h after their removal from the skin induced a significant increase in mean blood flux over baseline values, measured before the start of the iontophoresis. Mean blood flux immediately after the iontophoresis of ACh at the malathion treated site was not significantly different from that at the vehicle-control treated sites (598 ± 46 and 580 ± 105 PU respectively) (N.S., n = 5). However, the duration of the ACh-induced vasodilatation was prolonged by malathion 24 h after its removal from the skin compared with that at vehicle-control treated sites **(Figure 6.6)**. This is best demonstrated by calculation of the slopes of the recovery of the response to ACh at both malathion and vehicle-control treated sites for each individual. When the data were normalised to the maximum ACh-induced increase in mean blood flux in each subject, malathion 24 h after its removal from the skin, significantly reduced the rate of the recovery of the ACh-induced vasodilatation (slope: -0.14 ± 0.04 PU min^{-1}) compared to vehicle-control treated sites (slope: -0.27 ± 0.06 PU min^{-1}) ($P < 0.01$, n = 5). Further the slopes of the recovery obtained at malathion and vehicle-control treated sites 24 h after removal from the skin were not significantly different form those obtained at malathion (-0.12 ± 0.04 PU min^{-1}) and vehicle-control treated sites (-0.24 ± 0.03 PU min^{-1}) <1 h after their removal from the skin (N.S., n = 11). These data suggest that malathion exerts its effects for at least 24 h after its removal from the skin.

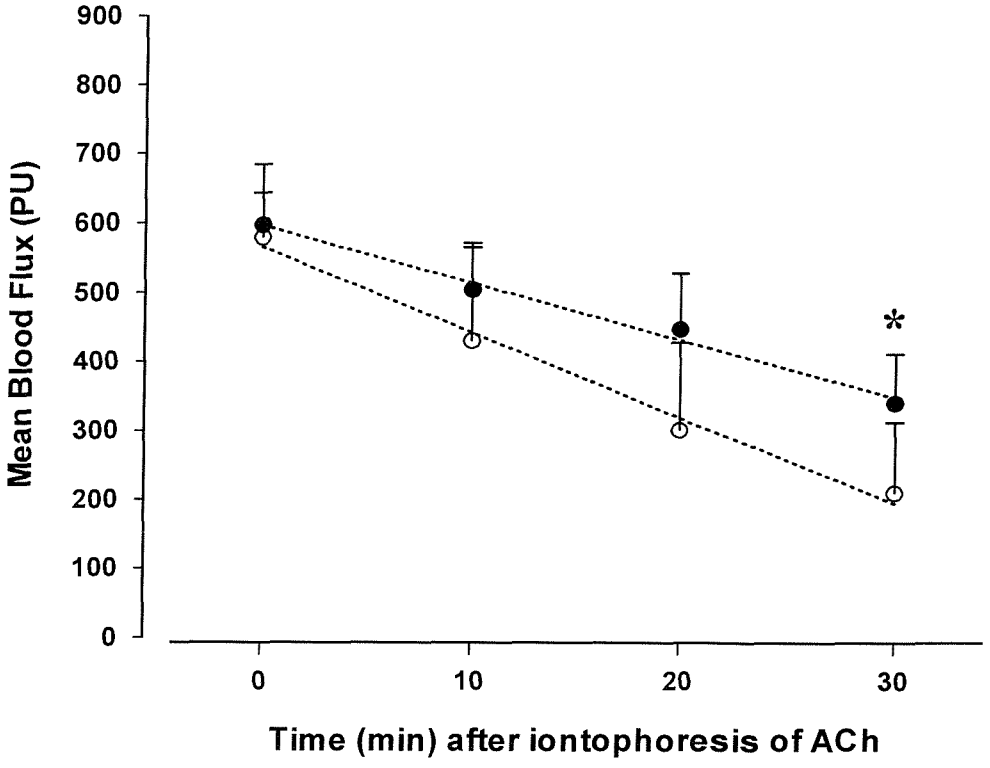

Figure 6.6 Prolonged effects of malathion on the microvascular responses to ACh a) Direct responses: Mean blood flux (PU) was measured immediately (0 min) and up to 30 min after the end of the iontophoretic protocol at both malathion (closed circles) and vehicle-control (open circles) treated sites 24 h after their removal from the skin using scanning laser Doppler imaging. Data are mean ± sem from five subjects (* $P < 0.05$,paired t-test).

b) Indirect (neurogenic) responses: The area of the ACh-induced erythema outside the area of iontophoresis was not significantly different at malathion treated sites (2 ± 0.7 cm^2) compared to the vehicle-control treated sites (1.3 ± 0.4 cm^2) 24 h after their removal from the skin (N.S., n = 5) **(Figure 6.7)**. Similarly no significant difference was observed in the mean blood flux measured within the area of the spread at malathion (385 ± 33 PU) and vehicle-control sites (305 ± 77 PU) (N.S., n = 5). However, malathion 24 h after its removal from the skin did extend the duration of the ACh-induced indirect response compared to vehicle-control treated sites. The slope of the recovery calculated from the maximum response to ACh at vehicle-control treated sites (-0.33 ± 0.01 cm^2 min^{-1}) was significantly greater compared to that at malathion treated sites (-0.18 ± 0.04 cm^2 min^{-1}) (P = 0.03, n = 5).

No significant difference was observed between the slopes obtained at <1 h and 24 h at malathion (-0.20 ± 0.03 and -0.18 ± 0.04 cm^2 min^{-1}) and vehicle-control (-0.33 ± 0.02 and -0.33 ± 0.01 cm^2 min^{-1}) treated sites respectively (N.S., n = 11). These data are in agreement with those obtained for the direct responses and suggest that malathion has its effects on the indirectly mediated ACh response for at least 24 h after exposure.

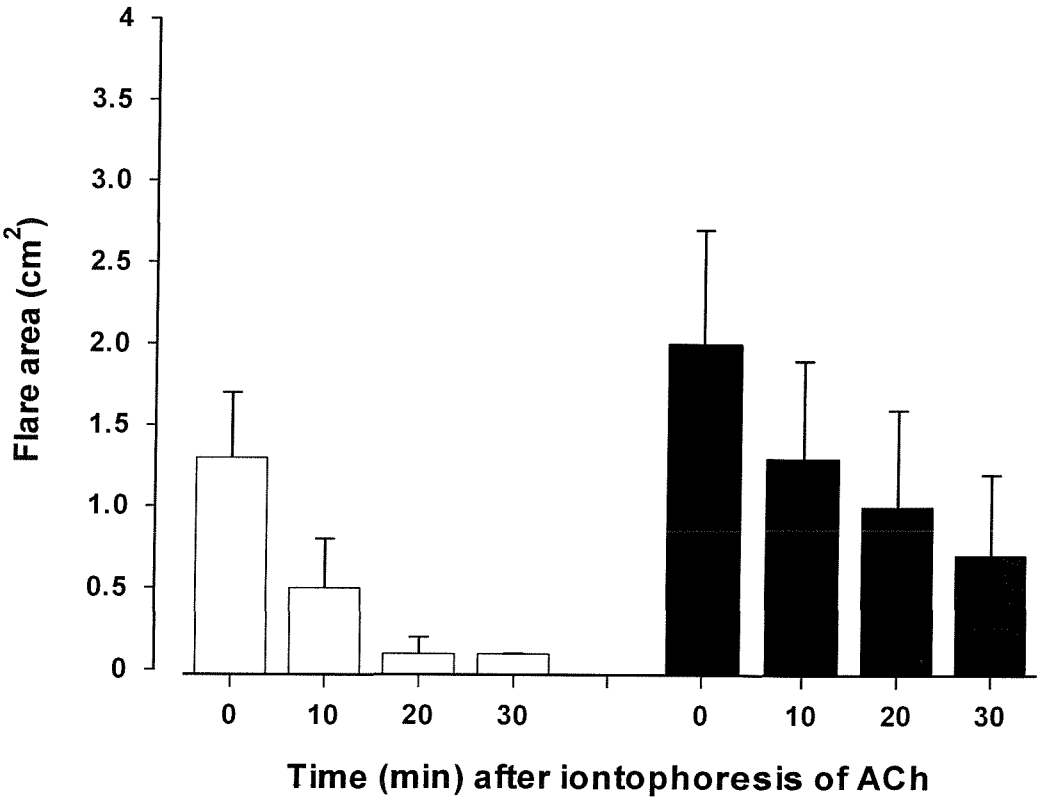

Figure 6.7 Prolonged effects of malathion on the microvascular responses to ACh b) Indirect responses: The area (cm^2) of the ACh-induced vasodilatation that spread outside the site of iontophoresis was measured at vehicle-control (open bars) and malathion (solid bars) treated sites at 10 min intervals after the end of the iontophoretic protocol using scanning laser Doppler imaging. Data are mean ± sem (N.S., n = 5, paired t-test).

6.4 Discussion

The hypothesis to be tested in this chapter was that the malathion-induced erythema following 5 h application to the skin was a result of the inhibition of AChE and the subsequent increase in tissue levels of ACh. Since it was not possible to assay directly the levels of ACh in the tissue an indirect method was used using exogenous ACh to test the activity of endogenous AChE. Application of malathion to the skin surface for 5 h prolonged the duration of the vasodilatation induced by exogenous ACh. These results support the suggestion that malathion via its inhibitory action on AChE reduces the rate at which exogenous and probably endogenous ACh is broken down in the tissue. Malathion was also found to augment the size of the ACh-induced vasodilatation that spread outside the area of iontophoresis (indirect neurogenic response). This was not totally unexpected as it was demonstrated previously that high concentrations of ACh delivered into the skin via microdialysis resulted in a widespread area of vasodilatation around the microdialysis probe **(see section 5.3.2)**. The mechanisms underlying this are unclear but that malathion modulates both the size and the duration of the indirect response may further support the idea that malathion inhibits AChE. Thus malathion increases the levels of ACh in the tissue space that may then induce the neurogenic spread of the vasodilator response.

Laser Doppler fluximetric results obtained during iontophoretic delivery of ACh or SNP show their vasodilator effects to be dose-dependent. Pre-treatment with malathion caused the dose-response curve to ACh to plateau unlike that at vehicle-control treated sites where the dose-dependent increase in skin blood flow was linear. This may be a result of the accumulation of ACh in the tissue, due to the inhibitory action of malathion on AChE, with subsequent saturation of the cholinergic receptors found at the site of application. Thus at higher doses of ACh no further vasodilatation can be induced. In addition malathion did not alter the intensity of the ACh-induced mean blood flux as measured from scanning laser Doppler images obtained immediately after the end of the iontophoresis protocol. These data are consistent with the LDF results and may suggest saturation of the cholinergic receptors due to accumulation of ACh in the tissue and/or a direct action of malathion on these receptors, to suppress the ACh-induced dilatation. A direct action malathion and other OP's on muscarinic receptors has been previously demonstrated *in vitro* in cardiac muscle and isolated cells (Eldefrawi *et al.*, 1992; Ward

& Mundy, 1996). However the action of OP's as agonists or antagonists on these receptors remains to be elucidated. The potential role of muscarinic receptors in the malathion-induced erythema and its effects on the ACh-induced vasodilatation will be further explored in **Chapter 7**.

There has been no attempt in this study to measure maximum vasodilatation in the skin. However the maximum blood flux value measured after iontophoretic delivery of ACh was 365 AU, ten times greater than values obtained after treatment with malathion (37 AU) and three times greater than values obtained after iontophoretic delivery of ACh at malathion treated sites (196 AU). These observations eliminate the possibility that the malathion-induced plateau is due to the inability of blood vessels to dilate further or a failure of the LDF probe to measure mean blood flux above a certain value. Similarly the scanning laser Doppler images showed no further difference in the ACh-induced vasodilatation in the presence and absence of malathion. This is not a result of maximum dilatation and/or a failure of the LDI to measure mean blood flux above a certain value as higher values of blood flux have been measured previously in this study **(see section 5.3.1)**.

Malathion did not alter the dose-dependent increase in mean blood flux induced by iontophoretic delivery of sodium nitroprusside. These data suggest that although malathion does itself cause an increase in skin blood flow, it does not affect the ability of the blood vessels to respond further to vasodilator mediators such as sodium nitroprusside.

As in many other studies an increase in cutaneous perfusion was also observed following the iontophoresis of distilled water alone (Morris & Shore, 1996; Noon *et al.*, 1998; Asberg *et al.*, 1999). Current induced vasodilatation is well recognised and is most likely secondary to activation of nociceptive C–fibres (Wårdell *et al.*, 1993c). In the present study the responses of the vasculature to iontophoretic delivery of distilled water, were at all times significantly smaller than than those to ACh and sodium nitroprusside.

ACh delivered at vehicle-control treated sites produced a vasodilator response that spread outside the area of iontophoresis. It has been reported previously that in man

iontophoresed ACh may stimulate peripheral nociceptive C-fibres to produce a flare response, which is abolished by anaesthetic and is absent in denervated skin (Westerman *et al.*, 1987; Benarroch & Low, 1991; Morris & Shore, 1996). Exposure to malathion enhanced by two-fold the size of the ACh-induced vasodilatation suggesting an increase in the levels of ACh in the tissue and/or increased sensitivity of nerves to ACh in the presence of malathion.

The possible mechanisms underlying the neurogenic response to ACh have been outlined in the introduction to this thesis in and may involve both the action of ACh on cholinergic receptors on nerve endings as well as the ACh-induced release of secondary mediators known to induce neurogenic inflammatory responses **Chapter 1 (section 1.5.2a)**. Although the data presented in this chapter cannot be used to distinguish between the two, it has been shown in this thesis that histamine is not involved in the ACh-induced indirect response in human skin. The possible neurogenic origins of the ACh-induced response are investigated further in **Chapter 7**.

The protocol developed in this chapter was also used to investigate the long-term effects of a single low-dose of malathion on the skin microvasculature. The results indicate that malathion even 24 h after its removal is effective and prolongs the duration of the response of the microvasculature to iontophoretically delivered ACh. It can be argued that the inhibitory action of malathion on AChE or its action on cholinergic receptors persist for up to 24 h after its removal from the skin. This conclusion is supported by the findings in chapter 3 where it was demonstrated that the erythema induced by malathion itself is still evident 24 h after removal from the skin. These findings are not unexpected since malathion is thought to be an irreversible inhibitor of AChE **(Chapter 1, section 1.2.1)** and reactivation of the enzyme is only possible by *de novo* synthesis and/or oxime treatment (Ray, 1998). It is also possible that malathion is still present in the skin 24 h after its removal from the surface of the skin. Recent studies performed in isolated perfused porcine skin flap revealed that malathion tends to be retained in the skin and subcutaneous fat (Chang *et al.*, 1994).

6.5 Summary

In summary the results in the present chapter show that acute exposure to a single low-dose of malathion modulates the microvascular response to exogenous ACh in healthy

human skin *in vivo*. The effects of malathion last for at least 24 h after its removal from the surface of the skin. It is concluded that the effects of malathion are mainly a result of the maintained inhibition of endogenous AChE with subsequent accumulation of exogenous and endogenous ACh in the tissue, which in turn acts on both the blood vessel wall and the nerves modulating the neurogenic vasodilator response in the skin.

CHAPTER 7: POTENTIAL MECHANISMS UNDERLYING THE MALATHION-INDUCED ERYTHEMA.
II) THE ROLE OF MUSCARINIC RECEPTORS AND NERVES

7.1 Introduction and Aims

The work so far presented suggests that malathion when applied to the skin causes a dilatation of the cutaneous vasculature through its inhibitory action on AChE and the subsequent increase in ACh in the tissue. The hypothesis to be tested in the present chapter is that excess ACh acts on muscarinic receptors found on endothelial cells in the skin, to mediate both the malathion-induced erythema and the malathion-induced modulation of the microvascular responses to exogenous ACh. It is also hypothesised that the indirect vascular responses to exogenous ACh augmented by malathion are neurogenically mediated.

The role of muscarinic receptors in the mediation of the effects of various OP's has been studied in mammalian brain tissue and cardiac muscle using a variety of muscarinic receptor antagonists such as pirenzepine and atropine (Eldfrawi *et al.*, 1992; Ward & Mundy, 1996). In a recent study in humans Grossmann *et al* reported that iontophoretically delivered atropine induces cutaneous vasodilatation that lasts for more than an hour (Grossmann *et al.*, 1995). Increase in cutaneous vasorelaxation induced by atropine delivered to the skin using intradermal injections have been previously reported and was blocked by treatment with antihistamines (Cavanah *et al.*, 1991). The contribution of local sensory nerves to the cutaneous vascular responses induced by iontophoretically delivered ACh has been previously explored using a local anaesthetic cream (EMLA, 5%) (Morris & Shore, 1996; Berghoff *et al.*, 2002). In that study treatment with EMLA for 2 h failed to block the ACh-induced vasodilatation (Morris & Shore, 1996).

It is the aim of this study to explore the effects of atropine and EMLA on the malathion-induced erythema and the malathion-induced changes in the vascular responses to the endothelium-dependent vasodilator ACh. Iontophoresis was used to deliver atropine in the skin and block cutaneous muscarinic receptors whereas local anaesthetic was applied in the form of an aqueous based cream to block activation of local sensory nerves by ACh. Changes in mean blood flux induced after administration of atropine and EMLA as well as malathion, ACh and/or vehicle-control were quantified using both the laser Doppler fluximetry probe and scanning laser Doppler imaging.

7.2 Materials and Methods

7.2.1 Subjects and experimental conditions

Two separate studies were conducted. In the first study the effects of atropine on the vascular response to malathion were explored in 5 healthy volunteers aged between 20-45 (1 man and 4 women). Ten healthy volunteers (6 men and 4 women, average age 28 ± 3 years) participated in the second study to explore the neurogenic nature of the ACh-induced responses at malathion and vehicle-control treated sites. Results from one volunteer who participated in the second study were excluded from the final data as this volunteer had an erythemateous response to EMLA. All subjects signed informed consent form the day before the experiment and the study was approved by the local ethics committee.

7.2.2 Application and/or delivery of drugs

Atropine: Iontophoresis was used to deliver atropine (10mM, in distilled water) and/or vehicle (distilled water) at 4 different sites (2 for atropine and 2 for distilled water) on the volar surface of the forearm **(Figure 7.1, Step 1)**. The iontophoretic protocol lasted for approximately 4 min and atropine was delivered in 4 consecutive doses each of 10 μA for 100 sec. Rest periods of 40 sec were allowed between each dose to minimize any non-specific current effects. The total dose of atropine delivered to the skin may be calculated using equation 2.1 and is approximately 0.1 mg, which is well below the recommended dose used for treatment after OP poisoning (0.6-1.2 mg).

Malathion and Acetylcholine: As previously described in **Chapter 6** malathion (10 mg ml^{-1} in an aqueous based gel) and/or vehicle-control (aqueous gel) was applied over the sites pre-treated with atropine and/or distilled water over an area of 2 x 2.5 cm^2 and left under occlusive dressing for 5 h. Two sites were treated with malathion and two sites with vehicle-control **(Figure 7.1, Step 2)**. At the end of the 5 h period ACh (2 % in distilled water) was delivered to all 4 sites **(Figure 7.1, Step 3)** using the iontophoretic protocol outlined previously (**Chapter 2** and **Chapter 6**).

Local anaesthetic: Where the effect of local anaesthetic on the neurogenic nature of the response to ACh was to be investigated EMLA cream was applied under occlusive dressing for 90 min to the areas previously treated for 5 h with malathion and/or vehicle-control. The cream was then gently removed from the skin surface using a wet cotton wool and a period of 10 min was allowed for any skin irritation to settle down.

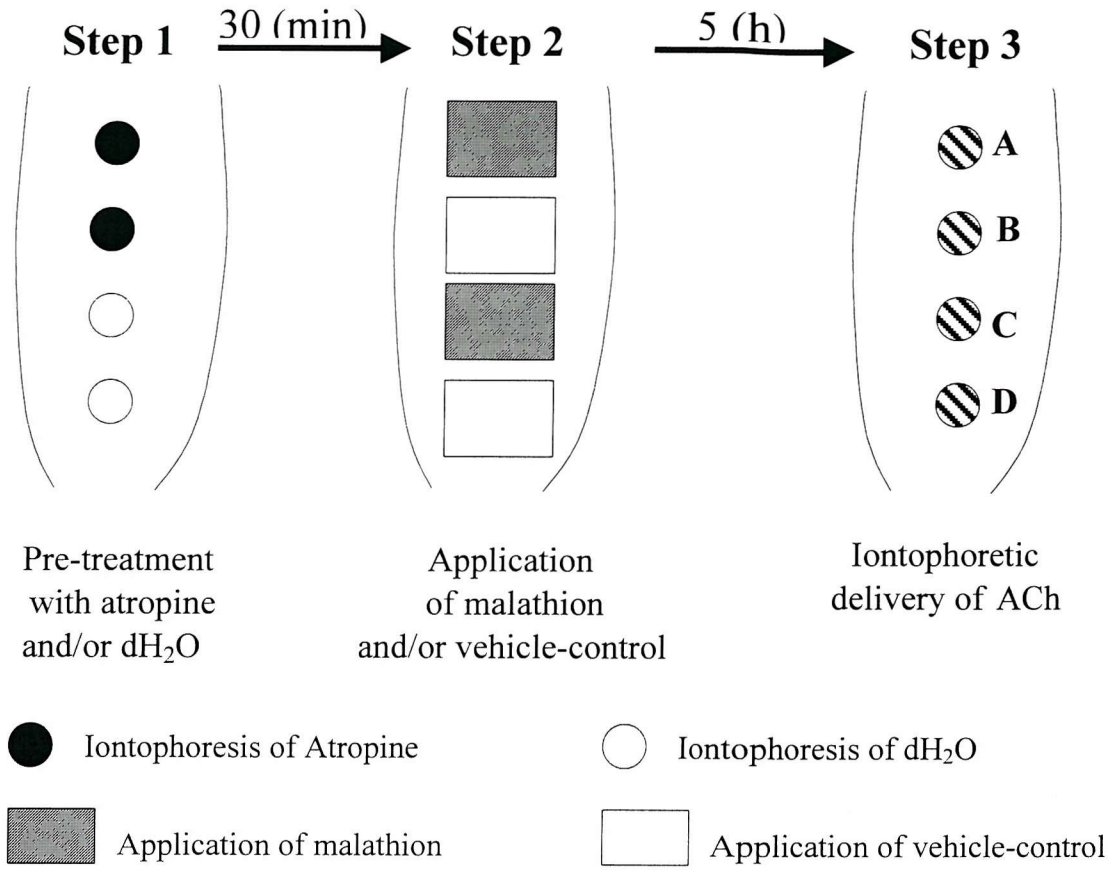

Figure 7.1 The experimental protocol used to explore the potential role of muscarinic receptors in the effects of malathion on the skin vasculature: Atropine (10 mM in distilled water) and/or distilled water (dH_2O) were iontophoretically delivered to the skin at four consecutive doses (each of 10 μA for 100 sec) **(Step 1)**. After the end of the iontophoresis protocol the iontophoresis chamber was removed and the responses of the skin vasculature to atropine were measured using scanning laser Doppler imaging (SLDI) at 10 min intervals for a period of 30 min. Malathion (10 mg ml^{-1} in aqueous based gel) and/or vehicle-control (aqueous based gel) were applied over an area of 2 x 2.5 cm^2 above the sites of iontophoresis and under occlusive dressing **(Step 2)**. Five hours later malathion and/or vehicle-control were removed from the skin and changes in mean blood flux were measured using SLDI. Acetylcholine was then iontophoretically delivered at all sites (**A:** +atropine / +malathion, **B:** +atropine / -malathion, **C:** -atropine / +malathion, **D:** -atropine / -malathion) **(Step 3)** as described in **Chapter 2**. Changes in mean blood flux were followed at 10 min intervals for a period of 30 min after the end of the iontophoresis protocol using SLDI.

7.2.3 Assessment of cutaneous blood flow

Laser Doppler fluximetry (LDF) was used to measure changes in skin blood flux during the iontophoretic delivery of ACh at sites pre-treated with atropine and/or distilled water as previously described in **Chapter 6**. Mean blood flux (AU) was calculated from the LDF measurements recorded during the rest periods between each dose. Changes in skin blood flux induced by atropine, malathion, ACh and/or vehicle were also measured using scanning laser Doppler images (SLDI) following removal of the iontophoresis chamber as previously described in **Chapter 6**. Mean blood flux (PU) from the recorded SLDI images before and after malathion application at sites pre-treated with atropine and/or distilled water was calculated within the treatment area (2 x 2.5 cm^2) box. In addition mean blood flux was measured within the area of iontophoresis of atropine and/or distilled water, which was defined as a circle (1 cm in diameter) that matched the size of the iontophoresis chamber. Any direct and/or indirect changes in mean blood flux induced by ACh, atropine and/or distilled water, were calculated as described previously in **Chapter 6**. In the second study mean blood flux was also calculated from SLDI recorded at malathion and vehicle-control treated sites before and after application of local anaesthetic cream (EMLA).

7.2.4 Statistical analysis

Where statistical comparisons were made a Student's t-test for paired data and/or analysis of variance (ANOVA) was used as appropriate. A probability value of $P < 0.05$ has been taken as significant. All subjects acted as their own controls.

7.3 Results

7.3.1 The role of muscarinic receptors in the malathion-induced erythema.

It was hypothesised that malathion through its inhibitory action on AChE results in the increase of ACh in the tissue, which then acts on muscarinic receptors, found on the endothelium to cause vasodilatation. Hence atropine was used to block muscarinic receptors and attenuate the malathion-induced erythema. Before that the effects of atropine itself on the cutaneous vasculature were explored.

7.3.1a The effects of atropine on the cutaneous microcirculation

i) Direct Effects (within the area of iontophoresis): Atropine caused an increase in mean blood flux of 61 ± 10 % over baseline that declined rapidly to a level of 27 ± 10 % above baseline ten minutes after the end of the iontophoresis protocol and to basal levels by 20-30 min **(Figure 7.2a)**. Iontophoresis of distilled water did not cause a significant increase in blood flux over baseline (100 ± 12 PU and 91 ± 5 PU respectively) (N.S., n = 10 sites in 5 subjects). The atropine-induced vasodilatation measured immediately after the end of the iontophoretic protocol was 4 times greater than that induced by iontophoresis of distilled water (390 ± 83 PU and 100 ± 12 PU respectively) ($P < 0.01$, n = 10 sites in 5 subjects).

ii) Neurogenic Effects (outside the area of iontophoresis): In addition to its direct effects iontophoretically delivered atropine induced an indirect vasodilator response that spread outside the area of iontophoresis. The size of the atropine-induced indirect response immediately after the end of the iontophoresis protocol was 1.3 ± 0.5 cm^2 and was significantly greater than that to distilled water (0 ± 0 cm^2) ($P < 0.05$, n = 10 sites in 5 subjects). The indirect (neurogenic) response was short lasting and had disappeared 20 min after the end of the iontophoresis protocol **(Figure 7.2b)**.

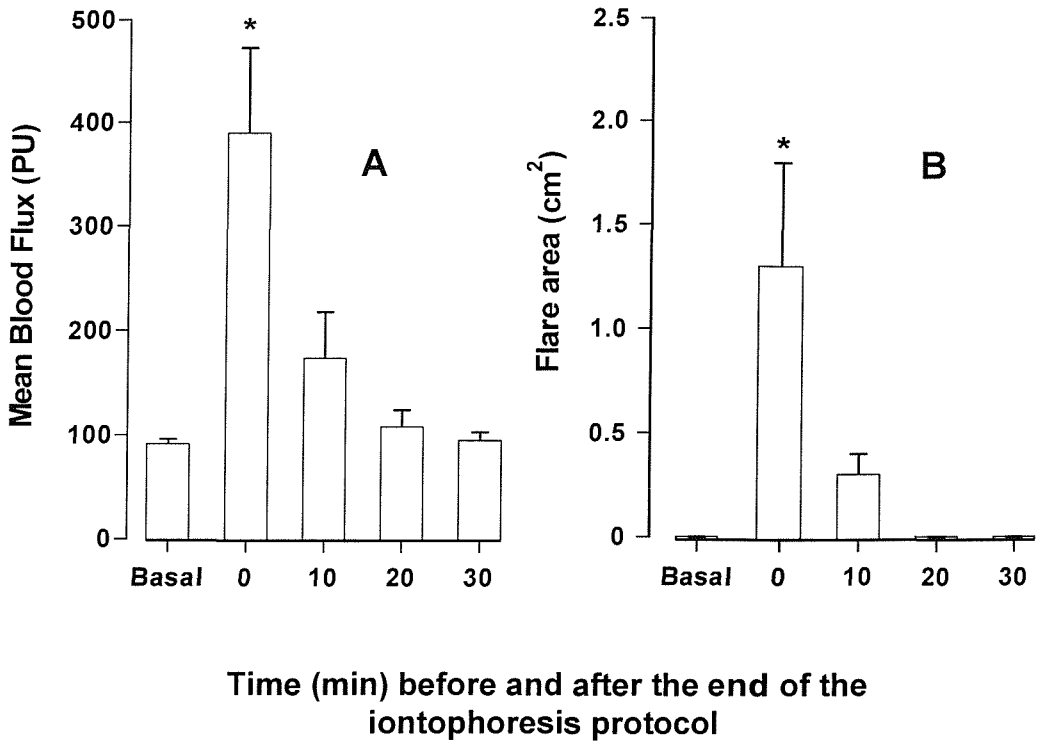

Figure 7.2 The effects of atropine on skin blood flux: After measuring basal blood flow, Atropine (10 mM) was delivered to the skin by iontophoresis. Immediately afterwards and at intervals for 30 min thereafter, mean blood flux **(A)** was measured within the area of iontophoresis using scanning laser Doppler imaging (*P < 0.01, n = 10 sites in 5 subjects). The area of the flare **(B)** that spread outside the site of iontophoresis was calculated from scanning laser Doppler images obtained before and after iontophoresis of atropine. Data are mean ± sem from 10 sites in 5 subjects.

7.3.1b Effects of atropine on the malathion-induced erythema

Pre-treatment with atropine significantly reduced the malathion-induced erythema measured within the area of iontophoresis by approximately 2-fold ($P < 0.03$, $n = 5$) **(Figure 7.3)**. Hence at sites pre-treated with atropine malathion increased mean blood flux measured within the area of iontophoresis by 25 ± 4.8 % whereas at sites pre-treated with distilled water malathion caused a 48 ± 4.5 % increase in mean blood flux over baseline **(Figure 7.3)**.

Mean blood flux was also measured over the area of malathion application (2 x 2.5 cm^2) at atropine and/or distilled water pre-treated sites. Pre-treatment with atropine caused a small but not significant reduction of the malathion-induced erythema measured over the total area of application compared to that at sites pre-treated with distilled water (158 ± 21 PU compared with 192 ± 19 PU respectively) (N.S., $n = 5$).

7.3.2 The role of muscarinic receptors and nerves in the effects of malathion on the cutaneous vascular responses to exogenous ACh.

7.3.2a Effects of atropine on the ACh-induced vasodilatation

i) Dose-response to ACh (LDF measurements): Acetylcholine in the absence of atropine induced a dose-dependent increase in mean blood flux measured using the laser Doppler fluximetry probe that was similar to that previously reported in **Chapter 6**. Pre-treatment with atropine shifted the ACh-induced dose-response curve to the right ($P < 0.05$, $n = 5$, ANOVA) **(Figure 7.4)**.

ii) Direct responses to ACh (LDI measurements): The ACh-induced increase in blood flux within the area of iontophoresis was significantly lower at atropine pre-treated sites (430 ± 113 PU) compared with that at sites pre-treated with distilled water (522 ± 84 PU) ($P < 0.05$, $n = 5$), which represents a reduction of 20%.

iii) Indirect responses to ACh (LDI measurements): Furthermore, ACh induced an indirect vasodilator response that spread outside the area of iontophoresis similar to that described previously in section **6.3.2**. Pre-treatment with atropine had little effect on the area of the ACh-induced indirect response (0.8 ± 0.3 cm^2) compared to that at sites pre-treated with distilled water (1.02 ± 0.4 cm^2) (N.S., $n = 5$).

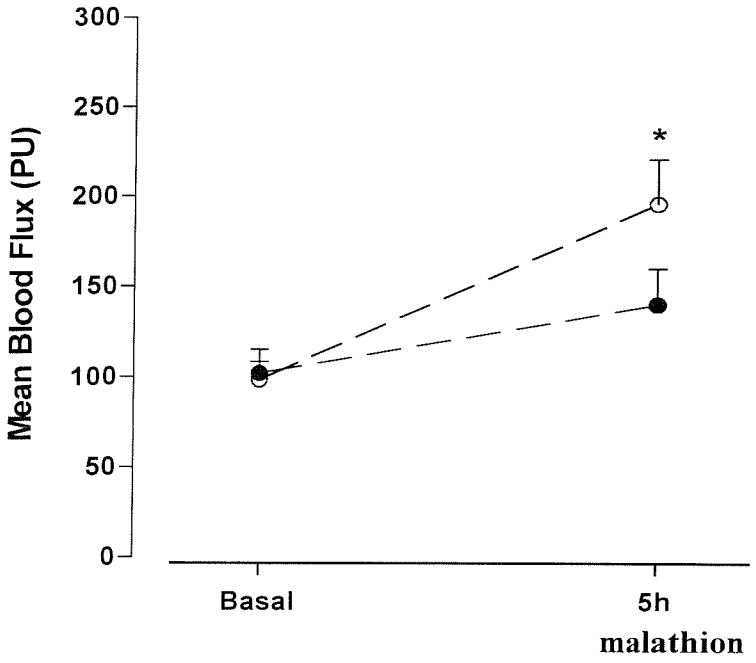

Figure 7.3 Effects of atropine on the malathion-induced erythema: Mean blood flux was measured within the area of iontophoresis at malathion sites pre-treated with iontophoretically delivered distilled water (open circles) and/or atropine (closed circles) using scanning laser Doppler imaging. Data are mean ± sem (* $P < 0.01$, $n = 5$).

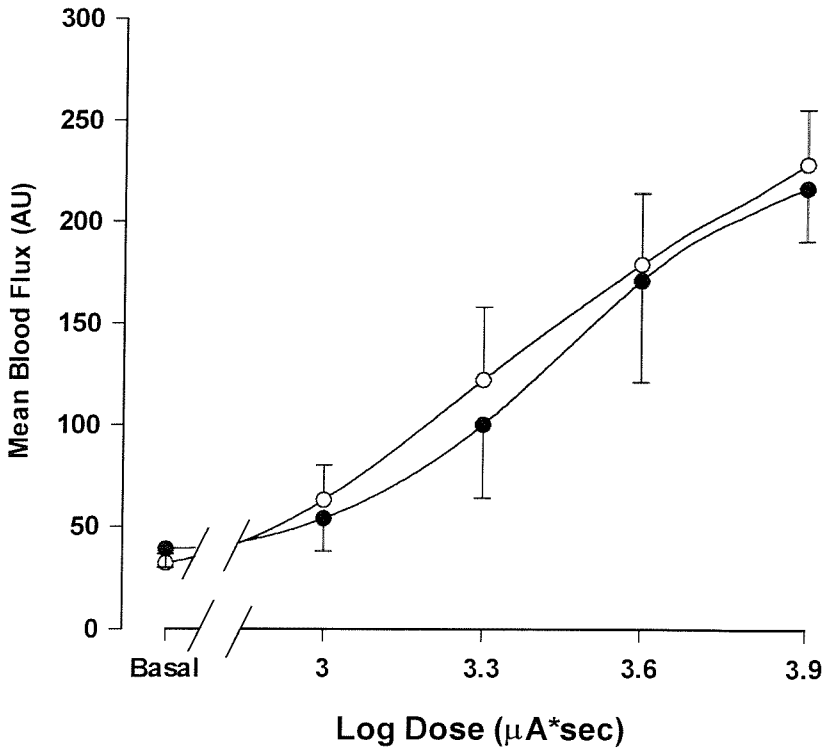

Figure 7.4 Effects of atropine on the ACh-induced dose-response: ACh delivered at sites pre-treated with distilled water and/or atropine (5 h before ACh delivery) caused a dose-dependent increase in mean blood flux. Atropine 5 h after its delivery to the skin shifted the dose-response curve to ACh rightwards (closed circles) and resulted in a significant reduction of the ACh-induced dose-response curve compared to that at sites pre-treated with distilled water (open circles) ($P < 0.05$, ANOVA).

7.3.2b Effects of atropine on the malathion-induced modulation of the vascular responses to exogenous ACh

i) Dose-response to ACh (LDF measurements): As described in **Chapter 6 (see section 6.3.1)** malathion shifted the dose-dependent increase in mean blood flux induced by ACh to the left (n = 5) **(Figure 7.5A)**. Pre-treatment with atropine prior to malathion exposure reversed the malathion-induced shift **(Figure 7.5B)**. Such that in the presence of atropine twice the dose of ACh was required to produce the same (2-fold) increase in blood flux over baseline.

ii) Direct Responses to ACh iontophoresis: Pre-treatment with atropine had little effect on the duration of the ACh-induced vasodilatation in the presence of malathion. Hence, 30 min after the end of the iontophoresis protocol the ACh-induced vasodilatation measured at atropine pre-treated sites in the presence of malathion was still significantly greater compared to that at sites pre-treated with distilled water in the absence of malathion (576 ± 101 PU and 209 ± 45 PU, respectively) ($P < 0.05$, $n = 5$).

iii) Indirect Responses to ACh iontophoresis: Iontophoresis of ACh at malathion treated sites caused a vasodilatation that spread outside the area of iontophoresis similar to that described in section **6.3.4**. Pre-treatment with atropine caused a small but not significant decrease in the size of the response compared to sites pre-treated with distilled water (2.98 ± 0.99 cm^2 and 4.02 ± 1.59 cm^2 respectively) (N.S., n = 5). Therefore, the ACh-induced indirect response at atropine pre-treated sites in the presence of malathion (2.98 ± 0.99 cm^2) was still significantly greater compared to that at distilled water pre-treated sites in the absence of malathion (1.02 ± 0.40 cm^2) ($P < 0.05$, $n = 5$). In addition pre-treatment with atropine had no effect on the duration of the ACh-induced response, which was still prolonged at malathion sites, compared to vehicle-control treated sites **(Figure 7.6)**.

7.3.2c Effects of local anaesthetic on the malathion-induced modulation of the vascular responses to exogenous ACh

i) Effects of EMLA on the skin microcirculation: Application of EMLA to the skin for a period of 1.5 h resulted in a 22.5 ± 4.3 % reduction of skin blood flow.

ii) Direct Responses to ACh iontophoresis: Application of local anaesthetic did not alter the direct responses of the microvasculature to exogenous ACh at either the malathion or vehicle-control treated sites **(Table 7.1)**. Furthermore application of EMLA did not alter the duration of the ACh-induced vascular responses at malathion treated sites which are still significantly greater compared to those at vehicle-control treated sites 20 and 30 min after the end of the iontophoresis protocol **(Table 7.1)**.

iii) Indirect Responses to ACh iontophoresis: As mentioned previously iontophoretic delivery of ACh to malathion and vehicle-control treated sites resulted in a vasodilator response spreading approximately 3 and 1.7 cm^2 outside the area of iontophoresis respectively. Local anaesthetic reduced the flare response to ACh at malathion treated sites by more than half (1.21 ± 0.34 cm^2 compared with 2.92 ± 0.68 cm^2, $P < 0.05$, $n = 6$) **(Figure 7.7)**. Application of EMLA also resulted in a small but not significant reduction in the size of the ACh-induced indirect response at vehicle-control treated sites (1.67 ± 0.49 cm^2 without EMLA compared with 1.19 ± 0.25 cm^2 with EMLA, $n = 6$, N.S.) **(Figure 7.7)**.

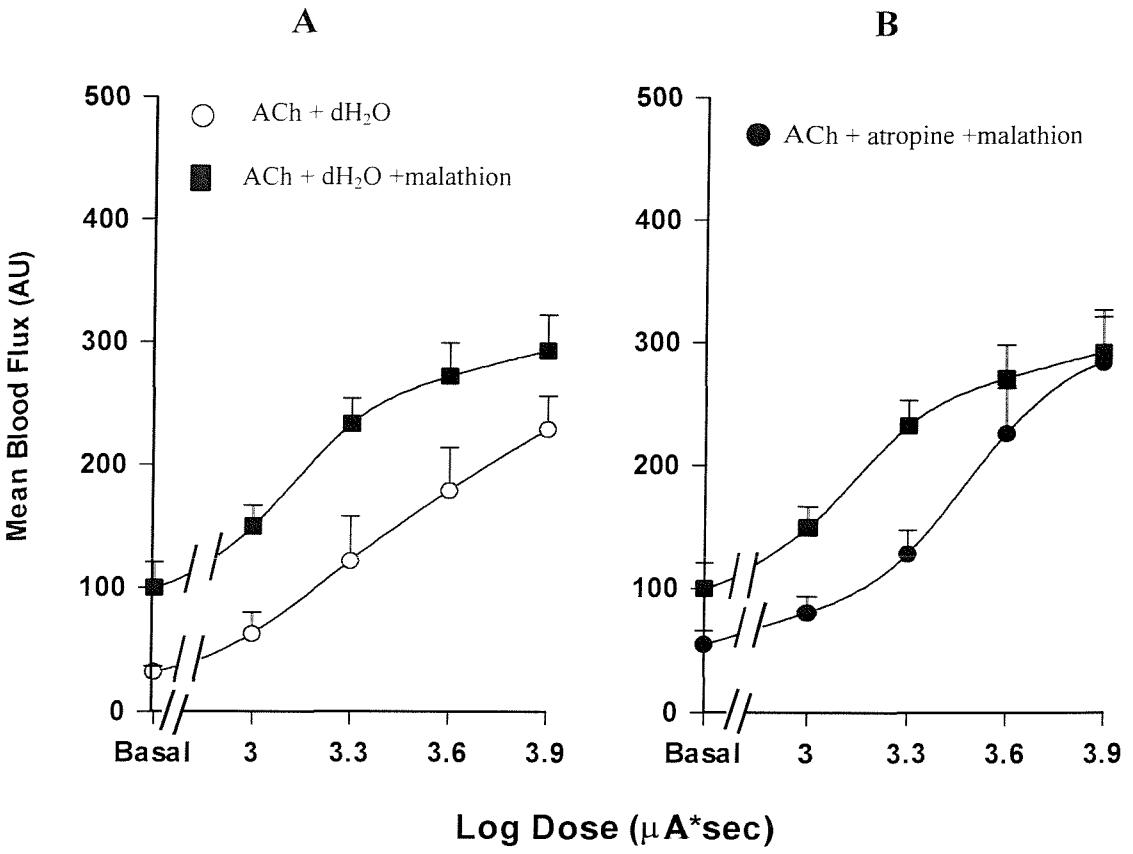

Figure 7.5 Effects of atropine on the vascular responses to ACh in the presence of malathion: Mean blood flux was measured using the laser Doppler fluximetry probe during iontophoretic delivery of ACh at sites pre-treated with distilled water in the absence malathion (open circles) and presence of malathion (closed squares) **(A)** (n = 5). Mean blood flux was also measured using the LDF probe during iontophoretic delivery of ACh at malathion (closed circles) and vehicle-control sites (open circles) pre-treated with atropine **(B)** (n = 5).

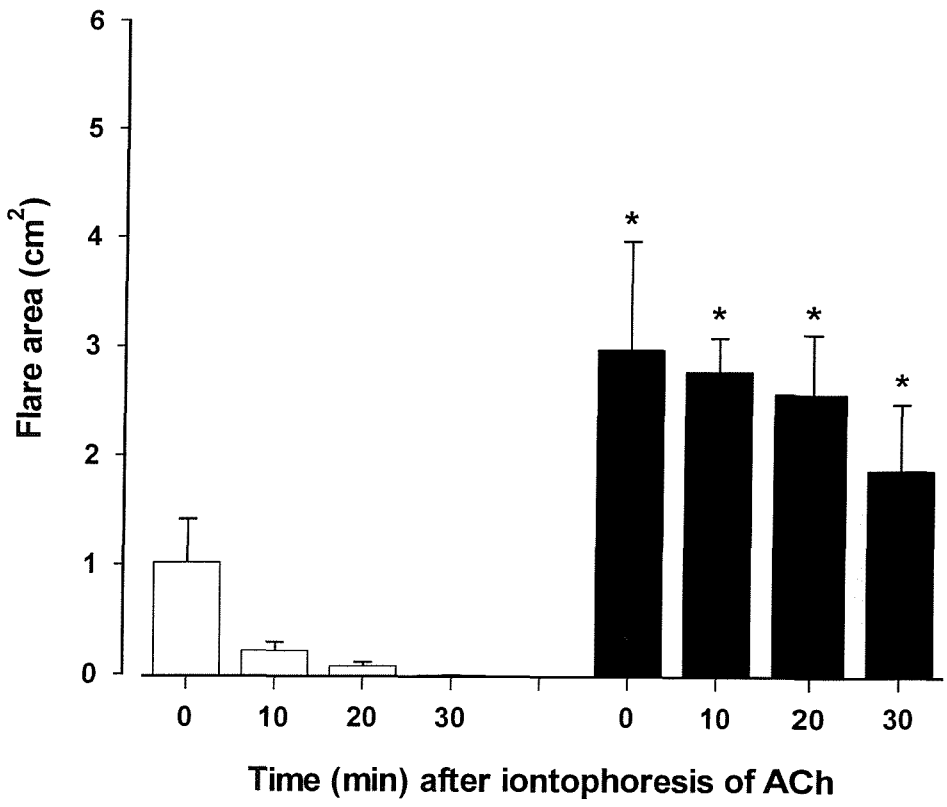

Figure 7.6 Effects of atropine on the indirect vascular responses to ACh: ACh was delivered at sites pre-treated with atropine (10 mM, iontophoretically delivered to both sites 5h before delivery of ACh) in the absence (open bars) and presence (closed bars) of malathion using iontophoresis. The area of the flare that spread outside the site of iontophoresis was measured from scanning laser Doppler images obtained immediately (0 min) and up to 30 min after the end of the iontophoresis protocol. Data are mean ± sem (* $P < 0.05$, $n = 5$, paired t-test).

	MEAN BLOOD FLUX (PU)-DIRECT RESPONSES			
Time (min)	**Control Without EMLA**	**Malathion Without EMLA**	**Control With EMLA**	**Malathion With EMLA**
0	530 ± 99	626 ± 63	712 ± 80	685 ± 93
10	388 ± 113	517 ± 54	378 ± 45	704 ± 100
20	233 ± 88 *	437 ± 64 *	156 ± 37 #	542 ± 122 #
30	101 ± 47 **	340 ± 54 **	107 ± 36 #	505 ± 92 #

Table 7.1 The effects of local anaesthetic on the ACh-induced direct responses: Summarises mean blood flux values (PU) calculated from scanning laser Doppler images within the area of iontophoresis in a circle of 1 cm in diameter at malathion and vehicle-control treated sites in the absence and presence of EMLA. Measurements were recorded immediately after the last dose of ACh (0 min) as well as 10, 20 and 30 min after the end of the iontophoretic protocol. The ACh-induced vasodilatation was prolonged at malathion treated sites compared to vehicle-control treated sites both in the presence and absence of EMLA (#$P < 0.05$ at 20 and 30 min) and (*$P < 0.05$, **$P < 0.001$ at 20 and 30 min) (paired t-test) respectively.

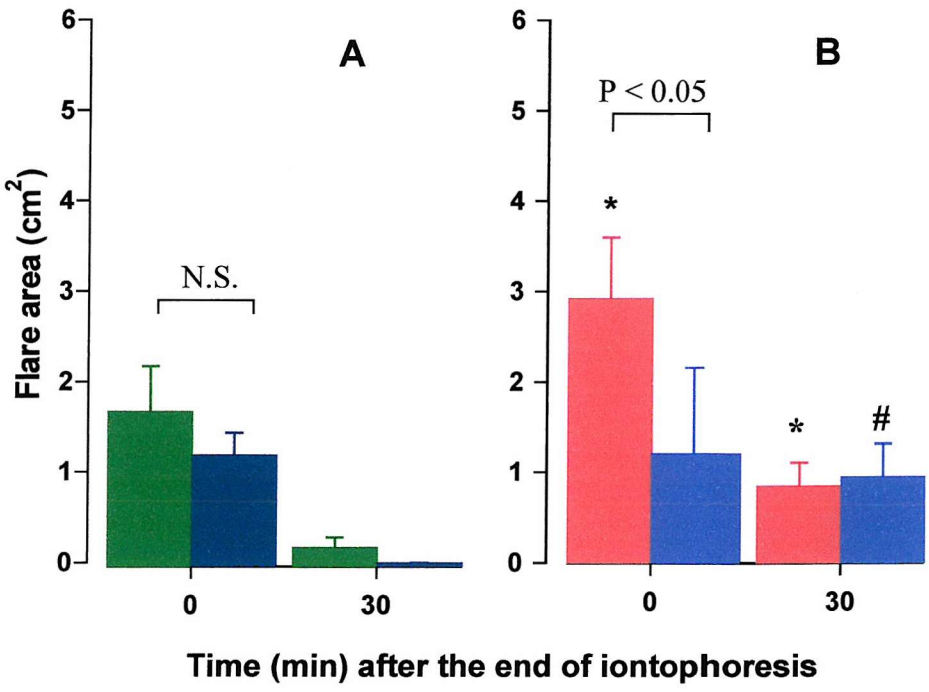

Figure 7.7 The effects of local anaesthetic on the ACh-induced indirect responses: The area of the neurogenic flare was measured from scanning laser Doppler images obtained immediately (0 min) and up to 30 min after the end of the iontophoresis protocol both at vehicle-control (green bars, Figure **A**) and malathion (red bars, Figure **B**) treated sites (* $P < 0.05$, n= 6, paired t-test). In addition SLDI images were obtained in the presence of EMLA both at vehicle-control treated sites (dark blue bars, Figure **A**) (N.S., n = 6, paired t-test) and malathion (light blue bars, Figure **B**) ($P < 0.05$, n = 6, paired t-test). Pre-treatment with EMLA did not affect the duration of the ACh-induced response, which 30 min after the end of the iontophoresis protocol was still greater at malathion treated sites (light blue bars) compared to vehicle-control (dark blue bars) treated sites (# $P < 0.05$, n= 6, paired t-test).

7.4 Discussion

This study set out to test whether malathion had its effects on the skin vasculature via muscarinic receptors. It was demonstrated, using atropine as a non-specific muscarinic receptor antagonist, that muscarinic receptors play a significant role in both the malathion-induced erythema and the malathion-induced modulation of the microvascular responses to ACh. It was also proposed that malathion through its inhibitory action on AChE resulted in an increase in tissue levels of ACh (both exogenous and endogenous), which in turn activates local sensory nerves to cause the indirect (flare) responses. This was confirmed as pre-treatment with local anaesthetic significantly reduced the ACh-induced indirect response in the presence of malathion.

7.4.1 The role of muscarinic receptors in the malathion-induced erythema and modulation of the microvascular responses to ACh

The present study confirms that atropine delivered iontophoretically to the skin induces a dilatation that resolves completely by 30 min. The atropine-induced dilatation observed in the present study was of similar magnitude as that reported by Grossmann and colleagues (120 AU compared with 100 AU) (Grossman *et al.*, 1995). However the response in the present study is of shorter duration compared to that reported previously.

Furthermore, data from the present study show that atropine results in a vasodilator response that spreads outside the area of iontophoresis. The atropine-induced indirect responses have been reported previously after intradermal injections of atropine in the skin of the forearm (Cavanah *et al.*, 1991). Cavanah and colleagues proposed a possible mechanism underlying the vasodilator responses to atropine in the skin. This suggests that atropine blocks an afferent nerve autoreceptor of the M1 or M2 subtype leading to the release of ACh and other vasoactive mediators with subsequent mast cell degranulation and/or direct action on the blood vessels. In the absence of atropine the autoreceptor would inhibit neurotransmission and the subsequent release of ACh. However the above mechanism fails to explain the inhibitory effect of atropine on the ACh-induced vasodilator response in the skin (Grossmann *et al.*, 1995).

Data from the present study demonstrate that atropine even 5 h after its delivery to the skin shifted the dose response to ACh rightwards. The fashion of the shift suggests that

atropine acts as a competitive antagonist on the cutaneous muscarinic receptors to block the ACh-induced dilatation. However, since only one dose of atropine was used and a 5 h period was allowed before iontophoresis of limited doses of ACh it is not possible to perform any further pharmacological analysis of these results. It is important for the present study that atropine 5 h after its delivery to the skin partially blocked the ACh-induced vasodilatation.

Atropine significantly reduced the intensity of the malathion-induced erythema. These results demonstrate that the effects of malathion on the skin microcirculation are in part mediated through cutaneous muscarinic receptors, which may be located on both cholinergic nerves in the skin as well as on non-neuronal cells including endothelial cells, keratinocytes and mast cells. Atropine at the dose used did not abolish completely the malathion-induced erythema. This is more likely because atropine was applied over a smaller area compared to the area of malathion application. Furthermore since malathion requires an incubation period of 5 h to induce a significant increase in mean blood flux it is not possible to know whether atropine under different circumstances would have blocked completely the malathion-induced erythema. The use of higher doses of atropine was not possible because it results in skin blistering.

Atropine reversed in part the malathion-induced reduction of the ACh-induced dose-response curve. These results confirm that muscarinic receptors do play some role in the effects of malathion on the responses of the vasculature to exogenous ACh. These effects may be a result of the accumulation of ACh in the tissue following the inhibition of AChE by malathion and/or of a direct action of malathion on the receptors (Eldefrawi *et al.*, 1992; Katz *et al.*, 1997). It is not possible to distinguish between the two mechanisms from the data obtained in this study.

7.4.2 The role of nerves on the malathion-induced erythema and modulation of the microvascular responses to ACh.

In the present study application of local anaesthetic induced vasoconstriction at the area of contact. These data are in consistent with the study by Bjerring and colleagues who demonstrated blanching of the skin after 30-60 min application of EMLA. In the same study it was shown that after prolonged application (> 2 h), EMLA caused an erythema measured over the area of application (Bjerring *et al.*, 1989). The possible mechanisms

underlying the biphasic responses to EMLA are yet to be investigated, although possible explanations, such as the direct effect of EMLA on vascular smooth muscle, producing vasoconstriction at low concentrations and vasodilatation at high concentrations has been previously suggested (Jacobs *et al.*, 1974).

Pre–treatment with local anaesthetic reduced the size of the ACh-induced indirect response at malathion treated sites by half immediately after the end of the iontophoresis protocol. These data suggest that the mechanism underlying the malathion-induced modulation of the vascular responses to ACh is in part neurogenic in nature. It has been previously suggested that the ACh-induced indirect effect is probably mediated by the action of ACh on peripheral nociceptive C-fibres (Benarroch & Low, 1991; Morris & Shore, 1996). The data in the present study cannot be used to evaluate whether these effects result from the action of ACh itself on local sensory nerves or whether secondary mediators are released in response to excess ACh to stimulate these nerve fibres.

Pre-treatment with local anaesthetic cream failed to abolish the ACh-induced indirect response at vehicle-control treated sites. These results are in consistent with that reported in a previous study and suggest that in the absence of malathion local sensory nerve activation may not be a major contributor to the responses of the microvasculature to iontophoretically delivered ACh. Data from the present study demonstrate that pre-treatment with local anaesthetic did not alter the malathion-induced increase in the duration of the vascular responses to exogenous ACh. These results verify that malathion modulates the vascular responses to ACh through its inhibitory effect on AChE and the subsequent prolongation of survival of ACh in the tissue.

7.5 Summary

In this study the combination of iontophoresis and SLDI allowed further investigation into the possible mechanisms underlying the effects of malathion on the skin microcirculation. It is concluded that the malathion-induced erythema is mediated via cutaneous muscarinic receptors that play a role in the malathion-induced modulation of the vascular responses to ACh. Malathion also augments the ACh-induced neurogenic responses and this is in part mediated via the activation of local sensory nerves by ACh itself and/or other secondary mediators released in response to excess ACh.

CHAPTER 8: GENERAL DISCUSSION

This thesis aimed to assess the effects of a single low-dose of malathion on the cutaneous vasculature following its topical application to the skin and to elucidate the mechanisms underlying these effects. The results showed that the organophosphorus compound malathion is absorbed through the skin of healthy human volunteers in amounts sufficient to cause a localised erythema. They also show that changes in local skin blood flow could influence the concentration of malathion recovered from the skin suggesting that the distribution of malathion may be influenced by the local vasculature. Studies to investigate the mechanisms underlying the effects of malathion on the cutaneous microcirculation provided evidence for an inhibitory action of malathion on endogenous acetylcholinesterase with the subsequent accumulation of acetylcholine in the tissue and over-stimulation of muscarinic receptors. The consequence of this was an increase in blood flow, activation of cutaneous nerves and neurogenic inflammation.

8.1 Percutaneous absorption of malathion and local skin blood flow

Despite the fact that the skin is an important route for the absorption of malathion, until now, the rate at which malathion is absorbed into the dermis and the influence of the factors such as cutaneous blood flow on its systemic distribution remained unclear. Results from the present study demonstrate that malathion does penetrate the epidermis and that it is possible to follow the rate of the percutaneous absorption of malathion following topical application *in vivo* in humans using the technique of cutaneous microdialysis. The recovery of malathion from the dermis was low and this is consistent with previous studies performed both *in vitro* (Carver *et al.*, 1989; Chang *et al.*, 1994; Wester *et al.*, 1996) and *in vivo* in man (Wester *et al.*, 1983).

The use of microdialysis overcame the limitations of various methods used in the past to study the absorption of xenobiotics following topical application. Using this non-invasive technique it was possible to demonstrate, *in vivo* in humans, the penetration of a toxic compound, such as malathion, through the skin. The presence of an intact microcirculation while measuring penetration *in vivo* in man is novel since similar studies for malathion and other organophosphates have only been previously performed using *in vitro* models, such as the isolated porcine skin flap (Chang *et al.*, 1994).

Although not in great detail this study also examined a number of factors that affected the penetration of malathion and its recovery from the tissue using microdialysis. The effect of

the formulation was briefly explored using Derbac M, an aqueous based shampoo used for the treatment of head lice in children. In this study malathion was not recovered from the tissue following topical application of the formulation to the skin. This may be taken as evidence for reduced bio-availability of malathion in this preparation. However, treatment of head lice usually requires longer periods of treatment that may also be accompanied by hot baths and scratching of the scalp. The latter may result in removal of the epidermal barrier and consequently absorption of malathion in the tissue.

Several factors will affect the concentration of malathion in the tissue and hence its availability for dialysis. These include both the detoxification of malathion by carboxylesterases and its metabolic oxidation to its active metabolite malaoxon. In addition, local blood flow plays an important role in the removal of xenobiotics from the tissue. Although the present study does not deal with the detoxification of malathion in the skin, it would have been possible using microdialysis to recover by-products, such as isomalathion and nitrophenols, that would indicate the break down of malathion in the tissue. If detoxification of malathion does not occur then malathion can undergo metabolic oxidation resulting in its conversion to its active metabolite malaoxon. In this study malaoxon was not detected in dermal dialysate. This is not surprising because the conversion of malathion to malaoxon has been shown to take as long as 4 h in human plasma (Mason *et al.*, 1992) and thus it is unlikely that it would be available for dialysis within the 5 h experimental period. Furthermore once formed malaoxon binds to AChE and the resulting complex is too large to pass the pores of the probes. Finally if both detoxification and removal of malaoxon from the tissue are taken into consideration, the levels of malaoxon available for dialysis would be very low to be detected in the dialysate.

Although the present study does not provide direct evidence for bio-activation of malathion in the tissue, malathion at the concentration measured within the dermis, caused a marked and long-lasting erythema. Irritant responses after patch test with malathion and other OP's have been reported previously in farmers with contact dermatitis but not in healthy farmers (Sharma & Kaur, 1990). In addition, cases of non-specific skin rash, urticaria as well as angioedema after repeat spraying of a mixture of malathion corn syrup bait have been reported in a more recent study in southern California (Schanker *et al.*, 1992). In the present study there was no obvious oedema after 5h exposure to malathion, nor did the subjects report any sensation of discomfort or itch during exposure. In addition

there was no evidence that malathion in the aqueous preparation used, behaved as a direct activator of mast cells to release histamine. This is the first study to report alterations in cutaneous perfusion after short-term exposure to a single low-dose of malathion topically applied to healthy human skin *in vivo* in subjects that have not knowingly been in contact with organophosphates.

It was hypothesised that changes in local skin blood flow will influence tissue levels of malathion and therefore its recovery in the dialysate. This hypothesis was further confirmed in the present thesis using sodium fluorescein as the diffusible tracer the concentration of which in the dialysate was shown to be dependent upon local blood flow. Many recent studies have used microdialysis as the sampling method of choice to provide information about the physiology of the tissue space *in vivo* as well as to assess the transcutaneous delivery of xenobiotics. Thus the present data will have significant implications for the use of dialysis as a technique to assay tissue concentrations of a substance accurately, under conditions where blood flow is not constant. Results from this study also demonstrate that reducing the vascular compartment by constriction of the arteriolar vascular bed with noradrenaline results in an increase in the concentration of malathion in the dialysis fluid and by implication the concentration of malathion in the extravascular space. The results presented in this thesis are in agreement with the previous data (Riviere and Williams, 1992; Singh and Roberts, 1994) and confirm that the local vasculature does play a significant role in the removal of substances from the dermis.

As mentioned previously malathion when applied on the surface of the skin results in an increase in the cutaneous vascular perfusion. Since this project demonstrates that removal of malathion from the dermis is dependent upon local skin blood flow it may be speculated that agents, like malathion, which themselves increase dermal vascular perfusion may enhance their own systemic uptake and subsequent systemic distribution through a direct effect on the local vasculature. The importance of these findings is vast since increasing levels of malathion in the tissue will lead to severe adverse health effects. Hence the effects of vascular perfusion on the systemic distribution of malathion must be taken into consideration especially in cases such as the treatment of head lice where topical application of malathion is often accompanied by hot baths and occupational exposure which is associated with exercise and subsequent increase in blood flow.

8.2 Mechanisms underlying the effects of malathion on the cutaneous vasculature

While the effects on human health of acute exposure to high levels of organophosphates is well documented the effects of exposure to low-levels of OP's which do not themselves evoke cholinergic symptoms such as salivation, meiosis, bradycardia and eventually skeletal muscle paralysis are less well understood.

It was the aim of the present study to elucidate the mechanisms underlying the effects of a single low-dose of malathion on the cutaneous microcirculation in human skin *in vivo*. Organophosphates have their main action through the inhibition of acetylcholinesterase, which leads to the rapid accumulation of acetylcholine in the tissue and the accompanying cholinergic symptoms. The potential of organophosphates to cause low-level toxicity has been recently reviewed (Ray *et al.*, 2001) and is mainly a result of the nature of the reaction of the OP's with acetylcholinesterase and other serine esterases that is dependent on both concentration and duration of exposure.

In the present study an analytical method was developed to quantify changes in the tissue levels of endogenous acetylcholine and thus demonstrate AChE inhibition following exposure to a single low-dose of malathion. However, although identification of ACh was possible it was technically difficult to quantify the levels of endogenous ACh. Therefore, it was decided to explore the effects of malathion on the responses of the microvasculature to exogenous ACh.

This study demonstrates that short-term exposure to a single low-dose of malathion results in altered vascular function. This is expressed as prolonged duration of the ACh-induced increase in cutaneous perfusion and local axon-reflex mediated vasodilatation in response to low-doses of exogenous ACh. The mechanisms underlying the effects of malathion on vascular function are yet to be elucidated, although they probably originate from malathion's inhibitory action on endogenous AChE and the subsequent accumulation of exogenous and endogenous ACh in the tissue. Both ACh and AChE are expressed in neuronal (cholinergic nerve endings) and non-neuronal (endothelial cells, keratinocytes and mast cells) constituents of the skin (Wessler et al., 1998). The role of ACh as an important neurotransmitter and its necessity for a normal tissue function are well established. Non-neuronal ACh is involved in the regulation of important cell functions such as mitosis, cell mobility, cell-cell interactions and immune functions. By implication,

interaction of malathion, even in low-doses, with the components of the cholinergic system found in the skin may affect normal skin biology.

It is possible that malathion is having its effects by its direct actions on the receptors (Eldefrawi *et al.*, 1992; Katz *et al.*, 1997) together with its inhibitory action on AChE and possibly other serine esterases found in non-neuronal tissue **(Figure 1.2)** (Ray *et al.*, 2001). Since the experiments in the present study were all performed in human skin *in vivo* it was not possible to distinguish between the three mechanisms and further work *in vitro* is required to dissect further the mechanisms underlying the effects of malathion on the vascular tissue. Preliminary *in vitro* studies using human dermal microvascular endothelial cells have been conducted to characterise their AChE activity in the presence and absence of non-cytotoxic concentrations of malathion and malaoxon. The data demonstrate a 30 % inhibition of the enzyme activity by malaoxon but not by malathion. This may suggest that it is necessary for malathion to be transformed into malaoxon in order to have its effects on the vasculature. However, previous *in vitro* studies mainly in neuronal cells have shown that malathion itself can inhibit AChE and, therefore, has cytotoxic effects (may result in cell death) (Jianmongkol *et al.*, 1999). Thus, it is also possible that malathion results in altered vascular function via its direct actions on AChE found in cholinergic nerve endings and/or other non-neuronal cells in the skin.

Further work must be done to explore the effects of malathion and malaoxon on muscarinic receptors and on other serine hydrolases found on endothelial cells since interaction of OP's with non-neuronal cholinergic receptors has been shown to result in cell death (Grando, 1997). Various serine hydrolases such as carboxylesterases are located in the skin and although their main role is the detoxification of xenobiotics they have been also shown to be involved in metabolising cholesterol esters and testosterone biosynthesis.

This study demonstrates that the effects of malathion on the cutaneous vasculature lasted for up to 24 h after its removal from the skin. Hence the present study provides evidence for prolonged modulation of the physiological functions of the cutaneous vasculature following short-term exposure to a single low-dose of malathion. The implications of the above findings are of great importance in cases of occupational exposure, which is mainly associated with chronic low-dose contact with malathion and other OP's. This raises important questions on whether the effects of malathion on the physiological functions of

the vasculature (mainly through its interaction with AChE and other serine esterases) are associated with increased susceptibility to inflammation.

In conclusion this thesis provides important evidence that malathion is absorbed through the skin and that its systemic distribution is dependent upon local blood flow. Although bio-activation of malathion to malaoxon has not been demonstrated in this study, it has been shown that even a short-term exposure to a low-dose of malathion results in the increase of cutaneous perfusion. By implication, this study shows that malathion, via its effects on the cutaneous vasculature, favours its own systemic distribution and has the potential, therefore, to cause severe adverse effects.

The main outcome of this work is that short-term exposure to a single low-dose of malathion results in prolonged (up to 24 h) modulation of the cutaneous vascular function that manifest both as an erythemateous response and as altered vascular responses to ACh. This is mainly through the inhibition of AChE and the accumulation of ACh in the tissue. The latter via its effects on both the endothelium and the cutaneous nerves plays an important role in the regulation of vascular relaxation. Thus malathion through its inhibitory effects on endogenous AChE promotes neurogenic inflammation and may result in endothelial dysfunction. Hence one might speculate that malathion, through its effects on endothelial function, might increase susceptibility to infection or affect wound healing process. In addition interaction of malathion with AChE expressed in other non-neuronal cells such as immune cells may lead to suppression of the immune system and result in further toxic effects.

This study provides strong evidence that the vasculature can be used as a model tissue to study the potential biochemical effects of both acute and chronic exposure to low-levels of OP's which themselves do not cause the cholinergic symptoms associated with acute high-doses of OP's. This is of great importance since, up to now, epidemiological research exploring the effects of chronic exposure (mainly occupational) to low-doses of OP's has focused on psychometric and neurological measurements. The results of the present study contribute to a further understanding of the potential toxic effects caused after exposure to low-doses of malathion. In addition, these findings illustrate the use of studying the cutaneous vasculature to gain knowledge of drug absorption and toxicity and provide a risk assessment and possible diagnosis of OP exposure.

APPENDIX

Appendix : Materials and Instruments

Acetic acid glacial: (Code A/0400/PB08, Fisher Scientific UK Limited, Leisc., UK)

Acetylcholine Chloride: (Acetylcholine Chloride 100g, Lot 119H2605 Sigma-Aldrich Company Ltd, Poole, Dorset, UK)

Aqua Gel: (Aquagel, Adams Healthcare, Leeds, UK)

Autosampler: (Model 7673, Hewlett Packard Co., Avondale, USA).

Battery powered iontophoresis controller: MIC 1 (Moor Instruments Ltd, Devon, UK)

Capillary column: (DB-1 (100% methyl), length 30 m; i.d. 0.32 mm; film thickness 0.25 μm) (J&W Scientific Inc. Folsom CA, USA).

Cellophane tape: (SellotapeTM, Sellotape GB Ltd., Dunstable, UK)

Comfeel: (Coloplast Ltd, Peterborough, UK)

Cuprophane membranes: Renal dialysis capsule (Focus 90H Hemophan Hollow Fibre Dialyser, National Medical Care, Rockleigh,USA).

Derbac M: (0.5% w/w Derbac M, Seton Healthcare Group, Oldham, UK).

EMLA: (EMLA, Astra Pharmaceuticals Ltd., Kings Langley, UK)

Flame photometric detector: (Model 19256A, Hewlett Packard Co., Avondale, USA).

Fluoresence Plate reader: Cytofluor 4000 Microplate fluoresence reader, Biosearch technologies Inc., CA, USA)

Gas Chromatograph (GC): (Model 5890, series II, Hewlett Packard Co., Avondale, USA)

GC vials: (Chrompack International BV, Middelburg, The Netherlands).

Glyceryltrinitrate: (Nitronal®, Lipha Pharmaceuticals Ltd, Middlesex, UK)

Glyceryltrinitrate (patches): (Transiderm-Nitro5 patches, Novartis Pharmaceuticals UK limited, Surrey, UK)

Hexane: (Prolabo, Fontenay, France)

Hydrogen: (BOC Gases, Guildford, UK)

Laser Doppler Fluximetry probe: (Moor Instruments Ltd, Devon, UK)

Malaoxon: (Malaoxon Pestanal® 250mg, (Riedel-de-Haën, RdH Laborchemikalien GMbH Sigma)

Malathion: (Malathion Pestanal® (O,O-dimethyl-S-(1,2-dicarb-ethoxyethyl) phosphorodithioate) 250mg), (Riedel-de-Haën, RdH Laborchemikalien GMbH, Sigma UK Ltd)

Mecarbam: (Mecarbam Pestanal® (ethyl (diethoxy-phophinthionyl) acetyl-n-methyl carbamate) 100mg) (Riedel-de-Haën, RdH Laborchemikalien GMbH Sigma)

Microdialysis Pumps: (Univentor 801 syringe pump, Biotech Instruments Ltd, Kimpton, Herts., UK).

Needles: (23G x 1 $^{1/4}$", 0.6 x30 mm, Nr.14, Lot: 97H11A2, Terumo Europe N.V., 3001 Lenven-Belgium)

Nitric Oxide analyzer: (NOA^{TM} model 280, Sievers Instruments Inc., CO 80301, USA)

Nitrogen: (BOC Gases, Guildford, UK)

Noradrenaline (NA): (Levophed® Abbott Labs, N. Chicago, IL, USA)

Perspex electrode chamber: (Moor Instruments Ltd, Devon, UK)

Phosphate Buffered Saline (PBS): 0.01M phosphate buffered saline (PBS) with a pH 7.4 at 25 °C

Portex tubing: (Fine Bore polythene tubing, 0.28 ID, 0.61 OD, Portex Limited, Kent, UK)

Scanning Laser Doppler Imager (SLDI): (MLDI 5030, Moor Instruments Ltd, Devon, UK)

Sodium Fluorescein: (Minims fluorescein 2%, Chauvin Pharmaceuticals Ltd, Essex, UK)

Sodium Iodide (NaI): (Sodium Iodide anhydrous 99+%, Lot: A009686002, Acros Organics, Geel, Belgium)

Sodium Nitrite ($NaNO_2$): (Code S/5640/53, Fisher Scientific UK Limited, Leisc., UK)

Sodium Nitroprusside: (Sodium Nitroprusside Dihydrate 50mg, David Bull Laboratories DBL®, Warwick, UK)

Tegaderm: (3M Tegaderm™ , Astra Pharmaceuticals Ltd., Kings Langley, Herts., UK)

Toluene: (Toluene GPC, Fisons Scientific Equipment, Loughborough, UK)

Ultrasonograph: (Dermascan C, version 3, Cortex technology handsund, Denmark).

Wire: (Stainless steel AISI 302 wire, diameter 100 μm, Goodfellow Cambridge Ltd, Huntingdon, Cambs. UK)

96-well plates: (Costar® cluster plate 3632, Corning, NY 14831, USA).

BIBLIOGRAPHY

Safety of malathion dusting powder for louse control (1960) *Bulletin of World Health Organisation* **22**, 503-514

World Health Organisation IPCS Database 1993 Computer Program

Hazardous substances data bank 1997 Computer Program

Abou-Mohamed G, Kaesemeyer WH, Caldwell RB, Caldwell RW (2000) Role of L-arginine in the vascular actions and development of tolerance to nitroglycerin *British Journal of Pharmacology* **130** 211-218

Albery WJ, Guy RH, Hadgraft J (1983) Percutaneous absorption: transport in the dermis *International Journal of Pharmaceutics* **15** 125-148

Anderson C, Andersson T, Andersson RGG (1992) In vivo microdialysis estimation of hisatmine in human skin *Skin Pharmacology* **5** 177-183

Anderson C, Andersson T, Wårdell K (1994) Changes in skin circulation after insertion of a microdialysis probe visualised by laser Doppler perfusion imaging *Journal of Investigative Dermatology* **102** 807-811

Ansel JC, Armstrong CA, Song I, Quinlan KL, Olerud JE, Caughman, SW, Bunnett NW (1997) Interaction of the skin and nervous system *Journal of Investigative Dermatology Symposium Proceedings* **2** 23-26

Asahina A, Hosoi J, Grabbe S, Granstein RD (1995) Modulation of Langerhans cell function by epidermal nerves *Journal of Allergy and Clinical Immunology* **96** 1178-1182

Asberg A, Holm T, Vassbotn T, Andreassen AK, Hartmann A (1999) Nonspecific microvascular vasodilation during iontohporesis is attenuated by application of hyperosmolar saline *Microvascular Research* **58** 41-48

Ault JM, Riley CM, Meltzer NM, Lunte CE (1994) Dermal microdialysis sampling in

vivo *Pharmaceutical Research* **11** 1631-1639

Averbeck D, Averbeck S, Blais J, Moysan A, Hüppe G, Moliére P, Prognon P, Vigny P, Dubertet L (1989) Suction blister fluid: its use for pharmacodynamic and toxicological studies of drugs and metabolites in vivo in human skin after topical or systemic administration *Models Dermatology* **5-11** editors Maibach HI, Lowe NJ

Bakry MNS, El-Rashidy AH, Eldefrawi AT, Eldefrawi ME (1988) Direct actions of organophosphate anticholinesterases on nicotinic and muscarinic acetylcholine receptors *Journal of Biochemical Toxicology* **3** 235-259

Bayliss WM (1901) On the origin from the spinal cord of the vasodilator fibres of the hind-limb, and on the nature of these fibres *Journal of Physiology* **26** 173-209

Baynes RE and Riviere JE (1998) Influence of inert ingredients in pesticide formulations on dermal absorption of carbaryl *American Journal of Veterinary Research* **59** 168-175

Benarroch EE and Low PA (1991) The acetylcholine-induced flare response in evaluation of small fiber disfunction *Annals of Neurology* **29** 590-595

Benfeldt E and Serup J (1999) Effect of barrier perturbation on cutaneous penetration of salycilic acid in hairless rats: *in vivo* pharmacokinetics using microdialysis and non-invasive quantification of barrier function *Archives in Dermatoogical Research* **291** 517-526

Benfeldt E, Serup J, Menné T (1999) Effect of barrier perturbation on cutaneous salicylic acid penetration in human skin: in vivo pharmacokinetics using microdialysis and non-invasive quantification of barrier function *British Journal of Dermatology* **140** 739-748

Benfeldt E, Serup J, Menné T (1999a) Microdialysis vs suction blister technique for in vivo sampling of pharmacokinetics in the human dermis *Acta Dermatologica Venereologica* **79** 338-342

Benveniste H and Hüttemeier PC (1990) Microdialysis: theory and application. *Progress in Neurobiology* **35** 195-215

Berghoff M, Kathpal M, Kilo S, Hilz MJ, Freeman R (2002) Vascular and neural mechanisms of ACh-mediated vasodilation in the forearm cutaneous microcirculation *Journal of Applied Physiology* **92** 780-788

Berridge MJ (1993) Inositol trisphosphate and calcium signalling *Nature* **361** 315-325

Bjerring P, Andersen PH, Arendt-Nielsen L (1989) Vascular response of human skin after anaelgesia with EMLA-cream *British Journal of Anaesthesiology* **63** 655-660

Bito L, Davson H, Levi EM, Murray M, Snider N (1966) The concentration of free amino acids and other electrolytes in cerebrospinal fluid in vivo dialysate of brain and blood plasma of the dog *Journal of Neurochemistry* **13** 1057-1067

Bolz SS, de Wit C, Pohl U (1999) Endothelium-derived hyperpolarizing factor but not NO reduces smooth muscle Ca^{2+} during acetylcholine-induced dilation of microvessels *British Journal of Pharmacology* **128** 124-134

Braverman IM (1997) The cutaneous microcirculation: Ultrastructure and micro-anatomical organization *Microcirculation* **4** 329-340

Braverman IM, Keh A, Goldminz D (1990) Correlation of Laser Doppler wave patterns with underlying microvascular anatomy *Journal of Investigative Dermatology* **95** 283-286

Brunner M, Schmiedberger A, Schmid R, Eichler HG, Piegler E, Eichler HG, Müller M (1998) Direct assessment of peripheral pharmacokinetics in humans: comparison between cantharides blister fluid sampling, *in vivo* microdialysis and saliva sampling *British Journal of Clinical Pharmacology* **46** 425-431

Buchli R, Ndoye A, Rodriquez JG, Zia S, Webber RJ, Grando SA (1999) Human skin fibroblasts express m2, m4, and m5 subtypes of muscarinic acetylcholine receptors

Journal of Cellular Biochemistry **74** 264-277

Camara AL, Braga MFM, Rocha ES, Santos MD, Cortes WS, Cintra WM, Aracava Y, Maelicke A, Albuquerque EX (1997) Methamidophos: an anticholinesterase without significant effects on post-synaptic receptors or transmitter release *Neurotoxicology* **18** 589-602

Carver MP, Williams PL, Riviere JE (1989) The isolated perfused porcine skin flap. III. Percutaneous absorption pharmacokinetics of organophosphates, steroids, benzoic acid, and caffeine *Toxicology and Applied Pharmacology* **97** 324-337

Cavanah DK and Casale TB (1991) Cutaneous responses to anticholinergics evidence for muscarinic subtype participation *Journal of Allergy and Clinical Immunology* **87** 971-976

Chang SK, Williams PL, Dauterman WC, Riviere JE (1994) Percutaneous absorption, dermatopharmacokinetics and related bio-transformation studies of carbaryl, lindane, malathion and parathion in isolated perfused porcine skin *Toxicology* **91** 269-280

Cheesman AR and Benjamin N (1994) Lack of tolerance in forearm blood vessels in man to glyceryltrinitrate *British Journal of Clinical Pharmacology* **37** 441-444

Church MK (1997) Investigating bradykinin-induced reactions in the skin through microdialysis *Clinical and Experimental Allergy* **27** 28-32

Church MK and Clough GF (1997) Scanning Laser Doppler Imaging and dermal microdialysis in the investigation of skin inflammation *ACI International* **9** 41-46

Clough GF (1999) Role of nitric oxide in the regulation of microvascular perfusion in human skin *in vivo Journal of Physiology* **516** 549-557

Clough GF, Bennett AR, Church MK (1998) Effects of H_1 antagonists on the cutaneous vascular response to histamine and bradykinin: a study using scanning laser Doppler imaging *British Journal of Dermatology* **138** 806-814

Clough GF, Bennett AR, Church MK (1998a) Measurement of nitric oxide concentration in human skin in vivo using dermal microdialysis *Experimental Physiology* **83** 431-434

Contreras HR and Bustos-Obregón E (1999) Morphological alterations in mouse testis by a single dose of malathion *Journal of Experimental Zoology* **284** 355-359

Costello CT and Jeske AH (1995) Iontophoresis: Applications in transdermal medication delivery *Physical Therapy* **75** 554-563

Cross SE, Anderson C, Roberts MS (1998) Topical penetration of commercial salicylate esters and salts using human isolated skin and clinical microdialysis *British Journal of Clinical Pharmacology* **46** 29-35

de Boer J, Plitjer-Groendijk H, Korf J (1993) Microdialysis probe for transcutaneous monitoring of ethanol and glucose in humans *Journal of Applied Physiology* **75** 2825-2830

de Wit C, Esser N, Lehr HA, Bolz SS, Pohl U (1999) Pentobarbital-sensitive EDHF comediates ACh-induced arteriolar dilation in the hamster microcirculation *American Journal of Physiology* **276** H1527-H1534

Department of Health (DOH) (1999) Committee on toxicity of chemicals in food, Organophosphates.

Douglas WW and Ritchie JM (1960) The excitatory action of acetylcholine on cutaneous non-myelinated fibres *Journal of Physiology* **150** 501-514

Doyle MP and Duling BR (1997) Acetylcholine induces conducted vasodilation by nitric oxide dependent and independent mechanisms *American Journal of Physiology* **272** H1364-H137

Eady DJ (1993) Neuropeptides in skin *British Journal of Dermatology* **128** 597-605

Eglen RM, Hegde SS, Watson N (1996) Muscarinic receptor subtypes and smooth muscle function *Pharmacological Reviews* **48** 531-565

Eldefrawi AT, Jett D, Eldefrawi ME (1992) Direct actions of organophosphorus anticholinesterases on muscarinic receptors *Organophosphates: Chemistry, Fate and Effects* 257-270

Elias PM (1983) Epidermal lipids, barrier function and desquamation *Dermatology* **80** 44

Fantozzi R, Masini E, Blandina P, Mannaioni PF, Bani-Sacchi T (1978) Release of histamine from rat mast cells by ACh *Nature* **273** 473-474

Feldmann RJ and Maibach HI (1974) Percutaneous penetration of some pesticides and herbicides in man *Toxicology and Applied Pharmacology* **28** 126-132

Fjallbrandt N and Iggo A (1961) The effect of histamine, 5-hydroxytryptamine and acetylcholine on cutaneous afferent nerve fibres *Journal of Physiology* **156** 578-590

Foreman JC (1988) The skin as an organ for the study of neuropeptides *Skin Pharmacology* **1** 77-83

Foreman JC (1991) The pharmacology of neuropeptides in mast cells and skin: its implications for the physiology of blood flow in normal and diseased human skin *Asia Pacific Journal of Pharmacology* **6** S1-S9

Goldsmith PC, Leslie TA, Hayes NA, Levell NJ, Dowd PM, Foreman JC (1996) Inhibitors of nitric oxide synthase in human skin *Journal of Investigative Dermatology* **106** 113-118

Grando SA (1997) Biological functions of keratinocyte cholinergic receptors *Journal of Investigative Dermatology Symposium proceedings* **2** 41-48

Grando SA, Kist DA, Qi M, Dahl MV (1993). Human keratinocytes synthesize, secrete,

and degrade acetylcholine *Journal of Investigative Dermatology* **101** 32-36

Grossmann M, Jamieson MJ, Kellogg Jr DL, Kosiba WA, Pergola PE, Crandall CG, Shepherd AMM (1995) The effect of iontophoresison the cutaneous vasculature: Evidence for current-induced hyperemia *Microvascular Research* **50** 444-452

Guy RH and Hadgraft J (1984) Prediction of drug disposition kinetics in skin and plasma following topical administration *Journal of Pharmaceutical Sciences* **73** 883-887

Hegemann L, Forstinger C, Partsch B, Lagler I, Krotz S, Wolff K (1995) Microdialysis in cutaneous Pharmacology: Kinetic analysis of transdermally delivered nicotine *Journal of Investigative Dermatology* **104** 839-843

Heymann E, Hoppe W, Krusselmann A, Tschoetschel C (1993) Organophosphate sensitive and insensitive carboxylesterases in human skin. *Chemical and Biological Interactions* **87** 217-226

Holzer P and Jocic M (1994) Cutaneous vasodilatation induced by nitric oxide-evoked stimulation of afferent nerves in the rat *British Journal of Pharmacology* **112** 1181-1187

Holzer P, Jocic M, Peskar BA (1995) Mediation by prostaglandins of the nitric oxide-induced neurogenic vasodilatation in rat skin *British Journal of Pharmacology* **116** 2365-2370

Holzer P (1998) Neurogenic vasodilatation and plasma leakage in the skin *General Pharmacology* **30** 5-11

Hong J, Eo Y, Rhee J, Kim T (1993) Simultaneous analysis of 25 pesticides in crops using gas chromatography and their identification by gas chromatography-mass spectrometry *Journal of Chromatography* **639** 261-271

Horsmanheimo L, Harvima IT, Ylönen J, Naukkarinen A, Horsmanheimo M (1996)

Histamine release in skin monitored with the microdialysis technique does not correlate with the weal size induced by cow allergen *British Journal of Dermatology* **134** 94-100

Hsiao JK, Ball BA, Morrison PF, Mefford IN, Bungay PM (1990) Effects of different semipermeable membranes on in vitro and in vivo performance of microdialysis probes *Journal of Neurochemistry* **54** 1449-1452

Hwa JJ, Ghibaudi L, Williams P, Chatterjee M (1994) Comparison of acetylcholine-dependent relaxation in large and small arteries of rat mesenteric vascular bed. *American Journal of Physiology* **266** H952-H958

Jansson P, Krogstad AL, Lönnroth P (1996) Microdialysis measurements in skin: evidence for significant lactate release in healthy humans *American Journal of Physiology* **271** E138-E142

Jianmongkol S, Marable BR, Berkman CE, Talley TT, Thompson CM, Richardson RJ (1999) Kinetic evidence for different mechanisms of acetylcholinesterase inhibition by (1R) and (1S) stereoisomers of isomalathion *Toxicology and Applied Pharmacology* **155** 43-53

Johnson JA and Wallace KB (1987) Species-related differences in the inhibition of brain acetylcholinesterase by paraoxon and malaoxon *Toxicology and Applied Pharmacology* **88** 234-241

Johnson JM, Taylor WF, Shepherd AP, Park MK (1984) Laser Doppler measurement of skin blood flow: comparison with plethysmography *Journal of Applied Physiology* **56** 798-803

Joyner MJ and Dietz NM (1997) Nitric oxide and vasodilation in human limbs *Journal of Applied Physiology* **83** 1785-1796

Joyner MJ and Halliwill JR (2000) Sympathetic vasodilatation in human limbs *Journal of Physiology* **526** 471-480

Juan H (1982) Nicotinic nociceptors on perivascular sensory nerve endings *Pain* **12** 259-264

Katz EJ, Cortes VI, Eldefrawi ME, Eldefrawi AT (1997) Chlorpyrifos, Parathion, and their Oxons bind to and desensitize a nicotinic acetylcholine receptor: Relevance to their toxicities *Toxicology and Applied Pharmacology* **146** 227-236

Kehr J (1993) A survey on quantitative microdialysis theoretical models and practical implications *Journal of Neuroscience Methods* **48** 251-261

Kellogg Jr DL, Johnson JM, Kenney WL, Pérgola PE, Kosiba WA (1993) Mechanisms of control of skin blood flow during prolonged exercise in humans *American Journal of Physiology* **265** H562-H568

Kellogg Jr DL, Pérgola PE, Piest KL, Kosiba WA, Crandall CG, Grossmann M, Johnson JM (1995) Cutaneous active vasodilation in human is mediated by cholinergic nerve cotransmission *Circulation Research* **77** 1222-1228

Khan F, Davidson NC, Littleford RC, Litchfield SJ, Struthers AD, Belch JJF (1997) Cutaneous vascular responses to acetylcholine are mediated by a prostanoid-dependent mechanism in man *Vascular Medicine* **2** 82-86

Klapproth H, Reinheimer T, Metzen J, Münch M, Bittinger F, Kirkpatrick CJ, Höhle KD, Schemann M, Racké K, Wessler I (1997) Non-neuronal acetylcholine, a signalling moleculesynthesized by surface cells of rat and man *Naunyn-Schmiedeberg's Archives Pharmacology* **355** 515-523

Kodja G, Patzner M, Hacker A, Noack E (1998) Nitric oxide inhibits vascular bioactivation of glyceryl trinitrate: a novel mechanism to explain preferential venodilation of organic nitrates *Molecular Pharmacology* **53** 547-554

Krogstad AL, Jansson P-A, Lönnroth P, Lönnroth P (1996) Microdialysis methodology for the measurement of dermal interestial fluid in humans *British Journal of Dermatology* **134** 1005-1012

Linden M, Wårdell K, Andersson T, Anderson C (1997) High resolution laser Doppler perfusion imaging for the investigation of blood circulatory changes after microdialysis probe insertion *Skin Research and Technology* **3** 227-232

Macklin KD, Maus ADJ, Pereira EFR, Albuquerque EX (1998) Human vascular endothelial cells express functional nicotinic acetylcholine receptors *The Journal of Pharmacology and Experimental Therapeutics* **287** 435-439

Magnus IA and Thompson RHS (1954) Cholinesterase activity in human skin *British Journal of Dermatology* **66** 163-173

Malger W, Westerman RA, Mohner B, Handwerker HO (1990) Properties of transdermal histamine iontophoresis: differential effects of season, gender, and body region *Journal of Investigative Dermatology* **94** 347-352

Mason H, Waine E, McGregor A (1992) *In-vitro* studies on human cholinesterase (ChE) and biological effect monitoring of organophosphate pesticide exposure *Human and Experimental Toxicology* **11** 557-558

Maxwell DM (1992) The specificity of carboxylesterase protection against the toxicity of organophosphorus compounds *Toxicology and Applied Pharmacology* **114** 306-312

McCracken NW, Blain PG, Williams FM (1993) Nature and role of xenobiotic metabolizing esterases in rat liver, lung, skin and blood *Biochemical Pharmacology* **45** 31-36

Merino V, Guy RH, Hochstrasser D, Guy RH (1999) Noninvasive sampling of phenylalanine by reverse iontophoresis *Journal of Controlled Release* **61** 65-69

Minton NA and Murray VSG (1988) A review of organophosphate poisoning *Medical Toxicology* **3** 350-375

Misery L (1997) Skin, immunity and nervous system *British Journal of Dermatology* **137** 843-850

Mize NK, Buttery M, Daddona P, Morales C, Cormier M (1997) Reverse iontophoresis: monitoring prostaglandin E_2 associated with cutaneous inflammation *in vivo* *Experimental Dermatology* **6** 298-302

Morris JL (1999) Cotransmission from sympathetic vasoconstrictor neurons to small cutaneous arteries in vivo *American Journal of Physiology* **277** H58-H64

Morris SJ and Shore AC (1996) Skin blood flow responses to the iontophoresis of acetylcholine and sodium nitroprusside in man: possible mechanisms *Journal of Physiology* **496** 531-542

Müller M, Brunner M, Schmid R, Putz EM, Schmiedberger A, Wallner I, Eichler HG (1998) Comparison of three different experimental methods for the assessment of peripheral compartment pharmacokinetics in humans *Life Sciences* **62** PL 227-PL 234

Müller M, Burgdorff T, Jansen B, Singer EA, Agneter E, Dorner G, Brunner M, Eichler HG (1997) *In vivo* drug-response measurements in target tissues by microdialysis *Clinical Pharmacology and Therapeutics* **62** 165-170

Ndoye A, Buchli R, Greenberg B, Nguyen VT, Zia S, Rodriquez JG, Webber RJ, Lawry MA, Grando SA (1998) Identification and mapping of keratinocyte muscarinic acetylcholine receptor subtypes in human epidermis *Journal of Investigative Dermatology* **111** 410-416

Noon JP, Walker BR, Hand MF, Webb DJ (1998) Studies with iontophoretic administration of drugs to human dermal vessels in vivo cholinergic vasodilatation is mediated by dilator prostanoids rather than nitric oxide *British Journal of Clinical Pharmacology* **45** 550

Obeid AN, Boggett DM, Barnett NJ, Dougherty G, Rolfe P (1988) Depth discrimination in laser Doppler skin blood flow measurement using different lasers *Medical and Biological Engineering and Computing* **26** 415-419

Pérgola PE, Kellogg Jr DL, Johnson JM, Kosiba WA, Solomon DE (1993) Role of

sympathetic nerves in the vascular effects of local temperature in human forearm skin *American Journal of Physiology* **265** H785-H792

Petersen LJ (1997) Quantitative measurement of extracellular histamine concentrations in intact human skin in vivo by the microdialysis technique: methodological aspects *Allergy* **52** 547-555

Petersen LJ, Church MK, Skov PS (1997) Histamine is released in the wheal but not the flare following challnge of human skin in vivo: a microdialysis study *Clinical and Experimental Allergy* **27** 284-295

Petersen LJ, Kristensen JK, Bülow J (1992) Microdialysis of the interstitial water space in human skin in vivo: Quantitative measurement of cutaneous gulcose concentrations *Journal of Investigative Dermatology* **99** 357-360

Petersen LJ, Mosbech H, Skov PS (1996) Allergen-induced histamine release in intact human skin in vivo assessed by skin microdialysis technique: Characterization of factors influencing histamine releasability *Journal of Allergy and Clinical Immunology* **97** 972-979

Petersen LJ and Skov PS (1995) Methacholine induces wheal and flare reactions in human skin but does not release histamine in vivo as assessed by the skin microdialysis technique *Allergy* **50** 976-980

PluthJM, Nicklas JA, O'Neill JP, Albertini RJ (1996) Increased frequency of specific genomic deletions resulting from *in vitro* malathion exposure *Cancer Research* **56** 2393-2399

Qiao GL and Riviere JE (1995) Significant effects of application site and occlusion on the pharmacokinetcs of cutaneous penetration and biotransformation of parathion *in vivo* in swine *Journal of Pharmaceutical Sciences* **84** 425-432

Qiu Y, Peng Y, Wang J (1996) Immunoregulatory role of neurotransmitters *Advantages in Neuroimmunology* **6** 223-231

Ralevic V, Khalil Z, Dusting GJ, Helme RD (1992) Nitric oxide and sensory nerves are involved in the vasodilator response to acetylcholine but not to calcitonin gene-related peptide in rat skin microvasculature *British Journal of Pharmacology* **106** 650-655

Rao MR, Kanji VK, Sekhar V (1999a) Pesticide induced changes of nitric oxide synthase in rat brain *in vitro Drug and Chemical Toxicology* **22** 411-420

Ray D (1998) Organophosphorus esters: An evaluation of chronic neurotoxic effects MRC Institute for Enviroment and Health

Ray DE and Richards PG (2001) The potential for toxic effects of chronic, low-dose exposure to organophosphates *Toxicology Letters* **120** 343-357

Reilly DM, Ferdinando D, Johnston C, Shaw C, Buchanan KD, Green MR (1997) The epidermal nerve fibre network: characterization of nerve fibres in human skin by confocal microscopy and assessment of racial variations *British Journal of Dermatology* **137** 163-170

Reifenrath WG, Chellquist EM, Shipwash EA, Jederberg WW, Krueger GG (1984) Percutaneous penetration in the hairless dog, weanling pig and grafted athymic nude mouse:evaluation models for predicting skin penetration in man *British Journal of Dermatology* **III** 123-135

Rendell MS, Finnegan MF, Healy JC, Lind A, Milliken BK, Finney DE, Bonner RF (1998) The relationship of Laser-Doppler Skin blood flow measurements to the cutaneous microvascular anatomy *Microvascular Research* **55** 3-13

Riviere JE and Williams PL (1992) Pharmacokinetic implications of changing blood flow in the skin *Journal of Pharmaceutical Sciences* **81** 601-602

Rodgers K and Xiong S (1997) Effect of acute administration of malahtion by oral and dermal routes on serum histamine levels *International Journal of Immunopharmacology* **19** 437-441

Rodgers K and Xiong S (1997a) Effect of administration of malathion for 90 days on macrophage function and mast cell degranulation *Toxicology Letters* **93** 73-82

Rodriguez OP, Muth GW, Berkman CE, Kim K, Thompson CM (1997) Inhibiton of various cholinesterases with the enantiomers of malaoxon *Bulletin of Enviromental Contamination and Toxicology* **58** 171-176

Rook, Wilkinson and Ebling FJG (1996) *Textbook of Dermatology* editors Ebling FJG, Eady RAJ, Leigh IM

Sams C and Mason HJ (1999) Detoxification of organophosphates by A-esterases in human serum *Human and Experimental Toxicology* **18** 653-658

Sartorelli P, Aprea C, Bussani R, Novelli MT, Orsi D, Sciarra G (1997) In vitro percutaneous penetration of methyl-parathion from a commercial formulation through the human skin *Occupational and Enviromental Medicine* **54** 524-525

Saumet JL, Kellogg Jr DL, Taylor WF, Johnson JM (1988) Cutaneous laser Doppler flowmetry: influence of underlying muscle blood flow *Journal of Applied Physiology* **65** 478-481

Schaefer H and Redelmeir TE (1996) *Skin Barrier: Principles of percutaneous absorption.*

Schanker HM, Rachelefsky G, Siegel S, Katz R, Spector S, Rohr A, Rodriquiz C, Woloshin K, Papanek PJJ (1992) Immediate and delayed type hypersensitivity to malathion *Annals of Allergy* **69** 526-528

Sharma VK and Kaur S (1990) Contact sensitization by pesticides in farmers *Contact Dermatitis* **23** 77-80

Shastry S, Minson CT, Wilson SA, Dietz NM, Joyner MJ (2000) Effects of atropine and L-NAME on the cutaneous blood flow during body heating in humans *Journal of Applied Physiology* **88** 467-472

Singh P and Maibach HI (1994) Iontophoresis in drug delivery: Basic principles and applications *Critical Reviews in Therapeutic Drug Carrier Systems* **11** 161-213

Singh P and Roberts MS (1993) Dermal and underlying tissue pharmacokinetics of salicylic acid after topical application *Journal of Pharmacokinetics and Biopharmaceutics* **21** 337-373

Singh P and Roberts MS (1994) Effects of vasoconstriction on dermal pharmacokinetics and local tissue distribution of compounds *Journal of Pharmaceutical Sciences* **83** 783-791

Stenn KS, Goldenhersh MA, Trepeta RW (1986) Structure and function of the skin. *The Skin* 1-14

Stewart DJ, Elsner D, Sommer O, Holtz J, Bassenge E (1986) Altered spectrum of nitroglycerin action in long term treatment: nitroglycerin-specific venous tolerance with maintenance of arterial vasodepressor potency *Circulation* **74** 573-582

Wallengren J (1997) Vasoactive peptides in the skin *Journal of Investigative Dermatology Symposium Proceedings* **2** 49-55

Wallin BG (1990) Neural control of human skin blood flow *Journal of the Autonomic Nervous System* **30** S185-S190

Wang I, Andersson-Engels S, Nilsson GE, Wårdell K, Svanberg K (1997) Superficial blood flow following photodynamic therapy of malignant non-melanoma skin tumours measured by laser Doppler perfusion imaging *British Journal of Dermatology* **136** 184-189

Ward TR, Ferris DJ, Tilson HA, Mundy WR (1993) Correlation of the anti-cholinesterase activity of a series of organophosphates with their ability to compete with agonist binding to muscarinic receptors *Toxicology and Applied Pharmacology* **122** 300-307

Ward TR and Mundy WR (1996) Organophosphorus compounds preferentially affect second messenger systems coupled to M2/M4 receptors in rat frontal cortex *Brain Research Bulletin* **39** 49-55

Warren JB (1994) Nitric oxide and human skin blood flow responses to acetylcholine and ultraviolet light *FASEB J.* **8** 247-251

Warren JB, Loi RK, Wilson AJ (1994a) PGD_2 is an intermediate in agonist-stimulated nitric oxide release in rabbit skin microcirculation *American Journal of Physioliology* **266** H1846-H1853

Wårdell K, Jakobsson A, Nilsson GE (1993) Laser Doppler perfusion imaging by dynamic light scattering *IEEE Transactions on Biomedical Engineering* **40** 309-316

Wårdell K, Naver HK, Nilsson GE, Wallin BG (1993a) The cutaneous vascular axon reflex in humans characterized by laser Doppler perfusion imaging *Journal of Physiology* **460** 185-199

Washington C and Washington N (1989) Drug delivery to the skin *Physiological Pharmaceutics Biological Barriers to drug absorption* editors Wilson CG and Washington N, 109-120 Ellis Horwood Limited

Wessler I, Kirkpatrick CJ, Racke K (1998) Non-neuronal Acetylcholine, a locally acting molecule, widely distributed in biological systems: Expression and function in humans *Pharmacological Therapeutics* **77** 59-79

Wessler I, Kirkpatrick CJ, Racke K (1999) The cholinergic 'pitfall': acetylcholine, a universal cell molecule in biological systems, including humans *Clinical and Experimental Pharmacology* **26** 198-205

Wester RC, Maibach HI, Bucks DAW, Guy RH (1983) Malathion percutaneous absorption after repeated administration to man *Toxicology and Applied Pharmacology* **68** 116-119

Wester RC, Quan D, Maibach HI (1996) In Vitro percutaneous absorption of model compounds glyphosate and malathion from cotton fabric and through human skin *Food and Chemical toxicology* **34** 731-735

Westerman RA, Widdop RE, Hogan C, Zimmet P (1987) Non-invasive tests of neurovascular function: reduced resposes in diabetic mellitus *Neuroscience Letters* **81** 177-182

Xiong S and Rodgers K (1997) Effects of malathion metabolites on degranulation of and mediator release by human and rat basophilic cells *Journal of Toxicology and Enviromental Health* **51** 159-175

Zhu Y, Wong PSH, Cregor M, Gitzen JF, Coury LA, Kissinger PT (2000) In vivo microdialysis and reverse phase ion pair liquid chromatography/tandem mass spectrometry for the determination and identification of acetylcholine and related compounds in rat brain *Rapid Communications in Mass Spectrometry* **14** 1695-1700